

**Susitna-Watana Hydroelectric Project
(FERC No. 14241)**

Updated Fluvial Geomorphology Modeling Approach

**Attachment A:
FA-128 (Slough 8A) Hydraulic Modeling for Proof of
Concept**

Prepared for
Alaska Energy Authority



Prepared by
Tetra Tech Inc.
May 2014

This page intentionally left blank

TABLE OF CONTENTS

1	INTRODUCTION	1
2	2-D MODEL DEVELOPMENT AND CALIBRATION	2
2.1	Model Description.....	2
2.2	Model Development.....	2
2.2.1	Topographic Data and Model Geometry	2
2.2.2	Material Roughness Properties	3
2.2.3	Downstream Boundary Conditions.....	4
2.2.4	Other Model Parameters	4
2.3	Model Calibration/Validation	4
2.3.1	Calibration/Validation Data	5
2.3.2	Model Calibration Results	5
2.3.3	Model Validation	7
2.3.4	Review of Model Results by Fish and Aquatics IFS	8
2.4	Transfer of Hydraulic Model Simulations to Fish and Aquatics IFS.....	9
2.5	Conclusions	10
3	REFERENCES	11
4	TABLES	13
5	FIGURES	19

LIST OF TABLES

Table 2.3-1.	Summary of ADCP flow measurements at FA-128 (Slough 8A). (Table modified from ISR8.5).	13
Table 2.3-2.	Summary of water-surface elevation measurements at FA-128 (Slough 8A).....	14
Table 2.3-3.	Comparison of the predicted and measured flows collected on September 10, 2013, when the discharge in the river was approximately 26,124 cfs.	15
Table 2.3-4.	Comparison of the predicted and measured flows collected on July 2, 2013, when the discharge in the river was approximately 24,690 cfs.....	16
Table 2.3-5.	Summary of difference in velocity calibration statistics (predicted minus measured, ft/s).	16
Table 2.3-6.	Results of hydraulic model calibration/validation.....	17
Table 2.3-7.	Additional flow sources and water-surface elevations applied to the model.	17

Table 2.4-1. Summary of SRH-2D model output provided to the IFS team. 18

LIST OF FIGURES

Figure 1-1. FA-128 (Slough 8A) site location map and location of ADCP transects. 21

Figure 2.2-1. Bathymetric and topographic survey data for FA-128 (Slough 8A)..... 22

Figure 2.2-2. Triangulated Irregular Network (TIN) developed for the in-channel areas of FA-128 (Slough 8A) using the topographic and bathymetric data shown in Figure 2.2-3. 23

Figure 2.2-3. TIN topography including LiDAR in the overbank areas of FA-128 (Slough 8A). 24

Figure 2.2-4. FA-128 (Slough 8A) SRH-2D hydraulic model mesh..... 25

Figure 2.2-5. FA-128 (Slough 8A) SRH-2D hydraulic model topography. 26

Figure 2.2-6. Fine and coarse mesh areas in FA-128 (Slough 8A) delineated by the Instream Flow Study team (copied from ISR8.5 Figure 5.6-4). 27

Figure 2.2-7. Close-up of a portion of the FA-128 (Slough 8A) SRH-2D hydraulic model mesh. 28

Figure 2.2-8. Manning *n*-values applied to the SRH-2D models in FA-128 (Slough 8A). 29

Figure 2.2-10 Location of the measured water-surface elevations (WSEs) in FA-128 (Slough 8A). 31

Figure 2.3-1 Flow travel time along the middle reach from Gold Creek gage. The travel times at each Focus Area are reported in ISR 8.5. 32

Figure 2.3-2. Screen capture from SMS showing differences between the measured and predicted water-surface elevations from the hydraulic model at 26,124 cfs (September 10, 2013) in FA-128 (Slough 8A). The bars indicate the relative differences in water-surface elevations in the direction of the error. For example, if the color is in the lower half, then the predicted water-surface elevation is lower than the measured values. Green bars indicate differences of less than 1 foot, orange bars indicate differences greater than 1 foot. 33

Figure 2.3-3. Comparison of measured velocities with the predicted velocities at Transect 1A at 26,184 cfs (Sep 10, 2013). 34

Figure 2.3-4. Comparison of measured velocities with the predicted velocities at Transect 1B at 26,184 cfs (Sep 10, 2013). 34

Figure 2.3-5. Comparison of measured velocities with the predicted velocities at Transect 2A at 26,184 cfs (Sep 10, 2013). 35

Figure 2.3-6. Comparison of measured velocities with the predicted velocities at Transect 2B at 26,184 cfs (Sep 10, 2013). 35

Figure 2.3-7. Comparison of measured velocities with the predicted velocities at Transect 2C at 26,184 cfs (Sep 10, 2013). 36

Figure 2.3-8. Comparison of measured velocities with the predicted velocities at Transect 2D at 26,184 cfs (Sep 10, 2013).	36
Figure 2.3-9. Comparison of measured velocities with the predicted velocities at Transect 3A at 26,184 cfs (Sep 10, 2013).	37
Figure 2.3-10. Comparison of measured velocities with the predicted velocities at Transect 3B at 26,184 cfs (Sep 10, 2013).	37
Figure 2.3-11. Comparison of measured velocities with the predicted velocities at Transect 3C at 26,184 cfs (Sep 10, 2013).	38
Figure 2.3-12. Comparison of measured velocities with the predicted velocities at Transect 4C at 26,184 cfs (Sep 10, 2013).	38
Figure 2.3-13. Comparison of measured velocities with the predicted velocities at Transect 4D at 26,184 cfs (Sep 10, 2013).	39
Figure 2.3-14. Comparison of measured velocities with the predicted velocities at Transect 4E at 26,184 cfs (Sep 10, 2013).	39
Figure 2.3-15. Comparison of measured velocities with the predicted velocities at Transect 5A at 26,184 cfs (Sep 10, 2013).	40
Figure 2.3-16. Comparison of measured velocities with the predicted velocities at Transect 6 at 26,184 cfs (Sep 10, 2013).	40
Figure 2.3-17. Comparison of measured velocities with the predicted velocities at Transect 7 at 26,184 cfs (Sep 10, 2013).	41
Figure 2.3-18. Scatter plot showing difference in velocity (predicted – measured) at 26,124 cfs (Sept. 10, 2013) FA-128 (Slough 8A).	42
Figure 2.3-19. Scatter plot showing difference in velocity (predicted – measured) at 24,690 cfs (July 2, 2013) FA-128 (Slough 8A).	42
Figure 2.3-20. Distribution of difference in velocity (predicted – measured) at 26,124 cfs (Sept. 10, 2013) FA-128 (Slough 8A).	43
Figure 2.3-21. Distribution of difference in velocity (predicted – measured) at 24,690 cfs (July 2, 2013) FA-128 (Slough 8A).	43
Figure 2.3-22. Comparison of measured and predicted velocity magnitude and direction at Transect 1A at 26,184 cfs (Sep 10, 2013).	44
Figure 2.3-23. Comparison of measured and predicted velocity magnitude and direction at Transect 1B at 26,184 cfs (Sep 10, 2013).	45
Figure 2.3-24. Comparison of measured and predicted velocity magnitude and direction at Transect 2A at 26,184 cfs (Sep 10, 2013).	46
Figure 2.3-25. Comparison of measured and predicted velocity magnitude and direction at Transect 2D at 26,184 cfs (Sep 10, 2013).	47
Figure 2.3-26. Comparison of measured and predicted velocity magnitude and direction at Transect 3C at 26,184 cfs (Sep 10, 2013).	48

Figure 2.3-27. Comparison of measured and predicted velocity magnitude and direction at Transect 4C at 26,184 cfs (Sep 10, 2013).....	49
Figure 2.3-28 Comparison of measured and predicted velocity magnitude and direction at Transect 4E at 26,184 cfs (Sep 10, 2013).....	50
Figure 2.3-29. Screen capture from SMS showing differences between the measured and predicted water-surface elevations at 54,200 cfs (June 4, 2013) FA-128 (Slough 8A).	51
Figure 2.3-30. Screen capture from SMS showing differences between the measured and predicted water-surface elevations at 24,705 cfs (July 2, 2013) FA-128 (Slough 8A).	51
Figure 2.3-31. Screen from SMS capture showing differences between the measured and predicted water-surface elevations at 20,132 cfs (July 24, 2013) FA-128 (Slough 8A).	52
Figure 2.3-32. Screen capture from SMS showing differences between the measured and predicted water-surface elevations at 20,688 cfs (July 25, 2013) FA-128 (Slough 8A).	52
Figure 2.3-33. Screen capture from SMS showing differences between the measured and predicted water-surface elevations at 20,050 cfs (August 4, 2013) FA-128 (Slough 8A).	53
Figure 2.3-34. Screen capture from SMS showing differences between the measured and predicted water-surface elevations at 36,636 cfs (August 21, 2013) FA-128 (Slough 8A).....	53
Figure 2.3-35. Screen capture from SMS showing differences between the measured and predicted water-surface elevations at 32,200 cfs (September 8, 2013) FA-128 (Slough 8A).....	54
Figure 2.3-36. Screen capture from SMS showing differences between the measured and predicted water-surface elevations at 26,124 cfs (September 10, 2013) FA-128 (Slough 8A).....	54
Figure 2.3-37. Flow depths at FA-128 (Slough 8A) for 12,000 cfs – initial run.....	55
Figure 2.3-38. Location of the additional flows applied to the model to represent the groundwater flows in FA-128 (Slough 8A).	56
Figure 2.3-39. Flow depths at FA-128 (Slough 8A) for 12,000 cfs – run with point sources.....	57
Figure 2.4-1. Predicted depth distribution at 2,000 cfs at FA-128 (Slough 8A).	58
Figure 2.4-2. Predicted depth distribution at 4,000 cfs at FA-128 (Slough 8A).	59
Figure 2.4-3. Predicted depth distribution at 6,000 cfs at FA-128 (Slough 8A).	60
Figure 2.4-4. Predicted depth distribution at 8,000 cfs at FA-128 (Slough 8A).	61
Figure 2.4-5. Predicted depth distribution at 12,000 cfs at FA-128 (Slough 8A).	62
Figure 2.4-6. Predicted depth distribution at 16,000 cfs at FA-128 (Slough 8A).	63

Figure 2.4-7. Predicted depth distribution at 22,000 cfs at FA-128 (Slough 8A). 64
Figure 2.4-8. Predicted depth distribution at 30,000 cfs at FA-128 (Slough 8A). 65
Figure 2.4-9. Predicted depth distribution at 50,000 cfs at FA-128 (Slough 8A). 66

This page intentionally left blank

1 INTRODUCTION

As part of the Fluvial Geomorphology Modeling below Watana Dam Study (RSP Study 6.6), 2-dimensional (2-D) hydraulic and sediment-transport modeling (also referred to as bed evolution modeling) will be conducted to assess the potential effects of the Susitna-Watana Hydroelectric Project on the dynamic behavior of the river downstream of the proposed dam, with particular focus on potential changes in instream and riparian habitat (Tetra Tech 2013a). The Project will alter flow rates and sediment supply downstream of the dam and the channel form is expected to respond to the changes, which in turn, will alter future instream and riparian habitat conditions.

An Instream Flow Study - Technical Team Meeting (IFS-TT: Riverine Modeling) was held on November 13-15, 2013 to review and discuss riverine modeling and study integration efforts. During this meeting a Proof of Concept (POC) exercise was discussed to demonstrate modelling coordination between studies. The coordination involved Fish and Aquatics IFS (Study 8.5), Fluvial Geomorphology Modeling (Study 6.6), Ice Processes (Study 7.6), Water Quality Modeling (Study 5.6) and Groundwater (Study 7.5) efforts. This attachment documents the portion of the POC effort conducted as part of the Fluvial Geomorphology Modeling Study. It is part of the Updated Fluvial Geomorphology Modeling Approach Technical Memorandum (Updated Modeling Approach TM), which provides updates to several topics besides the POC effort including 1-D and 2-D model selection, and selection of representative years including the treatment of Pacific Decadal Oscillation (PDO).

As part of the Proof of Concept, a 2-dimensional hydraulic model (SRH-2D) was developed for a representative Focus Area (FA) FA-128 (Slough 8A) to evaluate local scale issues. FA-128 (Slough 8A) is shown in Figure 1-1 with several channel types highlighted. Local scale issues are generally defined on the scale of the habitat and geomorphic features within the Focus Areas. One-dimensional (1-D) models will be used to address reach scale issues at the scale of geomorphic reaches. The output from the hydraulic model will be used by the Fish and Aquatics Instream Flow Study (IFS) (Study 8.5) team to evaluate the habitat characteristics in the Focus Area. A 2-D sediment-transport model is also being developed to evaluate the potential changes in bed elevation (patterns and magnitude of change) and bed material characteristics under the post-dam conditions. As outlined in the Fluvial Geomorphology Modeling Approach TM (Tetra Tech 2013a), the predicted changes in bed elevations from the sediment transport models will be incorporated into the hydraulic model to evaluate future conditions. The hydraulic model will be re-run to evaluate the changes in habitat under with project conditions.

The purpose of this technical memorandum is to document the 2-D hydraulic model development, calibration/validation, and model output at FA-128 (Slough 8A) performed for the Proof of Concept. The Proof of Concept demonstrates integration of hydraulic modeling with habitat analyses and includes establishing model layout and boundary locations, developing the geometry and roughness parameters in the model domain, reviewing the quality of the model network, testing and calibrating the model, reviewing the model results, and making any final adjustments to the model before making production runs over a range of discharges required for habitat analyses. The steps of this process are described below.

2 2-D MODEL DEVELOPMENT AND CALIBRATION

2.1 Model Description

The hydraulic modeling was conducted using SRH-2D Version 3 software developed by the U.S. Bureau of Reclamation (USBR) (Huang and Greimann 2011). The SRH-2D mesh was developed with Version 11 of the Aquaveo Surface Water Modeling System (SMS) graphical user interface (Aquaveo 2013). SRH-2D is a finite-volume model, hydrodynamic model that computes water-surface elevations and horizontal velocity components for sub-, super-, and trans-critical free-surface flow in 2-D flow fields. SRH-2D uses a flexible mesh composed of triangular and quadrilateral elements which allows the resolution of the computational elements to vary throughout the model domain, which provides a significant advantage over models with a structured mesh because the density of the computational points can be increased in areas with large topographic variability and areas of special interest. Lower resolution is used in other areas to maintain reasonable model size and computational efficiency. For the hydraulic models of the study Focus Areas, significant detail is incorporated into the model network, especially at areas of habitat influence.

2.2 Model Development

Model development is described in terms of model geometry, material roughness or flow resistance properties, boundary conditions and other model parameters.

2.2.1 Topographic Data and Model Geometry

The topography of the Focus Area (channel and overbank) is represented by elevations assigned to each node in the mesh. The bathymetric and topographic surveys reported in the ISR for Study 8.5 (Figure 2.2-1) were used to develop a Triangulated Irregular Network (TIN) of the channels in the Focus Area (Figure 2.2-2). The Indexed 2011 LiDAR data reported in the February 2 Draft ISR for Study 6.6 was then included in the TIN, which includes approximately 2.5 million triangles, most of which are located in the overbank areas captured in the LiDAR data. The horizontal datum for the surveys and models are referenced to the State Plane Coordinate System, North American Datum of 1983 (NAD83) (Alaska, Zone 4) and the vertical datum is the North American Vertical Datum of 1988 (NAVD88).

The contour map (1-foot contour interval for display purposes) of the TIN surface is shown in Figure 2.2-3. It is an accurate representation of the bathymetry and topography of the entire Focus Area. The model network was developed also to accurately represent the bathymetry and topography, but with elements that are suitable for simulated flow through the model domain. The TIN is used to assign elevations to the mesh nodes, which are located at the element corners.

The mesh was constructed to extend upstream and downstream of the FA boundary and to extend between the valley walls (Figure 2.2-4). The mesh was extended approximately 300 feet downstream of the FA boundary to provide better prediction of the flow distribution between the main and side channel near the downstream boundary. The mesh also was extended approximately 2,000 feet upstream of the FA to provide better prediction of the velocity distribution at the upstream boundary of FA-128 (Slough 8A) and to better represent the flow split into the side channel located near the left (east) boundary of the model. The contour map (also 1-foot contour interval) of the model mesh is shown in Figure 2.2-5, and is an accurate

replication of the TIN, but with considerably fewer elements. The resulting mesh is 11,300 feet long and contains 263,224 elements and 203,407 nodes.

As shown in Figure 2.2-6, the mesh was varied to have fine resolution in areas identified by the IFS team, medium resolution in the main channel, and coarse resolution in the overbank. Figure 2.2-7 illustrates transitions between fine, medium, and coarse mesh. To maintain mesh quality, the transitions in element size cannot be too abrupt, but element to element area factors of around 2 are used to maintain good mesh quality. The typical side length of the triangular and quadrilateral elements in the fine mesh areas is 6 feet (~2 m). The medium sized elements are predominantly quadrilateral with a typical size of approximately 30 feet (~ 10 m) wide by 30 feet (~ 10 m) long. The overbank elements are typically comprised of triangular elements ranging in size from 6 to 130 feet (~2 m to 40 m), with a representative size of approximately 75 feet (25 m).

A quality control check of the mesh was conducted using the “mesh quality” option in SMS. The mesh quality check included a review of the change in area between adjacent elements (no more than a factor of 2 area change between adjacent elements), number of connecting elements (no more than 8) and the minimum and maximum element angles (10 and 130 degrees, respectively). As indicated above, quadrilateral elements were kept relatively square. Similarly, triangular elements are kept relatively equilateral. By avoiding long aspect ratios (length to width), a higher level of mesh quality is achieved and the results should well represent the area for habitat analysis. The mesh met all of the quality control metrics, and together with the high quality TIN, the mesh is considered to be of excellent quality.

2.2.2 Material Roughness Properties

SRH-2D uses Manning’s n -values to define boundary friction losses and a turbulence model, either a parametric turbulence model or k - ϵ turbulence model referred to as the two equation model to compute the energy losses due to internal turbulence. The K -epsilon (k - ϵ) turbulence model is referred to as a 2-equation model that is more complex and computationally intensive compared to the parametric model. The eddy viscosity in the k - ϵ model is calculated using two equations that account for the turbulence energy and dissipation due to bed friction. A sensitivity analysis of the parabolic and k - ϵ turbulence models showed that both the parabolic and k - ϵ models predicted very similar hydraulic values, and as a result, the less computationally intensive parametric turbulence model was selected for all the SRH-2D model simulations.

Six different roughness material types were used to represent the channel, islands and various overbank surfaces and vegetation zones (Figure 2.2-8). The roughness zones were developed based on the geomorphic mapping, aerial photography and field observations. The overbank roughness ranged from 0.08 for lightly vegetated areas to 0.17 for overbank areas with thick vegetation. Main channels, side channels and sloughs were assigned a Manning’s n -value of 0.03 based on field observations, similar experience with other rivers, and standard references (Chow 1959; Barnes 1967; Hicks and Mason 1991; Julien 1995). SRH-2D does not have the ability to vary the Manning’s n -values during a simulation. These values were used as initial estimates and the model calibration process was used to make final adjustments as needed.

A parametric turbulence model was used to calculate internal turbulence using the default parameter of 0.7. A sensitivity analysis of the parametric turbulence model was conducted by varying the turbulence model parameter between the typical range of 0.1 and 0.7 suggested by the literature (Pasternak 2011) and comparing the predicted velocity distributions with the measured values (the

velocity data are described in Section 2.3.1). Due to the high level of mesh refinement, the turbulence exchange parameter has a relatively small effect on the results. The results of the sensitivity analysis indicate that 0.7 is an appropriate value for the model.

2.2.3 Downstream Boundary Conditions

The downstream boundary conditions for the model consist of a specified water-surface elevation for the particular discharge that is being modeled. A stage versus discharge rating curve was developed from measured water-surface elevations collected over a range of flows and by fitting a curve to represent stage-discharge values greater and less than the measured values (Figure 2.2-9). The measured water-surface elevations used to develop the rating curve were located near the downstream boundary, but not at the boundary (Figure 2.2-10). Therefore, it was necessary to adjust the measured values using a slope approximation to determine the water-surface at the boundary. The blue squares on Figure 2.2-9 represent the measured water-surface elevations, and therefore vary slightly from the rating-curve.

The stage-discharge values above and below the measured values were developed by fitting a curve through the measured points. The channel thalweg at the downstream boundary represents the minimum value on the rating curve. The 1-D hydraulic model output will be used to develop the rating-curve; however, this model is not yet available. The stage-discharge rating-curve will be revised after the 1-D model is finalized.

2.2.4 Other Model Parameters

The model was run initially using a 5-second time step at a constant discharge for 48 hours. This period was sufficiently long to ensure the model reached steady-state conditions in most cases. For some simulations, the model reached steady-state conditions in as little as 12 hours. All simulations were run at a 5 second time interval.

Monitor lines and monitor points were included in the model to evaluate the hydraulic conditions at specified locations. A “monitor line” is a modeling option in SRH-2D used to compute flow and sediment flux across a specified line that is defined by connecting a series of mesh nodes. Monitor lines were located at the ADCP transect in order to make comparisons between the measured and predicted flows. Monitor points were specified at areas of interest which include water-surface elevation measurement locations and near the upstream and downstream boundaries of the model.

2.3 Model Calibration/Validation

The model was calibrated to water-surface elevations and velocity (magnitude and direction) measurements collected on September 10, 2013, when the discharge in the river was 26,124 cfs. In general, the calibration procedure consisted of adjusting the Manning’s n roughness values, so that the predicted water-surface elevations, velocities and flow distributions matched the measured values, to a reasonable tolerance. Using the final model calibration parameters, the model was validated against the other sets of water-surface elevation measurements collected over a range of flows.

2.3.1 Calibration/Validation Data

Two sets of Acoustic Doppler Current Profiler (ADCP) measurements are available for calibration. They were collected on July 2, 2013, and September 10, 2013, when the discharge in the river was 24,705 and 26,124 cfs, respectively (Table 2.3-1). The model was calibrated to the September 10, 2013 dataset as it had slightly higher flows.

The ADCP data were collected across transects (i.e., perpendicular to the main flow direction) and longitudinally (i.e., parallel to the river) (previously presented Figure 1-1) as part of Study 8.5. In Figure 1-1, transects are labelled with a “T” and the longitudinal profiles are labeled with an “L”. Typically, repeat ADCP measurements were conducted at transects in the main channel as part of the quality control procedures implemented to ensure accurate flow measurements (ISR Study 8.5 Appendix C). Depth-averaged velocities were calculated from the raw ADCP measurements using the RiverSurveyor Live (Version 3.7) (Sontek/YSI 2013) software and the discharge for each transect was provided by Study 8.5. Water-surface elevations were also surveyed at the ends of each transect.

Water-surface elevation measurements were collected on 16 occasions over a range of flows from approximately 16,880 to 54,200 cfs (Figure 2.2-10, Table 2.3-2). Water-surface elevation (WSE) measurements were collected on the same days as the ADCP measurements and therefore the corresponding discharges are known. The discharges associated with the WSE measurements collected at other times, were calculated using the following procedure:

1. A Project River Mile (PRM) was calculated for each WSE measurement.
2. The travel time for each WSE measurement was calculated based on measured travel times (reported in ISR Study 8.5) between Gold Creek and the Focus Areas (Figure 2.3-1).
3. A discharge for each WSE measurement was calculated based on the time of the measurement, the travel time from Gold Creek, and the 15-minute interval discharge measurements at the Gold Creek gage (USGS Gage# 15292000) which is located at PRM 140 (Figure 2.3-1). No adjustments were made to the discharges because minimal tributary flow was expected.
4. The average of the individual discharges was used for the model simulation corresponding to each set of water surface measurements.

The variation in discharge during the ADCP survey results in reasonable small changes in water-surface elevation, and therefore, the average discharge applied to the model is considered representative of the flow conditions at the time of the ADCP and water-surface elevation measurements.

2.3.2 Model Calibration Results

The hydraulic model was run using the previously detailed model parameters, which included Manning’s n roughness value of 0.03 for the main channel and side channels, at a discharge of 26,124 cfs (Table 2.3-1). The model output indicated that the model slightly under-predicted the measured water-surface elevations, but predicted the flow distributions in the main and side channels reasonably well. A sensitivity analysis of the channel roughness was conducted by varying the Manning’s n -values for the main channel and side channels. Increasing the Manning’s n -values improved the water-surface elevation calibration, but over predicted the flow

and velocities in the side channels. Decreasing the Manning's n -value resulted in a poorer calibration of the water-surface elevations, flow distributions and velocity distributions. It was concluded that a Manning's n -value of 0.03 provided the best calibration between the water-surface, flow measurements and velocity measurements, and therefore, all the subsequent simulations were conducted using a Manning's n -value of 0.03 for the main channel and side channels.

A comparison of the measured and predicted water-surface elevations at 26,124 cfs shows very good agreement (Figure 2.3-2). In Figure 2.3-2, the bars indicate the relative differences in water-surface elevations in the direction of the error. The bars show tick marks at 0 and ± 1 foot. If the bar is in the lower half, then the predicted water-surface elevation is lower than the measured values. Conversely, if the bar is in the upper half, then the model is over-predicting the water-surface elevation. Green bars indicate differences of less than 1 foot and orange bars indicate differences greater than 1 foot.

The differences between the measured and predicted water-surface elevation range from -1.2 to 0.0 feet, with an average difference of -0.3 feet, indicating the model is slightly under predicting the water-surface elevation across the FA. The largest differences occur at the confluence of a side channel and side slough and can be seen slightly to the left of center of Figure 2.3-2. The measured flow is only approximately 4 cfs at this location and the model predicts 10 cfs, so an adjustment of Manning's n is unrealistic since a error of 0.1 feet in water surface elevation will cause this difference in flow into the side channel or side slough, especially since the rest of the model calibrates well.

The predicted flow distributions match the measured values very well (Table 2.3-3). In the larger channels that convey more than 20 percent of the total flow, the differences are less than 5 percent. In the smaller channels, the differences are larger. For example, at T2C, the predicted value is 925 cfs compared to the measured value of 1,134 cfs, an 18-percent difference. At T7, the predicted value is 10.7 cfs compared to the measured value of 3.7 cfs, a 190-percent difference. Although these differences appear large, in the context of the overall model they are small, because 1,000 cfs is only 4 percent of the total flow and 10 cfs is less than 0.1 percent of the total flow. In terms of the percent of total flow, the model predicts amounts within 2 percent at all locations. This is considered a very good calibration.

Comparisons of the predicted and measured velocity magnitudes at the measured channel transects show very good agreement (Figures 2.3-3 through 2.3-17). The measured velocity data show considerable variation between repeat ADCP transects. For example, repeat ADCP measurements were collected at T1A and T1B (Figures 2.3-3 and 2.3-4, respectively) which show variation in the measured velocities of up to 3 ft/s. This is expected given the extremely turbulent flow conditions and the fact that the ADCP data are nearly instantaneous as the boat moves across the channel. In general, the predicted velocity distributions fall within the scatter of the measured data. Following are some comparisons of selected transects.

- At T1A (Figure 2.3-3), the predicted velocities are slightly lower along the left side of the channel and slightly higher along the right side compared to the measured values.
- T2D (Figure 2.3-8) shows very good agreement between the measured and predicted velocities.

- T6 and T7 (Figures 2.3-16 and 2.3-17, respectively) transects are located across smaller channels. At T6 the predicted velocities are approximately 0.75 ft/s higher than measured velocities. At T7, the predicted velocities match the measured data well at about 0.1 ft/s with the exception of what appears to be an anomalous measured velocity at station 40 feet.

The correlation (R^2 value) between measured and predicted velocity magnitudes is 0.85 (Figure 2.3-18) which indicates very good agreement. Pasternack (2011) suggests an R^2 value in the range of 0.4 to 0.8 indicates good calibration. The average difference in the velocities (predicted-measured) is 0.03 ft/s indicating the model is very slightly over predicting the velocities. The model very slightly under predicts high velocity flows and slightly over predicts low velocity flows.

Because the July 2, 2013, ADCP data set was collected at nearly the same discharge, it would not provide a strong validation test. However, it was used for comparison using the same model parameters and applicable boundary conditions. Figure 2.3-19 shows the predicted and measured velocities for this event. The correlation is slightly greater, but essentially the same as the September data. Given the inclusion of turbulence in the ADCP data, the agreement is excellent.

Histograms of the velocity differences for each event are shown in Figures 2.3-20 and 2.3-21. The histograms are similar and show the bulk of the data between ± 2 ft/s. Note: the value on the axis is the upper limit of the bin. For example, the 0 bin represents velocity differences from -0.5 to 0 ft/s, and the 0.5 bin represents differences from 0 to 0.5 ft/s. These results are summarized in Table 2.3-5. For both events, the mean and median differences are less than 0.1 ft/s and the standard deviation is less than 1 foot, so approximately 70 percent of the data are within ± 1 ft/s.

Comparisons of the predicted and measured velocity magnitudes and directions are shown in planform view for a series of selected transects (Figures 2.3-22 through 2.3-28). The same vector scaling and color are used for both model and measured results. The measured results cross the channel and the model results are regularly spaced at the element centroids. The direction of the velocity vectors and the velocity magnitude match the measured values very well. This data representation shows the influence of turbulence, where individual vectors are significantly different in magnitude or direction from the surrounding measurements.

2.3.3 Model Validation

The model was validated by running it over a range of flows corresponding to the water-surface elevation measurements (Table 2.3-2). Comparison of the differences in water-surface elevations (predicted-measured) show very good agreement, as shown in Figures 2.3-29 through 2.3-36 and summarized in Table 2.3-6, except at the highest modeled discharge of 54,203 cfs (June 4, 2013). At 54,203 cfs, the average difference in water-surface elevation is 0.66 feet (Figure 2.3-29). The 54,203 measurements are of limited spatial extent and were collected along a slough. The predicted water-surface elevations match the measured values well near the upstream confluence of the slough, but over-predict the water-surface elevations at the downstream confluence due to high water-surface elevations downstream from the confluence. Without a more complete distribution of water surface elevations throughout the FA, attempting to improve this area may create unknown issues in other areas. Where the data set consists of measurements throughout the area, agreement between the model and the measurements is good. Additional water surface data will be collected in 2014 to help resolve this issue

The average difference in water-surface elevations over the range of validation flows, excluding the 54,203 cfs results, is -0.04 feet, indicating the model is well validated over a range of flows from 20,069 to 36,636 cfs (Table 2.3-6).

2.3.4 Review of Model Results by Fish and Aquatics IFS

As part of the POC process, the hydraulic model was run over a series of flows from 2,000cfs to 50,000 cfs. The model output indicated that the predicted flows in the side channels and sloughs, especially in the vicinity of transects T4B and T4A, were not matching the field observations. Figure 2.3-37 shows the result of a 12,000 cfs run at FA-128 (Slough 8A). It shows water depths over the 2013 aerial image obtained when the river flow was approximately 11,700 cfs. Of particular interest is Slough 8A along the lower right side of aerial photo just above the railroad alignment and Half Moon Slough just left of center. The aerial photo shows ponded water in Half Moon Slough and water in Slough 8A, but the model shows these areas as dry. Review by the Fish and Aquatics IFS (Study 8.5) pointed to these areas as important for habitat analysis so they need to be more representatively included in the model results. Because SRH-2D is a surface water model, areas are only wet if water flows from upstream or is ponded from downstream. In either case there needs to be a connection to flowing open water. Based on field evidence from Studies 8.5 and 7.5, Slough 8A has a persistent groundwater flow source and Half Moon Slough intercepts the river-influenced groundwater table. Other areas of ponded water and potential trickle flow are evident in the aerial image.

To address this concern, the Fish and Aquatics IFS (Study 8.5) provided preliminary flows for Slough 8A and water surface elevations in Half Moon Slough. The SRH-2D model was run using a point source in Slough 8A of 4 cfs for the 12,000 cfs run and imposed a water surface elevation in Half Moon Slough. These are shown as points A and J in Figure 2.3-38. The model results for this run are shown in Figure 2.3-39. Also note that Skull Creek tributary has flow (24 cfs) in the revised run because flows were not yet available for this tributary when the original model was run. This illustrates that other flow sources (or sinks) can be simulated in the SRH-2D model, though additional information is required in order to assign flow rates to these points. SRH-2D can simulate sources and sinks as points at a single element, lines along a series of elements, and distributed between non-connected elements.

For the simulations ranging from 2,000 to 50,000 cfs, water-surface elevations were imposed in Half Moon Slough up to 22,000 cfs and small point source flow was included above that discharge. Table 2.3-7 shows the point sources and water surfaces used over the range of models. Two other locations (D and H) were included for some flows to demonstrate the potential for hyperheic connection down a side channel or side slough once the upstream breaching location becomes disconnected. These flows are for demonstration only and do not represent measured data. However, the model runs show that very small flows can be accommodated by SRH-2D without loss of continuity. Because SRH-2D is a finite volume model, flows of less than 1 cfs can be included and tracked without loss of continuity. With these additions the review comments of Fish and Aquatics IFS (Study 8.5) were adequately addressed and the range of hydraulic simulations for habitat analyses was conducted.

2.4 Transfer of Hydraulic Model Simulations to Fish and Aquatics IFS

The hydraulic model was run for the following range of flows specified by Study 8.5 using the previously described model parameters: 2,000, 4,000, 6,000, 8,000, 12,000, 16,000, 22,000, 30,000 and 50,000 cfs (Note: these flows were identified for the POC; the Fish and Aquatics IFS may specify additional flows for future habitat modeling efforts). Figures 2.4-1 through 2.4-9 show the water depths for these flows throughout the model domain. Areas outside the Focus Area are based on approximate data and should be considered as much less reliable. The complete results provided at each element for each run are listed in Table 2.4-1. The model output was provided in Excel spreadsheets. The element areas, D_{crit} , and bed shear were calculated outside the model.

Figure 2.4-1 shows the lowest flow, 2,000 cfs, which is a very rare open water condition, but is needed as a lower bound for data interpolation in the habitat analysis. The entire 2,000 cfs is conveyed through a single channel with no breaching flows. Point sources of 4 cfs in Slough 8A and 10 cfs in the large side channel branching in the from the main channel in the center of Figure 2.4-1 were included to demonstrate the possibility of a hyporheic or groundwater flow contributions. Had a value less than 10 cfs been used, the plotted depths would be very similar because of water collecting in the pools. At 4,000 cfs (Figure 2.4-2), the large side channel is breached with 22 cfs (red number indicates a lateral flow after breaching while the black numbers indicate hyporheic or groundwater flow) computed by the model and the remaining flow is conveyed by the main channel.

The plots for 6,000 and 8,000 cfs (Figures 2.4-3 and 2.4-4) show rapidly increasing side channel flow and two point sources, one in Sough 8A and one at the head of a side channel. The side channel flow was selected to demonstrate the simulation of small sources through the channel network. Even though the river inflow discharge is 6,000 cfs, the small contributions of flow track and the outflow is 6,017 cfs, with the inclusion of 12 cfs from Skull Creek and 5 cfs from the point sources. In Figure 2.4-4 two flow splits are shown. These two flows, and the flows shown in subsequent figures, represent individual overflows, so they accumulate in the lower side channel. For the 8,000 cfs run, the total cumulative flow in the side channel at the downstream end is 424 cfs, which includes point sources (7 cfs), lateral flows (401 cfs), and Skull Creek (16 cfs).

At 12,000 cfs (Figure 2.4-5) nearly all the side channels have breached and contain lateral flow. The one exception at this discharge is the side channel that crosses downstream of Half Moon Slough. This channel shows some water in the aerial photo, but appears to have little or no connection at the upstream end. The water may only be ponded, but it appears to be flowing at its downstream end. This channel may be a candidate for a small point source of flow. The Fluvial Geomorphology Modeling (Study 6.6) will work with the Groundwater (Study 7.5) and the Fish and Aquatics IFS (Study 8.5) to identify areas throughout the 10 Focus Areas where additional analysis or data collection are required to characterize groundwater response for incorporation as point sources in the hydraulic model (See ISR Part C Study 6.6 Section 7.1.2.1).

As flows progress through the 16,000-, 22,000-, 30,000- and 50,000-cfs river conditions (Figures 2.4-6 through 2.4-9) the lateral flow splits to the side channels and side sloughs increase dramatically. At 30,000 cfs total river discharge, the lateral flows of 14,500 cfs are nearly half of the total. At 50,000 cfs, the lateral flows are nearly 60 percent of the total river discharge at 29,000 cfs. At 50,000 cfs, the upstream end of Slough 8A connects. Slough 8A probably

connects at flows slightly greater than 30,000 cfs. The appropriate breaching flow will be incorporated into future models based on field work and analysis in to be conducted in 2014.

Each of the figures shows water either ponded in Half Moon Slough or small amounts of flow. The ponding elevations were estimated based on information from Fish and Aquatics IFS (Study 8.5) and the point source flows were assigned as a demonstration of potential for hyporheic exchange.

2.5 Conclusions

The 2-D hydraulic modeling effort conducted for the POC demonstrated that the SRH-2D model can be calibrated and validated for the conditions in the Middle Susitna River. The model produced WSEs and velocities in both the calibration and validation runs that provided close agreement with measured data. The model was also able to output the hydraulic conditions at the resolution required by the Fish and Aquatics IFS (Study 6.5) to perform habitat modeling.

A primary lesson learned from the POC is that groundwater and other point sources need to be considered and incorporated in the hydraulic model. Another item for FA-128 (Slough 8A) is the far upstream connection for Slough 8A. This connection needs to be estimated based on the 1-D model water surface elevations and breaching elevation. The 2-D model cannot efficiently be extended further because the main channel splits on the right side of the river and adequate survey is not available. Therefore use of the 1-D model is more applicable for estimating the split.

The model may have to be run for additional low flows to provide sufficient data for habitat analyses, such as 10,000 and 40,000 cfs. Models will be run for riparian habitat analyses as well. For the Riparian IFS (Study 8.6) flows ranging from 50,000 to 100,000 cfs may be adequate as these are approximately the range of 2- to 100-year flow frequency. The larger flows for the Riparian IFS are needed because of the importance of evaluating the frequency and duration of flows that inundate the floodplain.

3 REFERENCES

- Aquaveo, 2013. SMS Surface-water Modeling System, Version 11.1, User's Manual
- Huang, J.V. and Greimann, B.P., 2011. SRH-1D 2.8 User's Manual, Sedimentation and River Hydraulics – One Dimension, Version 2.8, U.S. Department of Interior, Bureau of Reclamation, Technical Service Center, Sedimentation and River Hydraulics Group. 227 p.
- Barnes, H.H., 1967. Roughness characteristics of natural channels. U.S. Geological Survey Water-Supply Paper 1849.
- Brailey Hydrologic, R2 Resource Consultants, Geovera and GWS. 2014. Fish and Aquatics Instream Flow Study (8.5). Appendix C 2013 Moving Boat ADCP Measurements. Initial Study Report. Prepared for Alaska Energy Authority, Anchorage, Alaska.
- Chow, V.T. 1959. Open Channel Hydraulics. McGraw-Hill, Inc.
- Hicks, D.M. and Mason, P.D., 1991. Roughness characteristics of New Zealand rivers. Water Resources Survey, DSIR Marine and Freshwater, Wellington, New Zealand.
- Julien P.Y., 1995. Erosion and sedimentation. Cambridge University Press, 280 p.
- Keller, E.A., 1971. Areal sorting of bed-load material: The hypothesis of velocity reversal. Geological Society of America Bulletin, v. 82, pp. 753-756.
- Pasternack, G.B. 2011. 2-D Modeling and Ecohydraulics Analysis. Published by the University of California at Davis, Davis, CA.
- R2 Resource Consultants, Inc. (R2). 2014. Fish and Aquatics Instream Flow Study. Initial Study Report (8.5) prepared for Alaska Energy Authority Susitna-Watana Hydroelectric Project. FERC No. 14241.
- Sontek/YSI, 2013. RiverSurveyor Live. Version 3.70, User's Manual.
- Tetra Tech. 2013a. Fluvial Geomorphology Modeling Approach. Draft Technical Memorandum. Revised June 30, 2013. Susitna-Watana Hydroelectric Project. Prepared for the Alaska Energy Authority. Anchorage, Alaska.
- Tetra Tech. 2013b. Development of Sediment Transport Relationships and an Initial Sediment Balance for the Middle and Lower Susitna River Segments. Susitna-Watana Hydroelectric Project. 2012 Study Technical Memorandum. Prepared for the Alaska Energy Authority. Anchorage, Alaska.

This page intentionally left blank

4 TABLES

Table 2.3-1. Summary of ADCP flow measurements at FA-128 (Slough 8A). (Table modified from ISR8.5).

Date/Time	Transect	Flow (cfs)					Total Flow cfs
		Far left	Left	Middle	Right	Far right	
7/2/13 13:14	T1		7,520		17,197		24,717
7/2/13 12:46	T2	6,204	236	766	17,710		24,916
7/2/13 12:12	T3		379	5,843	18,413		24,635
7/2/13 11:26	T4	9.10	374	2,629	12,818	8,745	24,575
7/2/13 10:58	T5			24,538			24,538
7/2/13 12:24	T6			231			
7/2/13 15:36	T7			2.95			
Average							24,690
9/10/13 14:03	T1		8,547		17,551		26,098
9/10/13 13:40	T2	6,960	250*	1,134	18,019		26,113
9/10/13 13:13	T3		473	6,331	19,328		26,132
9/10/13 12:20	T4		473	2,907	13,659	9,127	26,167
9/10/13 11:54	T5			26,184			26,184
9/10/13 13:26	T6			250			
9/10/13 15:10	T7			3.68			
Average							26,124

* No measurement, but should be similar to measurement at T6.

Table 2.3-2. Summary of water-surface elevation measurements at FA-128 (Slough 8A).

Date	Source	Discharge (cfs)	Number of WSE Measurements	Used for Model Calibration / Verification
4-Jun-2013	Geovera, LLC	54,203	96	Yes
5-Jun-2013	Geovera, LLC	49,635	80	No
27-Jun-2013	Geovera, LLC	19,076	63	No
28-Jun-2013	Geovera, LLC	28,200	49	No
2-Jul-2013 ^A	Geovera, LLC	24,705	32	Yes
24-Jul-2013	Geovera, LLC	20,132	129	Yes
25-Jul-2013	Geovera, LLC	20,688	163	No
26-Jul-2013	Geovera, LLC	20,497	199	Yes
4-Aug-2013	Geovera, LLC	20,069	44	Yes
9-Aug-2013	Geovera, LLC	16,879	2	No
18-Aug-2013	Geovera, LLC	16,900	1	No
20-Aug-2013	Tetra Tech, Inc.	24,209	1	No
21-Aug-2013	Tetra Tech, Inc.	36,636	2	Yes
8-Sep-2013	Tetra Tech, Inc.	32,200	2	Yes
10-Sep-2013 ^A	Geovera, LLC	26,124	32	Yes
12-Sep-2013	Geovera, LLC	31,400	1	No
^A ADCP Measurements Collected				

Table 2.3-3. Comparison of the predicted and measured flows collected on September 10, 2013, when the discharge in the river was approximately 26,124 cfs.

Transect	Measured		Hydraulic Model			
	Flow (cfs)	% of Total Flow	Predicted (cfs)	% of Total Flow	Difference. (cfs)	% Difference
T1A	8,547	33	8,595	33	48	0.6
T1B	17,551	67	17,528	67	-23	-0.1
T2A	6,960	27	6,766	26	-194	-2.8
T2B	250	0.96	336	1.3	86	34.3
T2C	1,134	4.3	925	3.5	-209	-18.4
T2D	18,019	69	18,096	69	77	0.4
T3A	473	1.8	619	2.4	146	30.9
T3B	6,331	24	6,155	24	-176	-2.8
T3C	19,328	74	19,325	74	-3	0.0
T4A	No Meas.		0			
T4B	473	1.8	619	2.4	146	30.9
T4C	2,907	11.0	3,367	12.9	460	15.8
T4D	13,659	52	13,015	50	-644	-4.7
T4E	9,127	35	9,123	35	-4	0.0
T5	26,184	100	26,124	100	-60	-0.2
T6	250	1.0	328	1.3	78	31.1
T7	3.7	0.014	10.7	0.041	7	190

Table 2.3-4. Comparison of the predicted and measured flows collected on July 2, 2013, when the discharge in the river was approximately 24,690 cfs.

Transect	Measured		Hydraulic Model			
	Flow (cfs)	% of Total Flow	Predicted (cfs)	% of Total Flow	Difference (cfs)	% Difference
T1A	7,520	30	7,703	31	183	2.4
T1B	17,197	70	16,998	69	-199	-1.2
T2A	6,204	25	6,150	25	-54	-0.9
T2B	236	1.0	272	1.1	22	8.9
T2C	766	3.1	779	3.2	13	1.6
T2D	17,710	72	17,500	71	-210	-1.2
T3A	379	1.5	427	2	48	12.6
T3B	5,843	24	5,741	23	-102	-1.7
T3C	18,413	75	18,532	75	118	0.6
T4A	9	0.04	15	0.1	6	62.5
T4B	374	1.5	412	1.7	38	10.3
T4C	2,629	11	3,063	12	434	16.5
T4D	12,818	52	12,502	51	-316	-2.5
T4E	8,745	35	8,713	35	-32	-0.4
T5	24,538	99	24,690	100	153	0.6
T6	231	0.9	255	1.0	24	10.5
T7	3.0	0.01	0.0	0.00	-3	-100

Table 2.3-5. Summary of difference in velocity calibration statistics (predicted minus measured, ft/s).

Statistic	2 July 2013	10 September 2013
Average	0.02	0.03
Median	0.01	0.06
Std.Dev	0.92	0.97
Minimum	-3.85	-5.74
Maximum	4.21	4.70
R ²	0.885	0.852

Table 2.3-6. Results of hydraulic model calibration/validation.

Model Run	Discharge (cfs)	Average Difference (ft) (predicted – measured)
4-Jun-13	54,203	0.66
2-Jul-13 ^A	24,705	0.11
24-Jul-13	20,132	-0.01
25-Jul-13	20,688	0.07
4-Aug-13	20,069	0.11
21-Aug-13	36,636	-0.07
8-Sep-13	32,200	-0.08
10-Sep-13 ^A	26,124	-0.30
^A ADCP Measurements Collected		

Table 2.3-7. Additional flow sources and water-surface elevations applied to the model.

River Discharge (cfs)	Point Source Flow (cfs)				WSE (feet)
	A	D	H	J	J
2,000	4	0	10		568.5
4,000	4	0	0		568.5
6,000	4	1	0		568.5
8,000	4	3	0		568.5
12,000	4	0	0		568.7
16,000	4	0	0		569.6
22,000	8	0	0	1	
30,000	23	0	0	2	
50,000	0	0	0	3	

Table 2.4-1. Summary of SRH-2D model output provided to the IFS team.

Parameter	Parameter Description
Point_ID	Element ID
Area_ft^2	Area of element (square ft)
Centroid_X_ft	Easting coordinate of element centroid (ft)
Centroid_Y_ft	Northing coordinate of element centroid (ft)
Bed_Elev_ft	Elevation of element centroid (ft)
Water_Elev_ft	Water surface elevation (ft)
Water_Depth_ft	Water depth (ft)
Vel_X_ft_p_s	Velocity component in the X-direction (ft/s)
Vel_Y_ft_p_s	Velocity component in the Y-direction (ft/s)
Vel_Mag_ft_p_s	Velocity magnitude (ft/s)
Froude	Froude number
Strs_lb_p_ft2	Shear Stress (lb/ft ²)
Dcrit_mm	Particle size of incipient motion (mm) - Shields Parameter = 0.045
Bed_Strs_lb_p_ft2	Bed Shear Stress (lb/ft ²)
Dcrit_Bed_Strs_mm	Particle size of incipient motion from bed shear stress (mm) - Shields Parameter = 0.045 and Manning n of 0.03

5 FIGURES

This page intentionally left blank

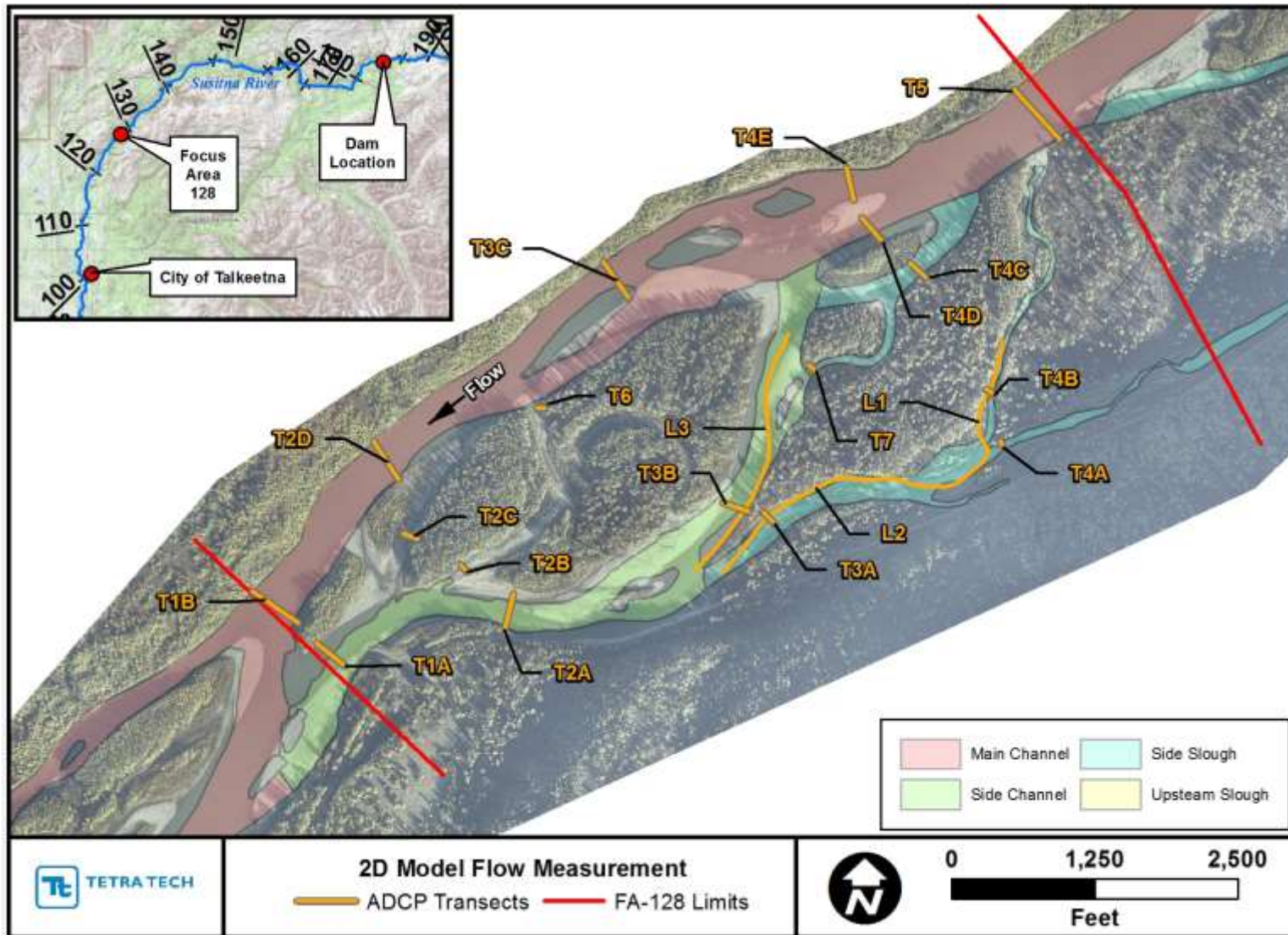


Figure 1-1. FA-128 (Slough 8A) site location map and location of ADCP transects.

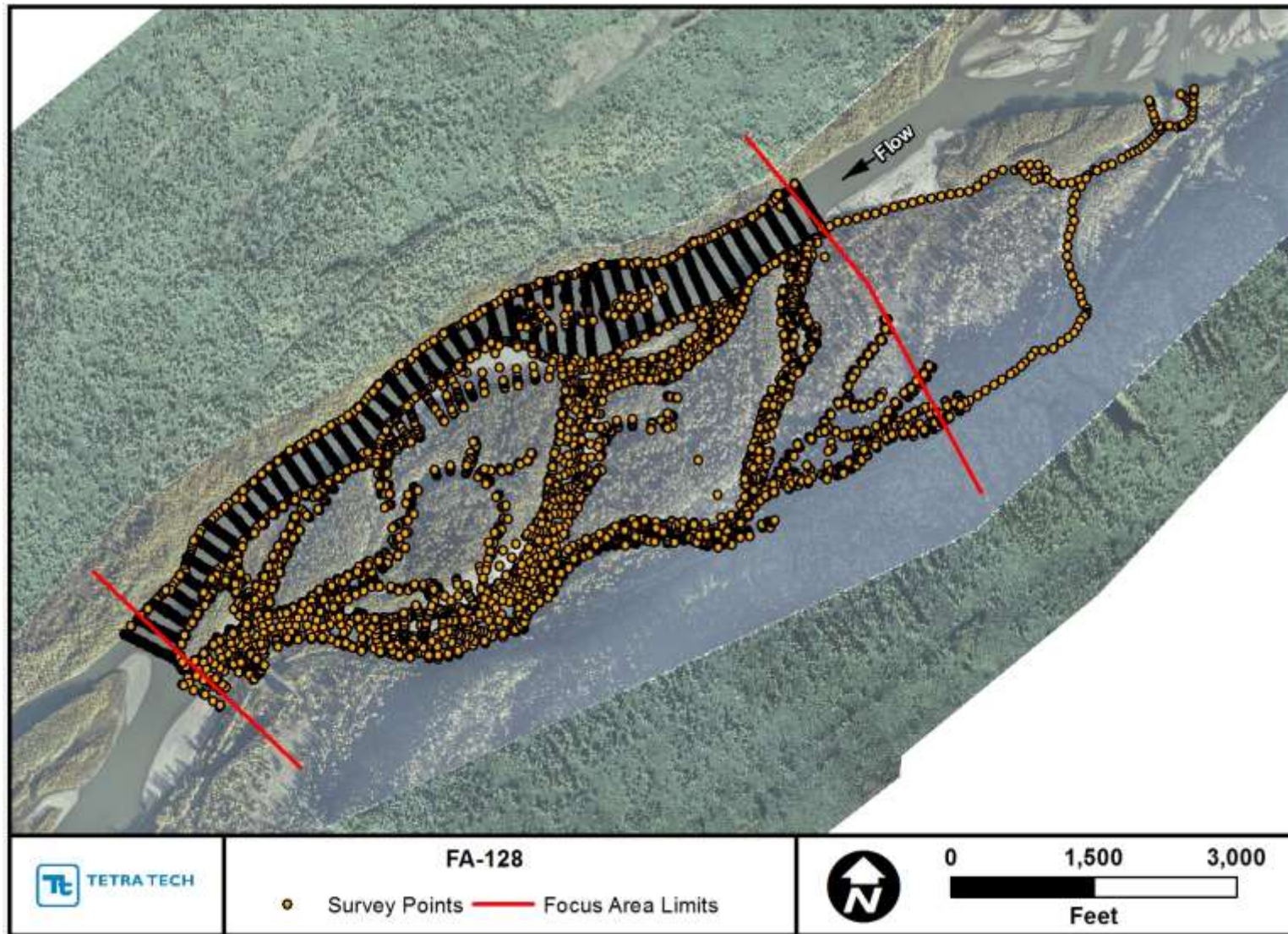


Figure 2.2-1. Bathymetric and topographic survey data for FA-128 (Slough 8A).



Figure 2.2-2. Triangulated Irregular Network (TIN) developed for the in-channel areas of FA-128 (Slough 8A) using the topographic and bathymetric data shown in Figure 2.2-3.

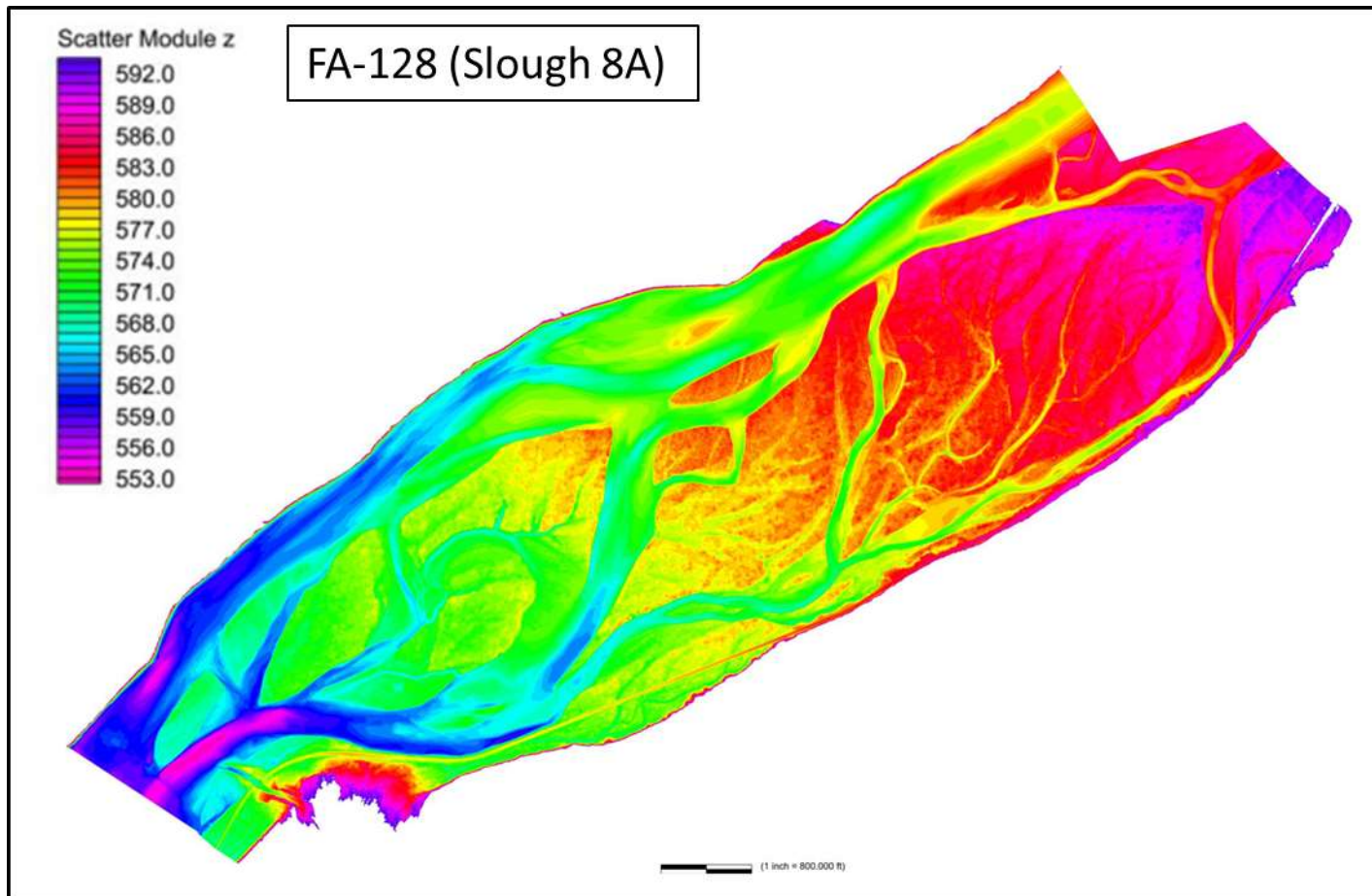


Figure 2.2-3. TIN topography including LiDAR in the overbank areas of FA-128 (Slough 8A).

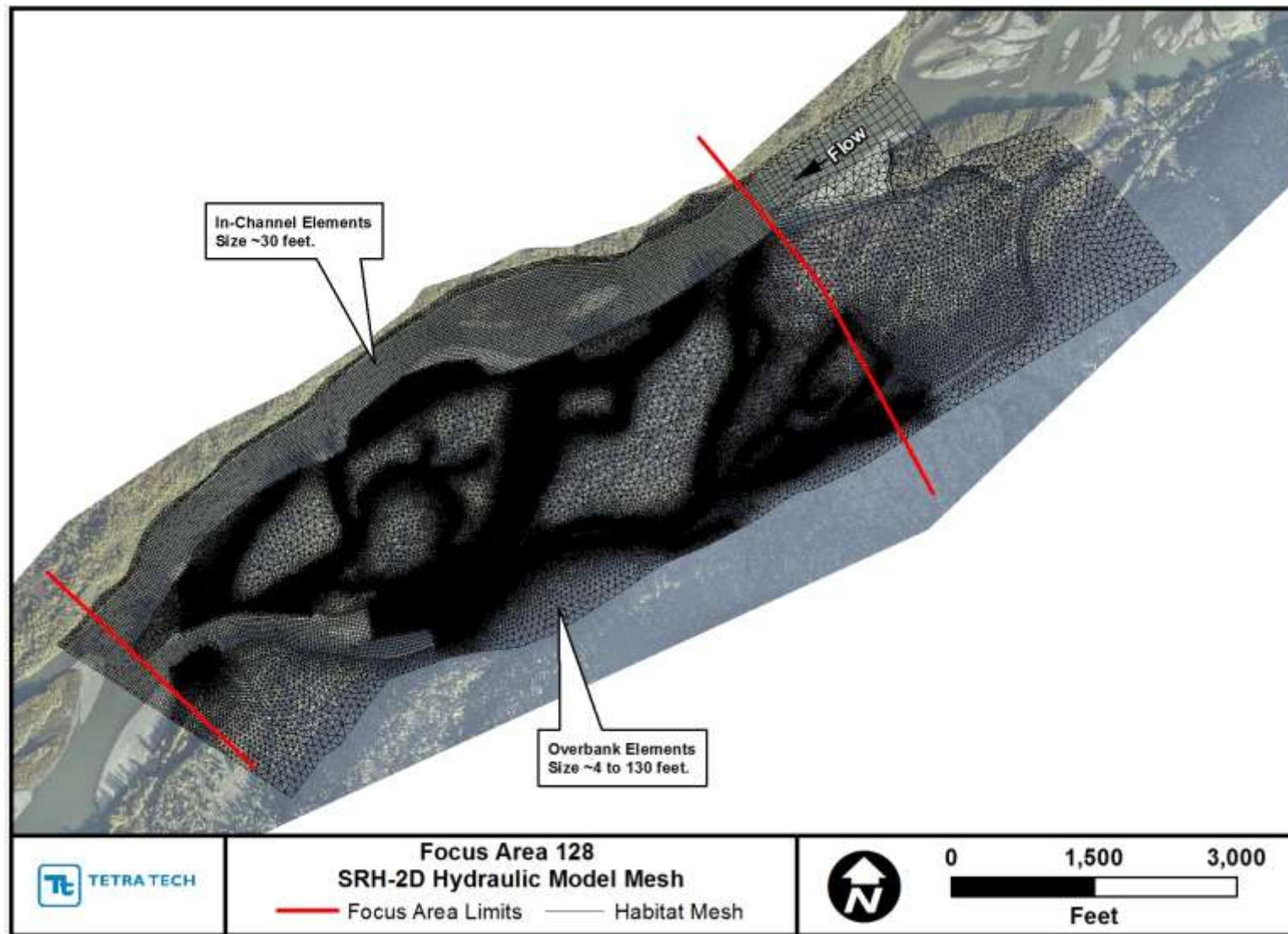


Figure 2.2-4. FA-128 (Slough 8A) SRH-2D hydraulic model mesh.

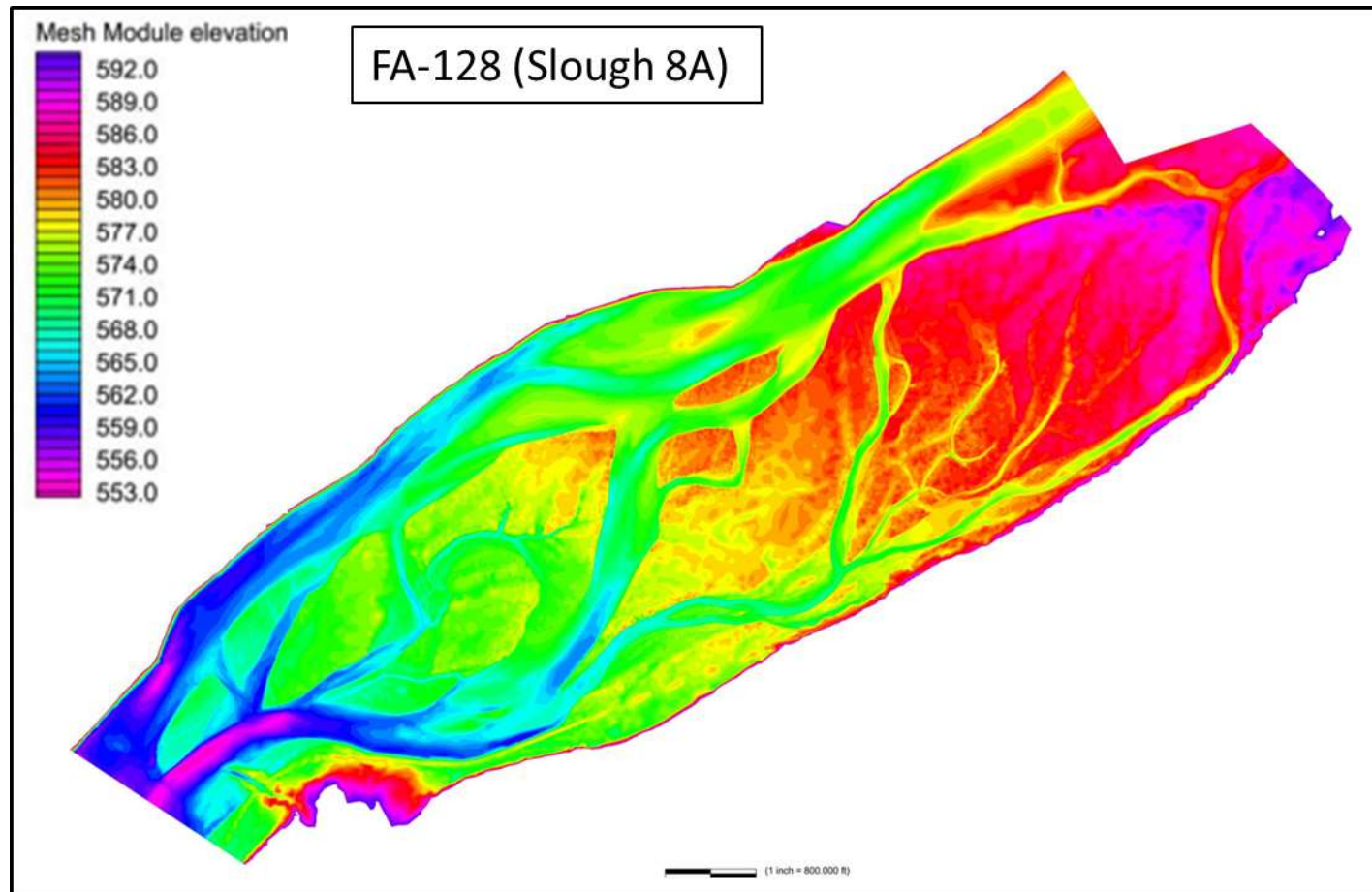


Figure 2.2-5. FA-128 (Slough 8A) SRH-2D hydraulic model topography.

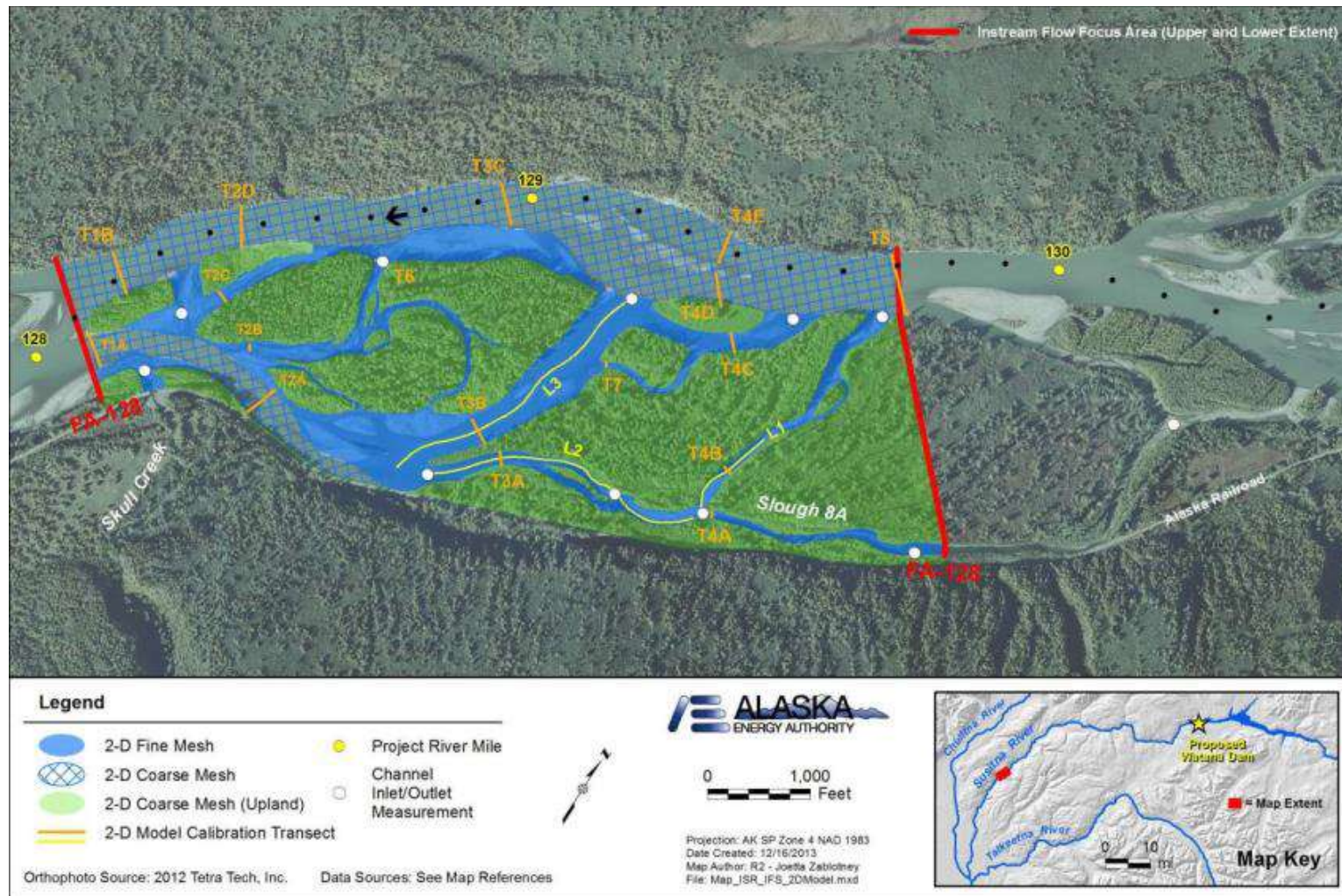


Figure 2.2-6. Fine and coarse mesh areas in FA-128 (Slough 8A) delineated by the Instream Flow Study team (copied from ISR8.5 Figure 5.6-4).



Figure 2.2-7. Close-up of a portion of the FA-128 (Slough 8A) SRH-2D hydraulic model mesh.

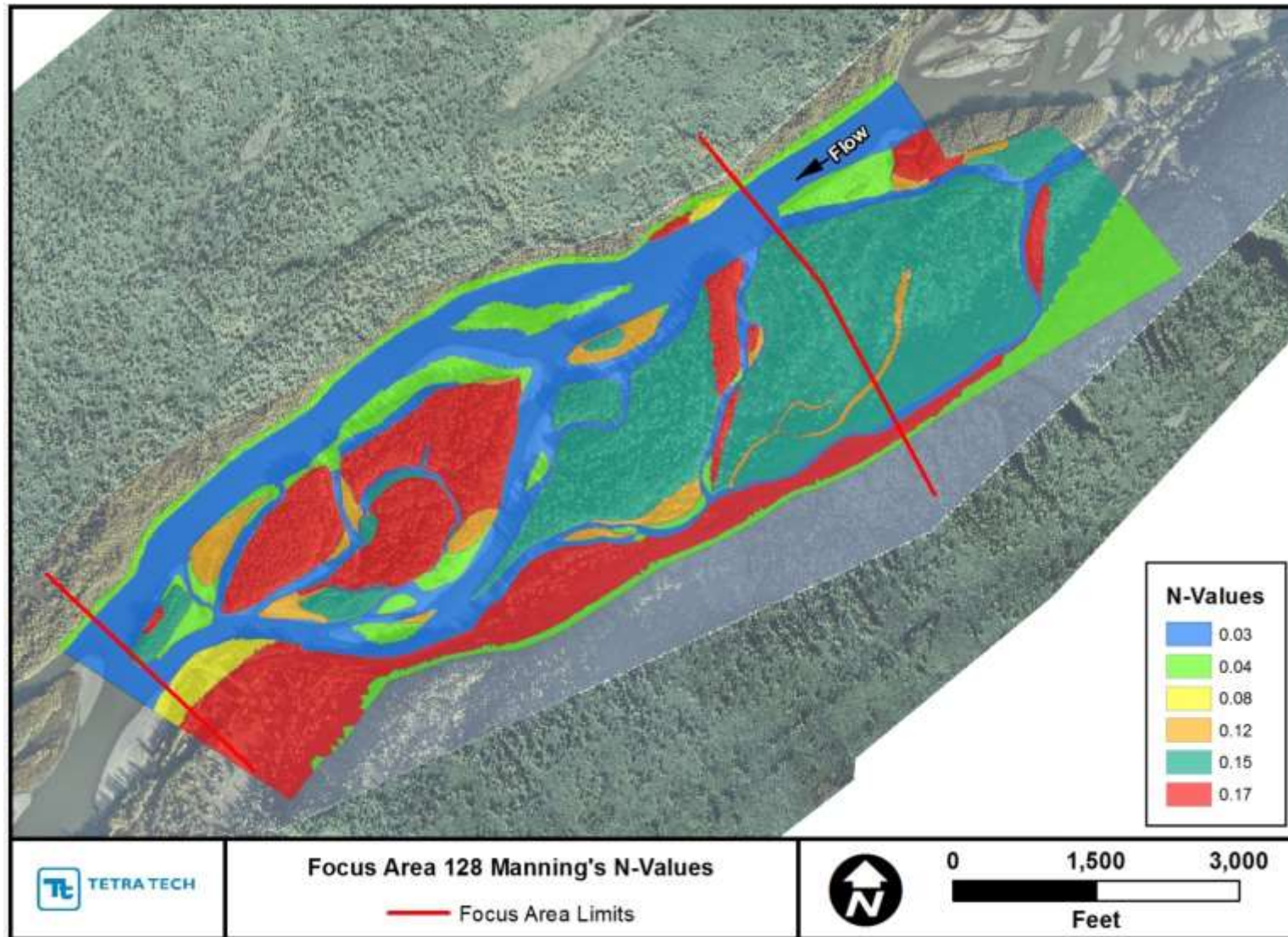


Figure 2.2-8. Manning n -values applied to the SRH-2D models in FA-128 (Slough 8A).

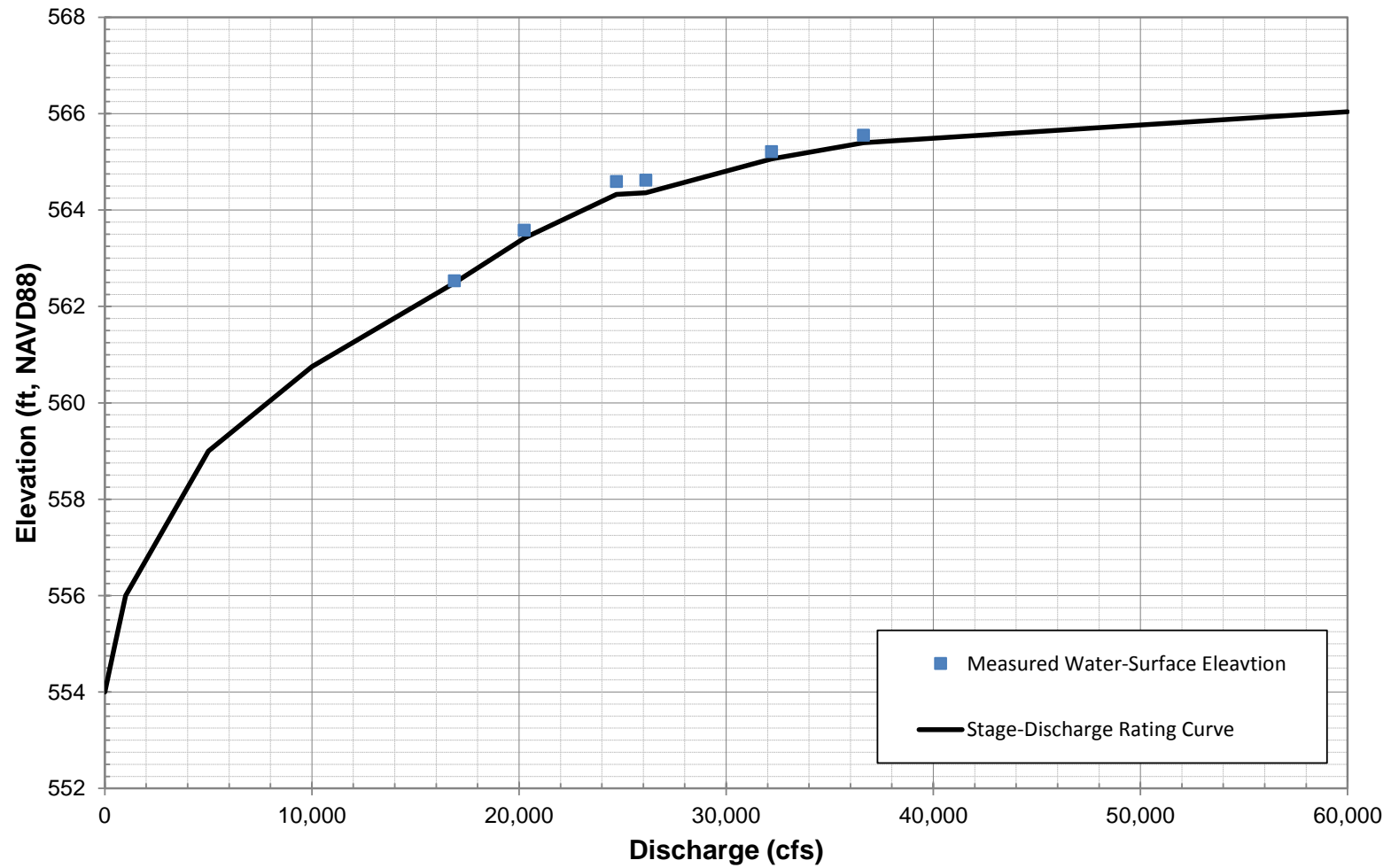


Figure 2.2-9. Stage-Discharge rating curve applied to the downstream boundary of the 2-D model in FA-128 (Slough 8A).

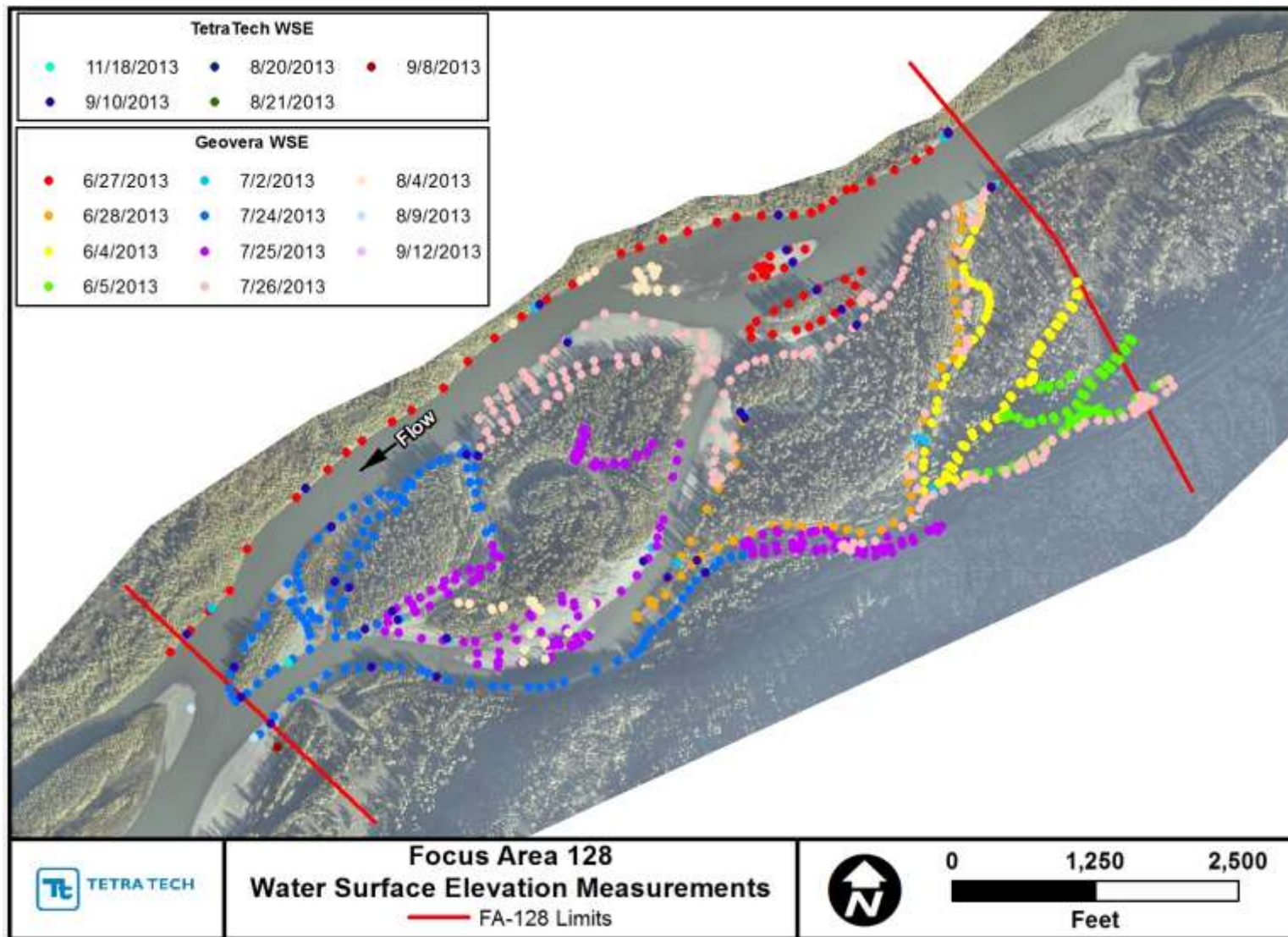


Figure 2.2-10 Location of the measured water-surface elevations (WSEs) in FA-128 (Slough 8A).

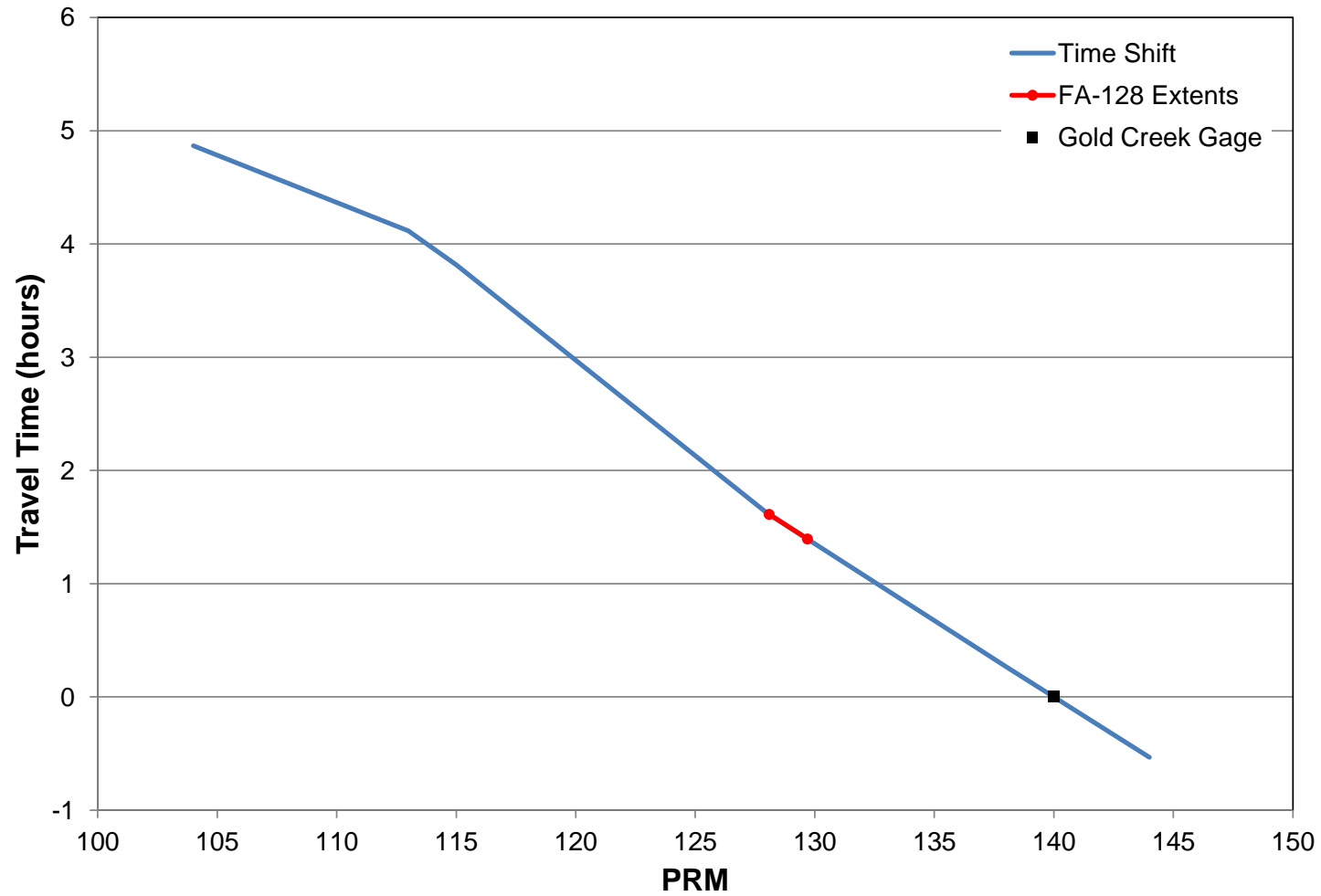


Figure 2.3-1 Flow travel time along the middle reach from Gold Creek gage. The travel times at each Focus Area are reported in ISR 8.5.

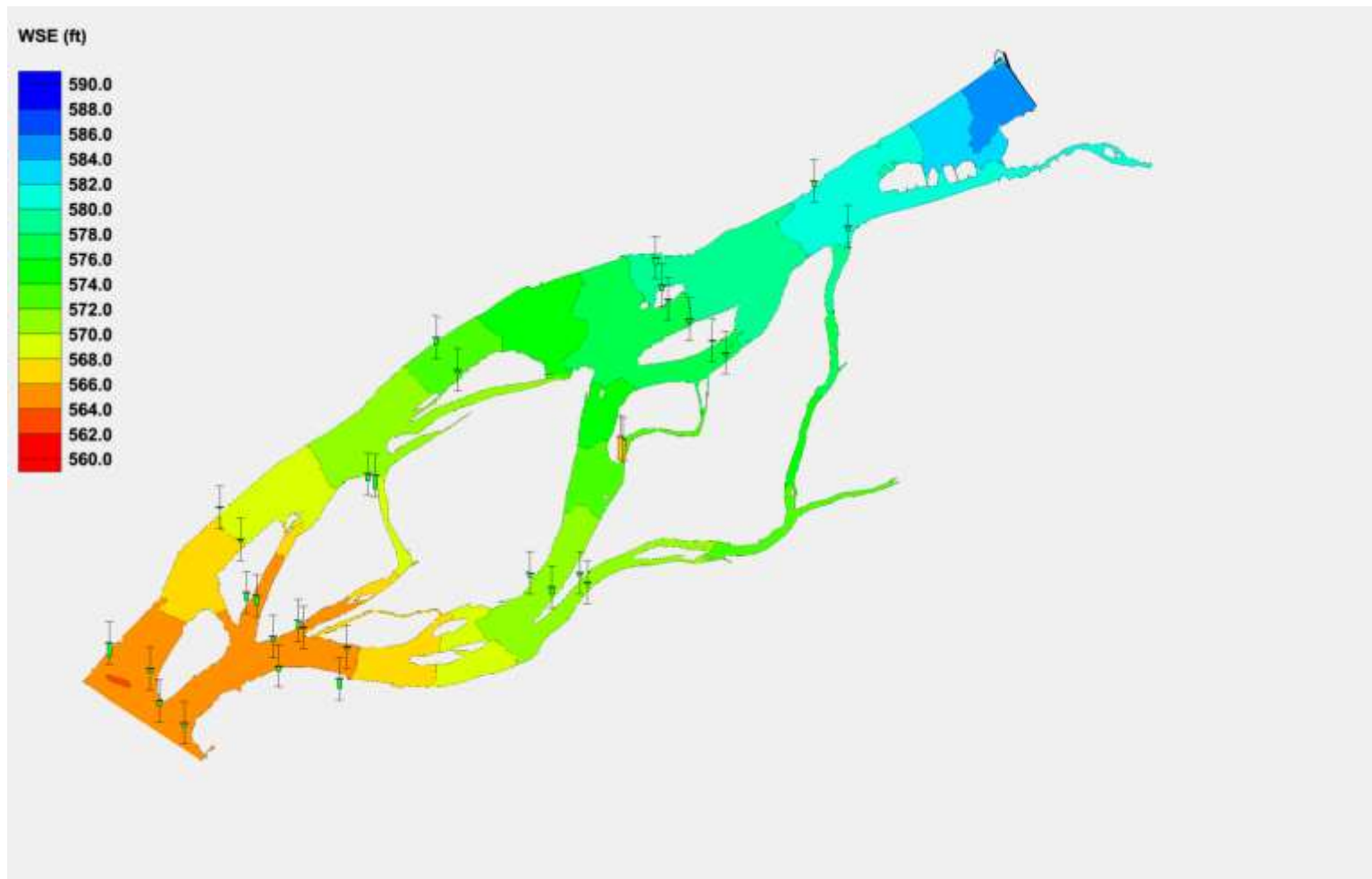


Figure 2.3-2. Screen capture from SMS showing differences between the measured and predicted water-surface elevations from the hydraulic model at 26,124 cfs (September 10, 2013) in FA-128 (Slough 8A). The bars indicate the relative differences in water-surface elevations in the direction of the error. For example, if the color is in the lower half, then the predicted water-surface elevation is lower than the measured values. Green bars indicate differences of less than 1 foot, orange bars indicate differences greater than 1 foot.

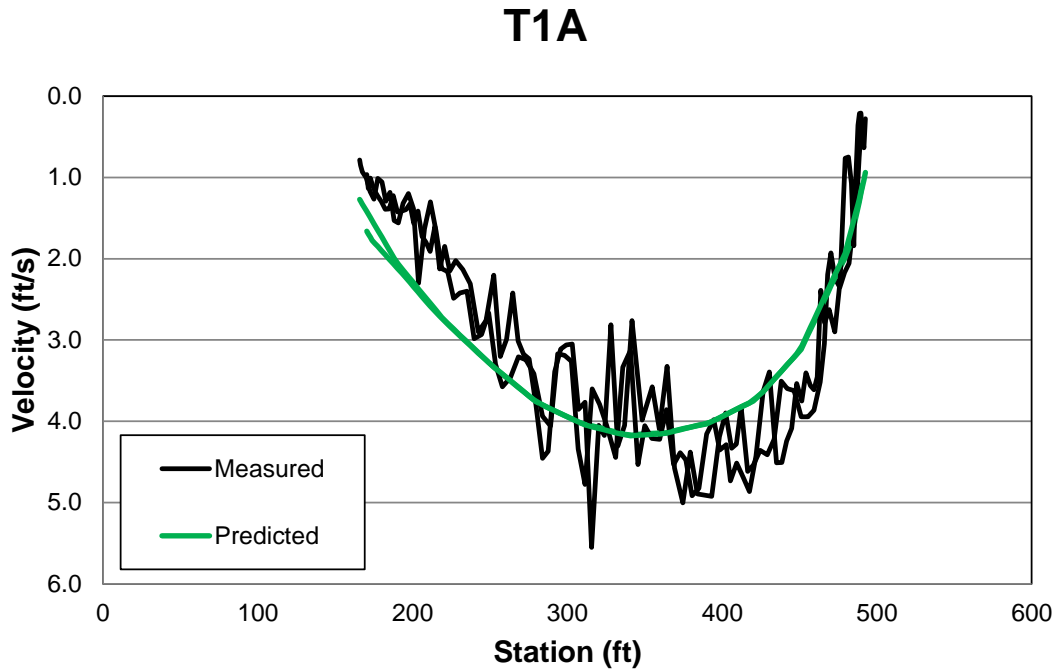


Figure 2.3-3. Comparison of measured velocities with the predicted velocities at Transect 1A at 26,184 cfs (Sep 10, 2013).

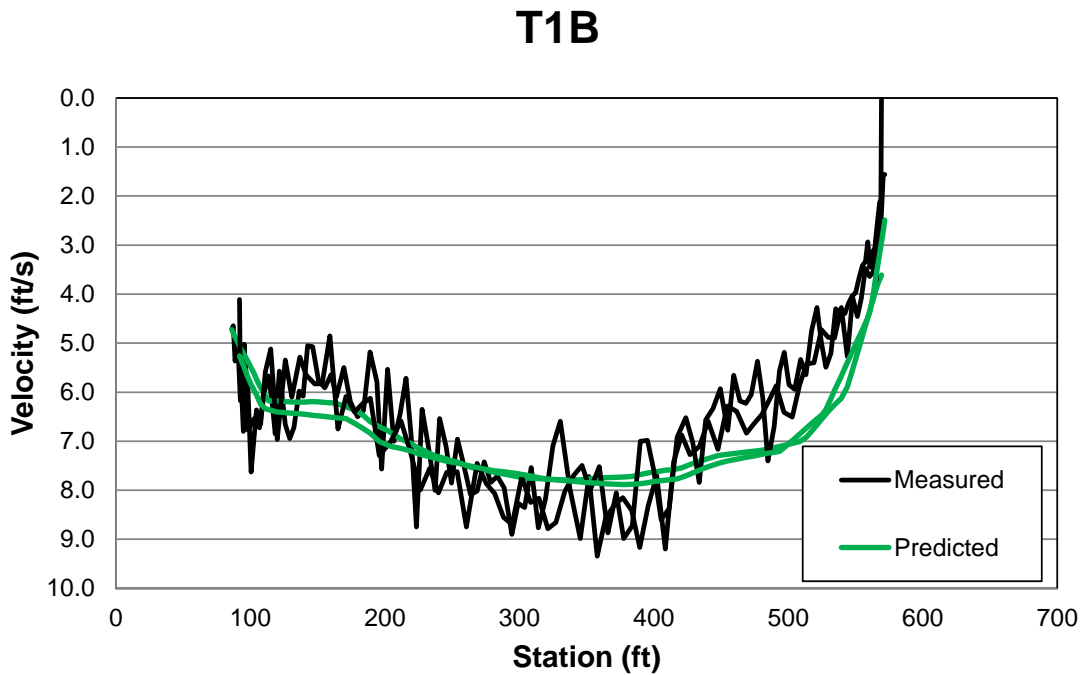


Figure 2.3-4. Comparison of measured velocities with the predicted velocities at Transect 1B at 26,184 cfs (Sep 10, 2013).

T2A

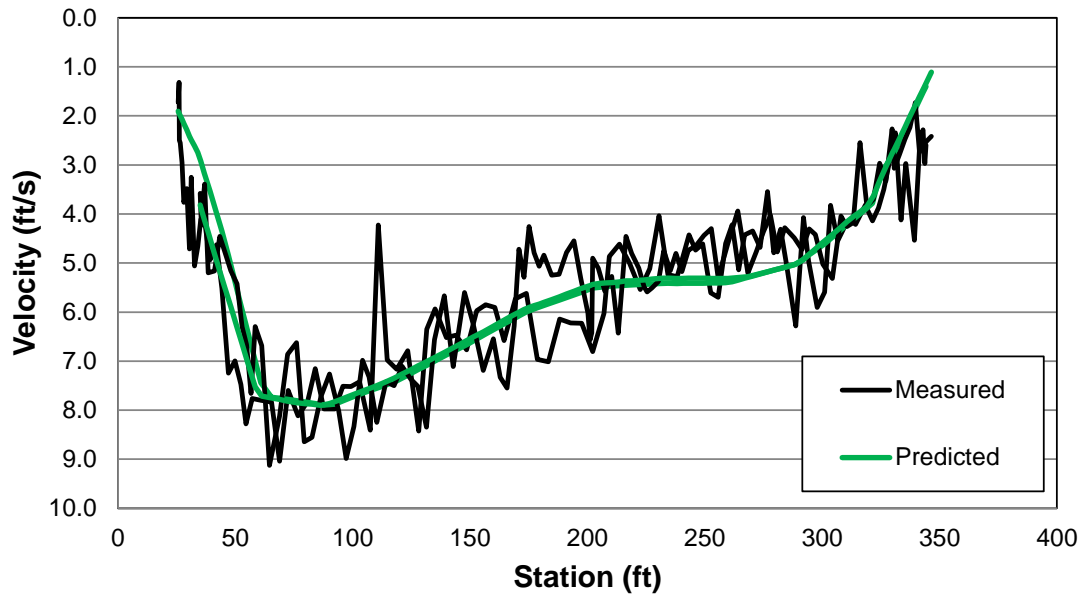


Figure 2.3-5. Comparison of measured velocities with the predicted velocities at Transect 2A at 26,184 cfs (Sep 10, 2013).

T2B

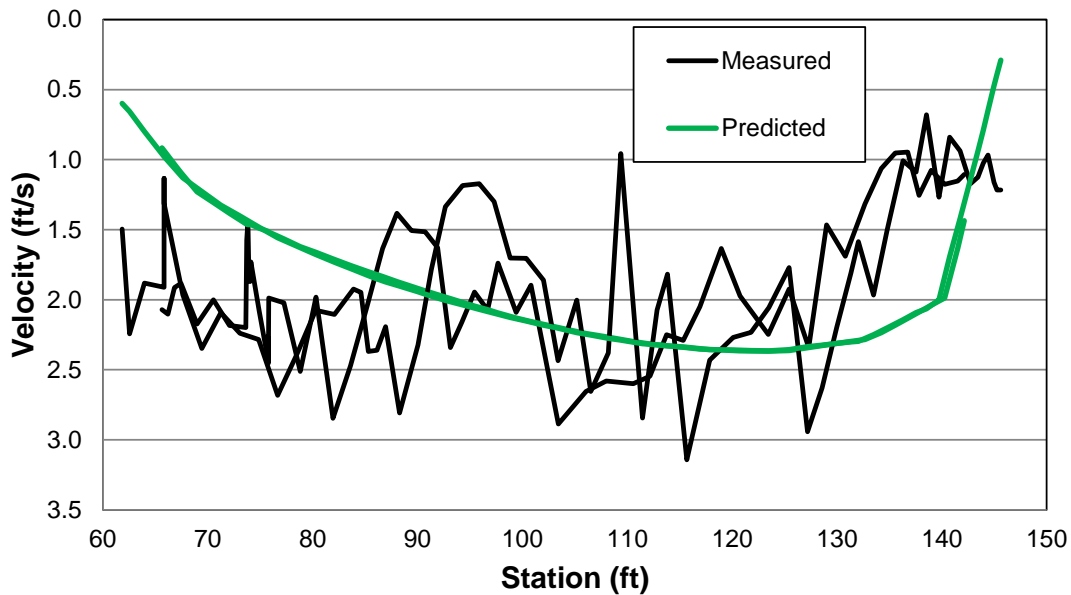


Figure 2.3-6. Comparison of measured velocities with the predicted velocities at Transect 2B at 26,184 cfs (Sep 10, 2013).

T2C

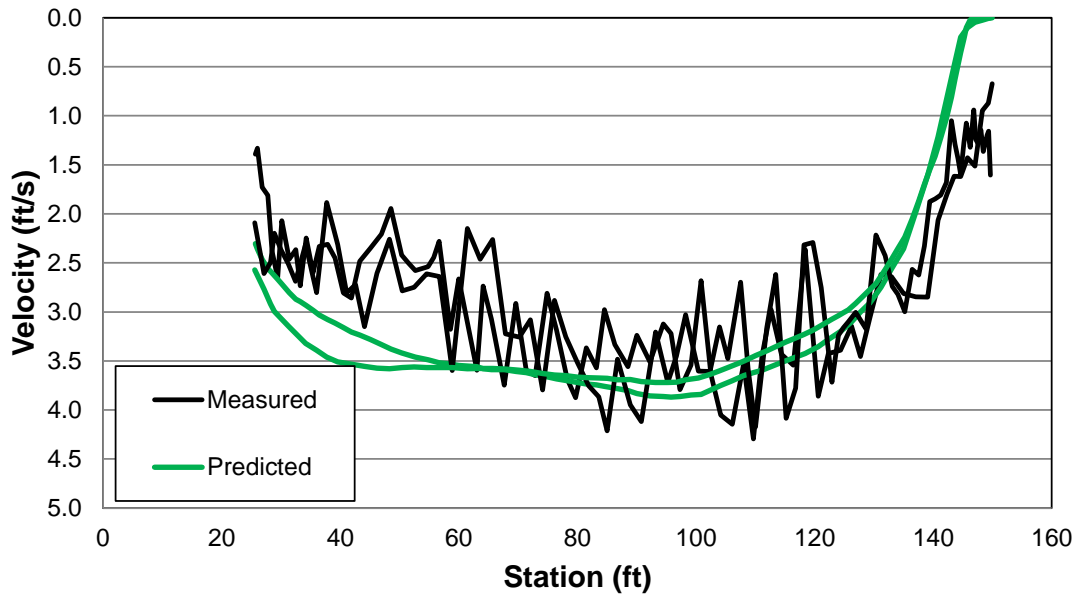


Figure 2.3-7. Comparison of measured velocities with the predicted velocities at Transect 2C at 26,184 cfs (Sep 10, 2013).

T2D

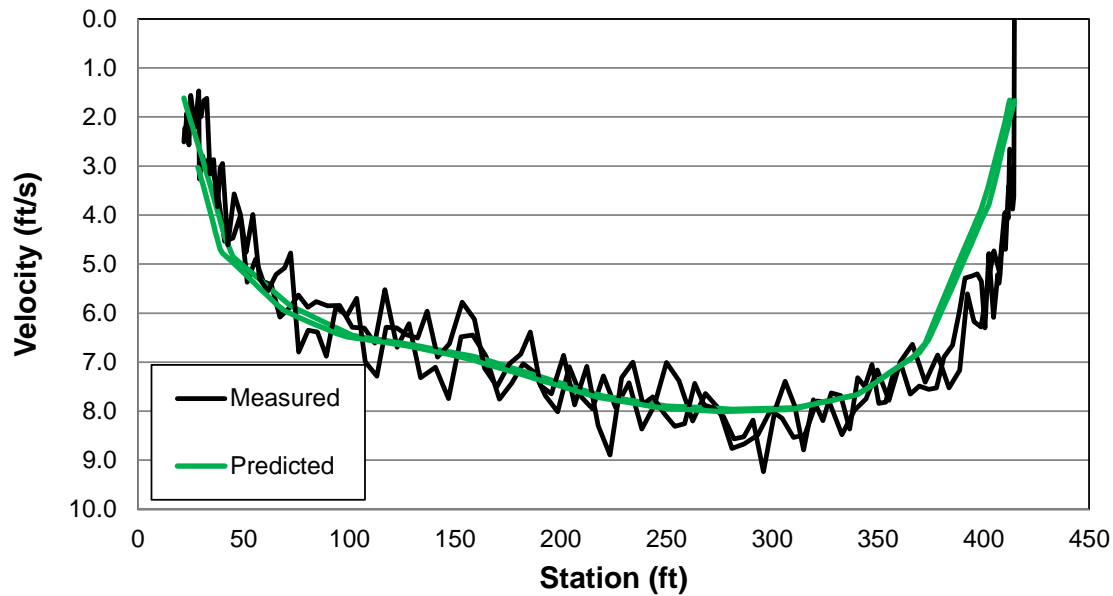


Figure 2.3-8. Comparison of measured velocities with the predicted velocities at Transect 2D at 26,184 cfs (Sep 10, 2013).

T3A

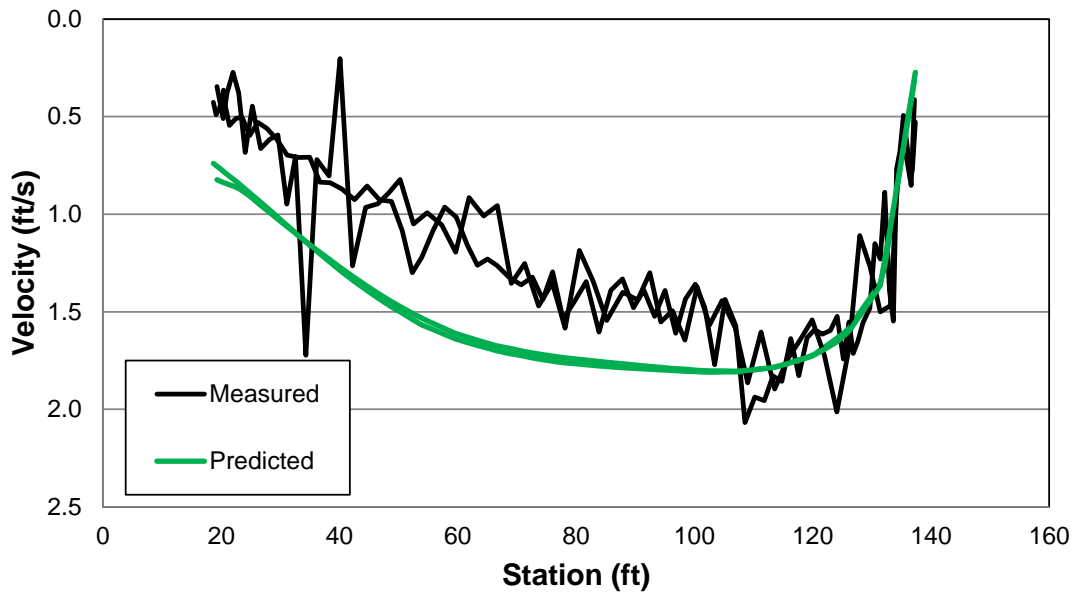


Figure 2.3-9. Comparison of measured velocities with the predicted velocities at Transect 3A at 26,184 cfs (Sep 10, 2013).

T3B

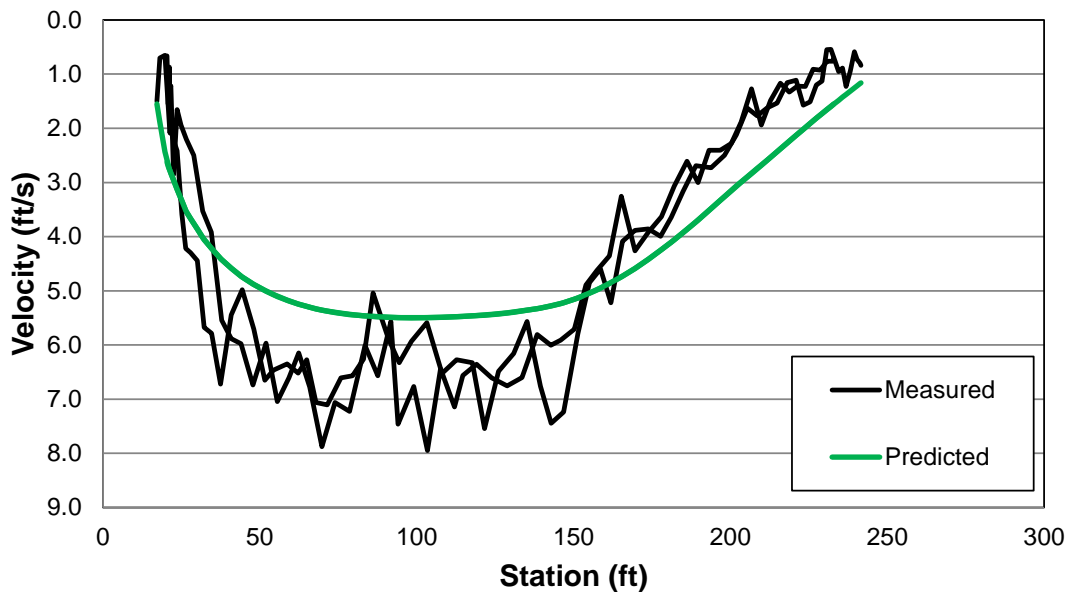


Figure 2.3-10. Comparison of measured velocities with the predicted velocities at Transect 3B at 26,184 cfs (Sep 10, 2013).

T3C

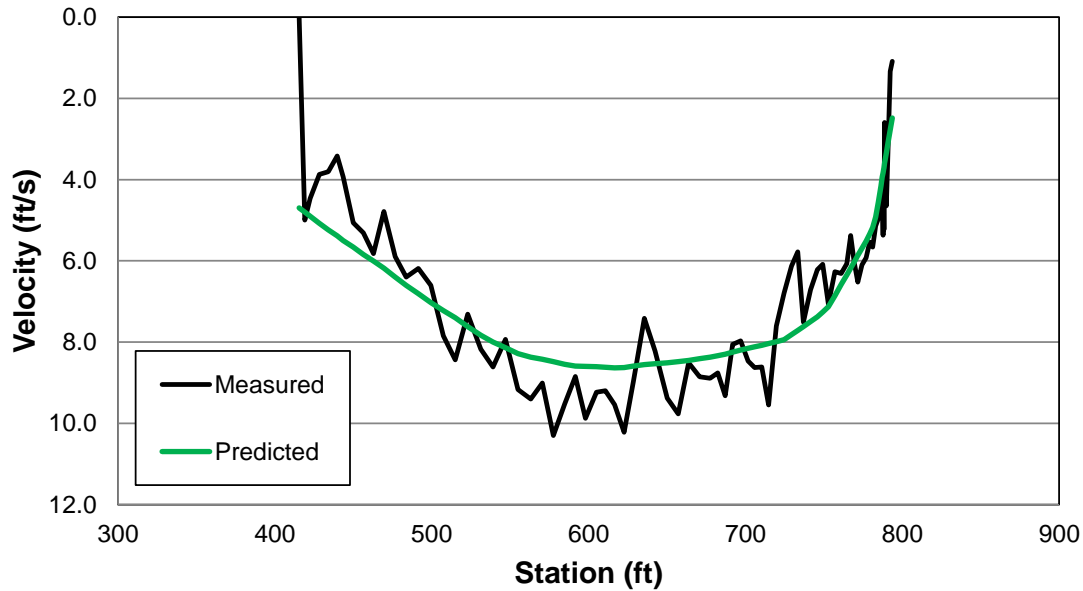


Figure 2.3-11. Comparison of measured velocities with the predicted velocities at Transect 3C at 26,184 cfs (Sep 10, 2013).

T4C

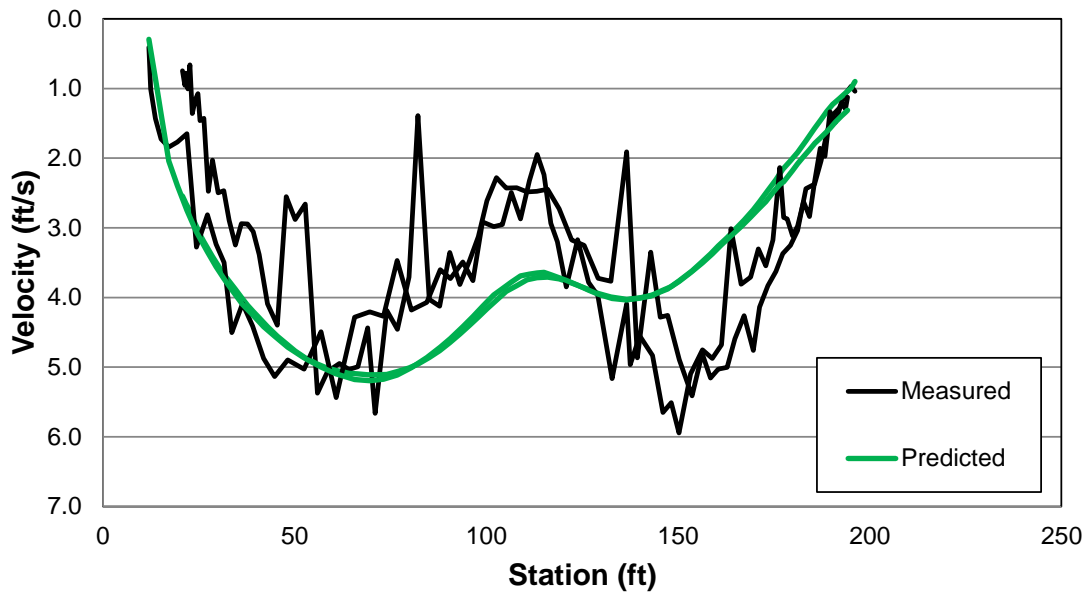


Figure 2.3-12. Comparison of measured velocities with the predicted velocities at Transect 4C at 26,184 cfs (Sep 10, 2013).

T4D

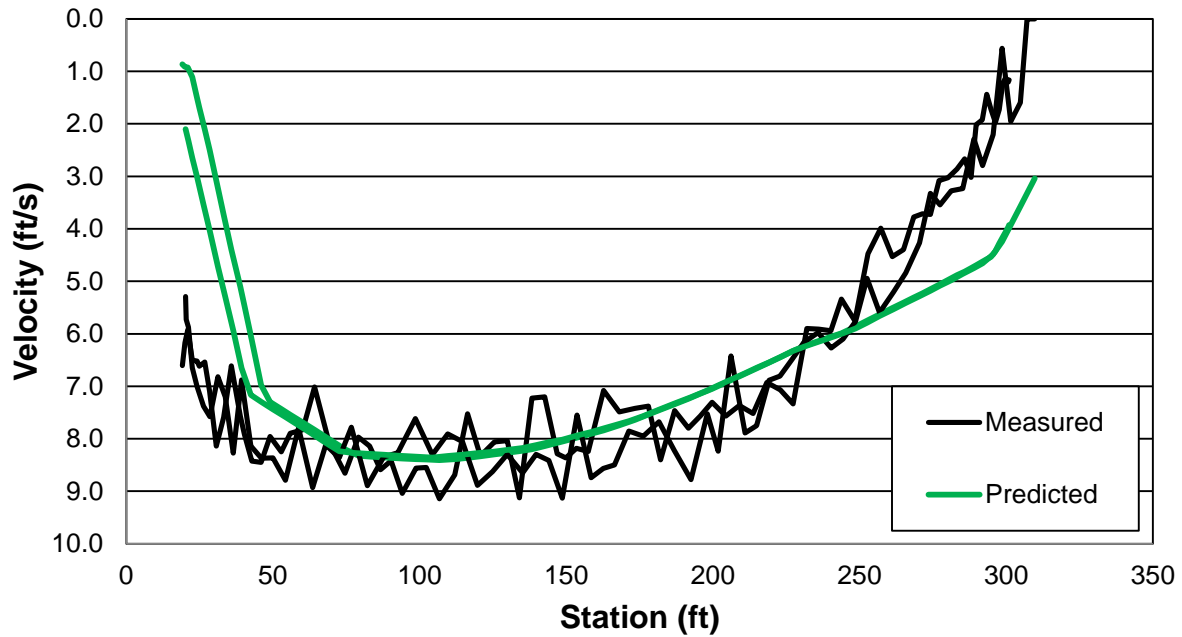


Figure 2.3-13. Comparison of measured velocities with the predicted velocities at Transect 4D at 26,184 cfs (Sep 10, 2013).

T4E

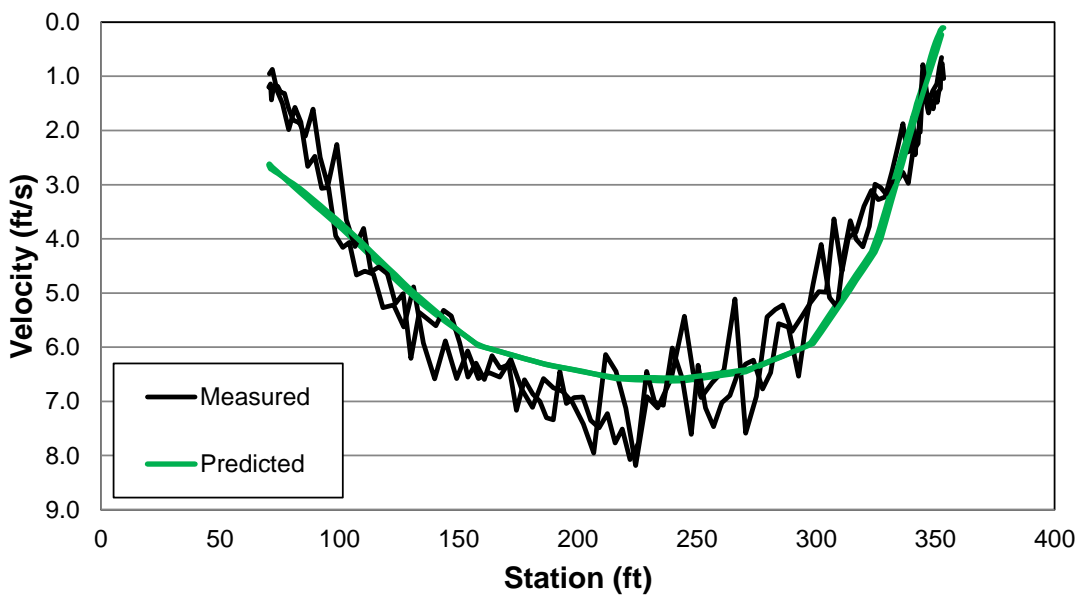


Figure 2.3-14. Comparison of measured velocities with the predicted velocities at Transect 4E at 26,184 cfs (Sep 10, 2013).

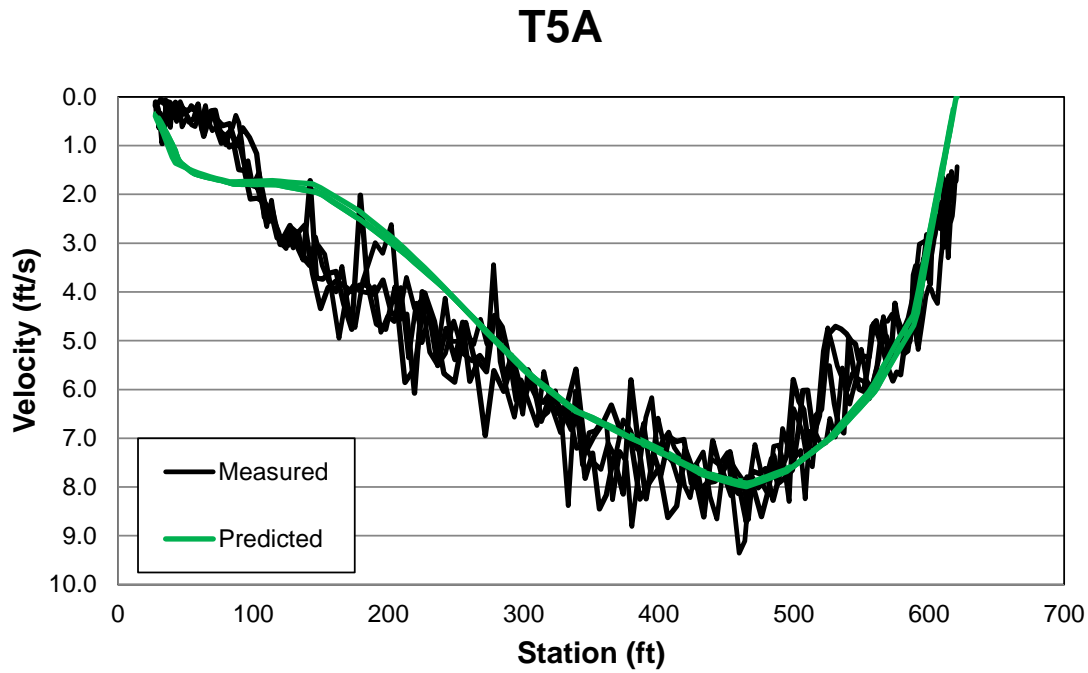


Figure 2.3-15. Comparison of measured velocities with the predicted velocities at Transect 5A at 26,184 cfs (Sep 10, 2013).

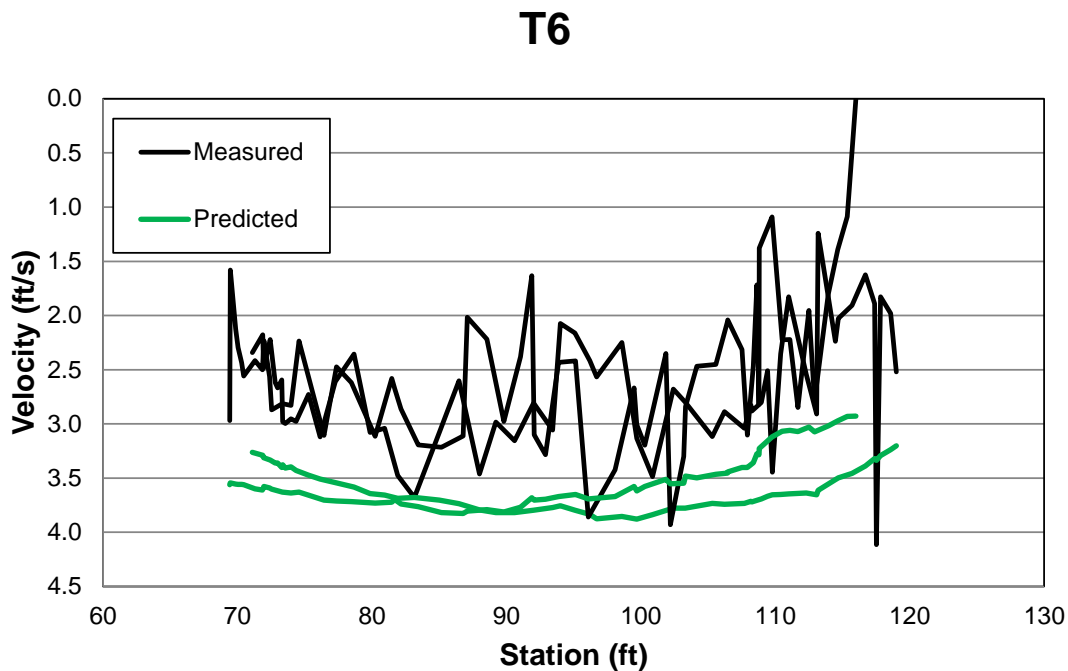


Figure 2.3-16. Comparison of measured velocities with the predicted velocities at Transect 6 at 26,184 cfs (Sep 10, 2013).

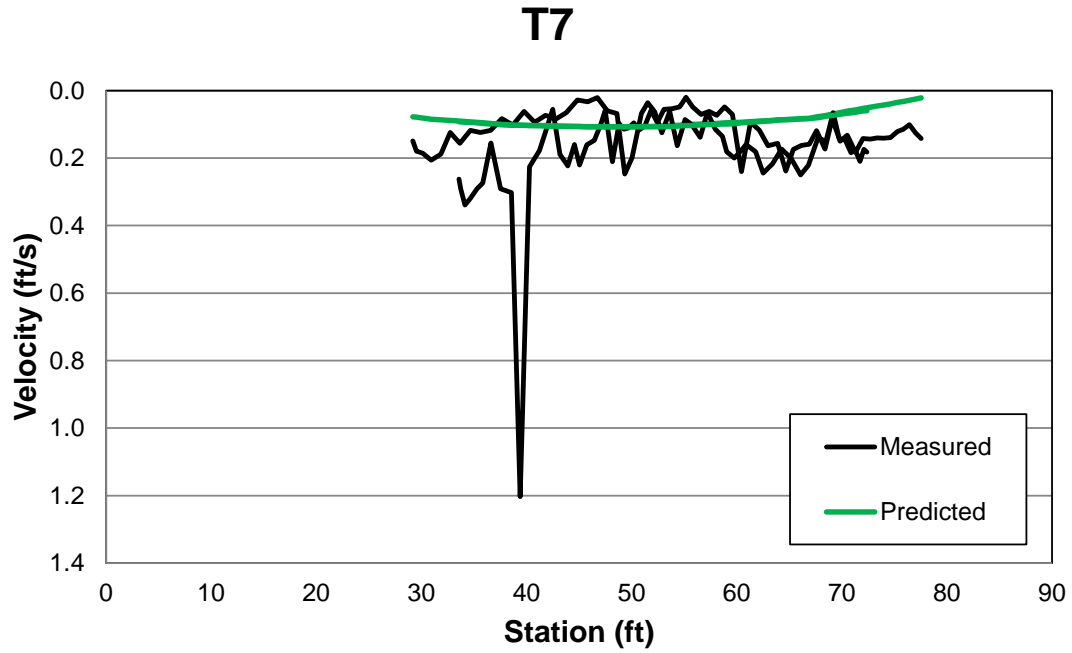


Figure 2.3-17. Comparison of measured velocities with the predicted velocities at Transect 7 at 26,184 cfs (Sep 10, 2013).

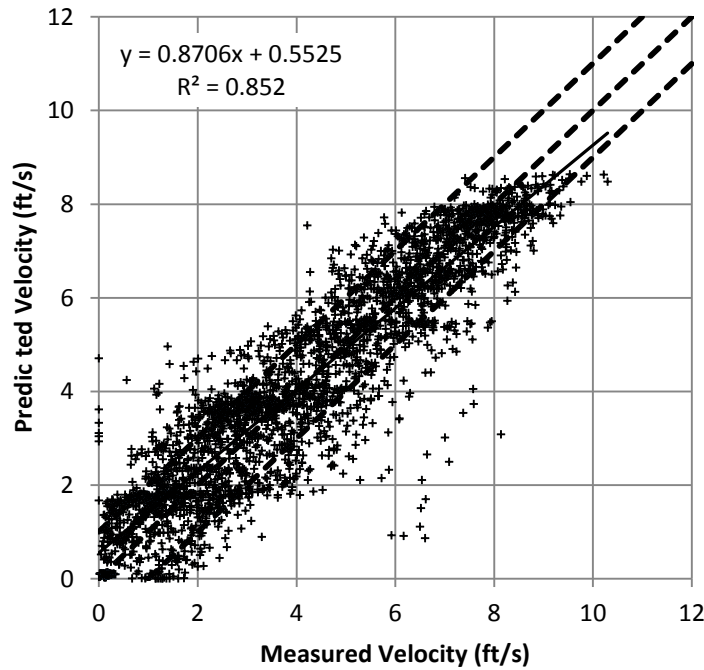


Figure 2.3-18. Scatter plot showing difference in velocity (predicted – measured) at 26,124 cfs (Sept. 10, 2013) FA-128 (Slough 8A).

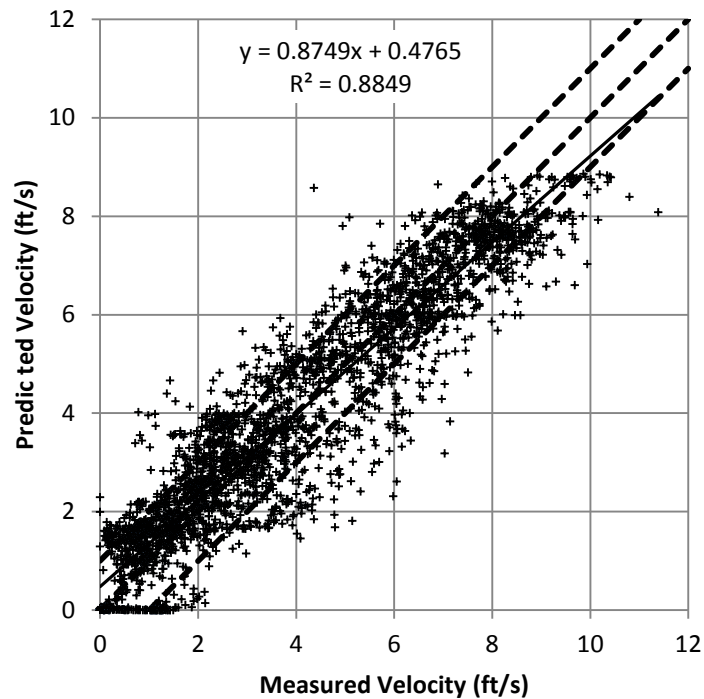


Figure 2.3-19. Scatter plot showing difference in velocity (predicted – measured) at 24,690 cfs (July 2, 2013) FA-128 (Slough 8A).

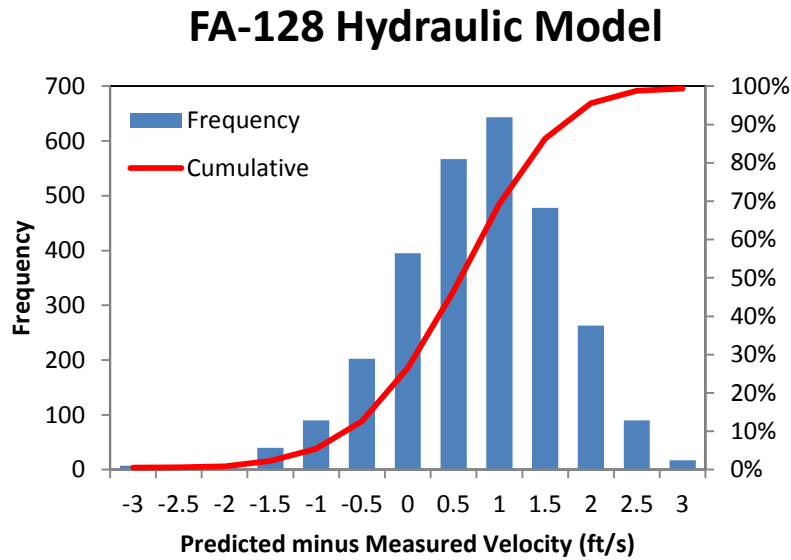


Figure 2.3-20. Distribution of difference in velocity (predicted – measured) at 26,124 cfs (Sept. 10, 2013) FA-128 (Slough 8A).

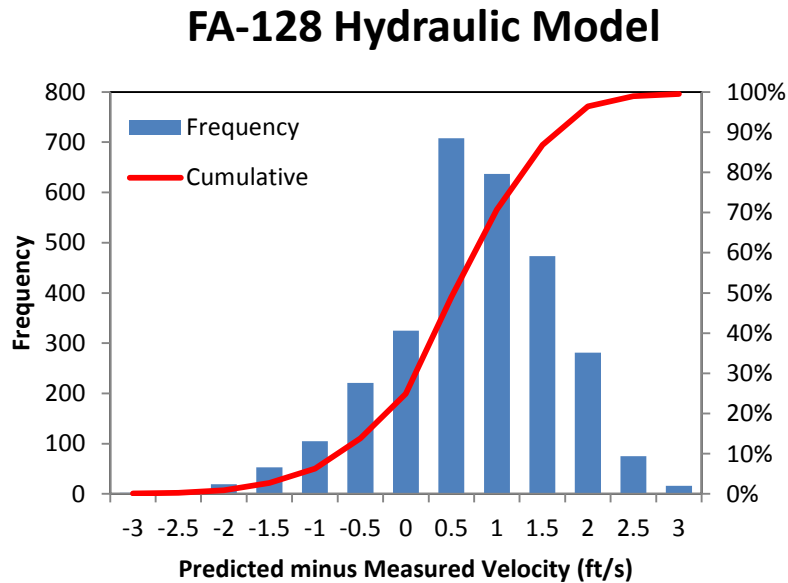


Figure 2.3-21. Distribution of difference in velocity (predicted – measured) at 24,690 cfs (July 2, 2013) FA-128 (Slough 8A).



Figure 2.3-22. Comparison of measured and predicted velocity magnitude and direction at Transect 1A at 26,184 cfs (Sep 10, 2013).

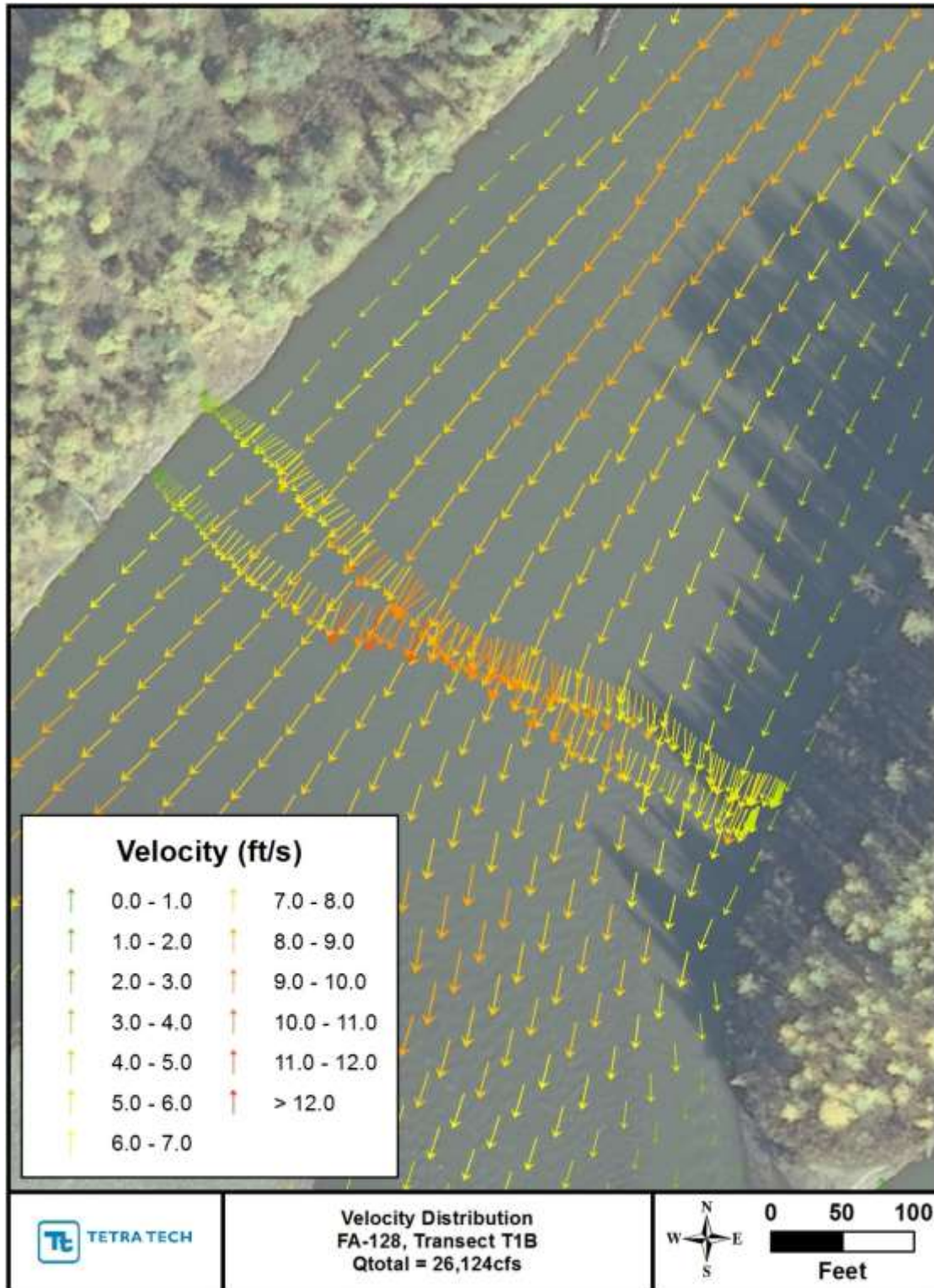


Figure 2.3-23. Comparison of measured and predicted velocity magnitude and direction at Transect 1B at 26,184 cfs (Sep 10, 2013).

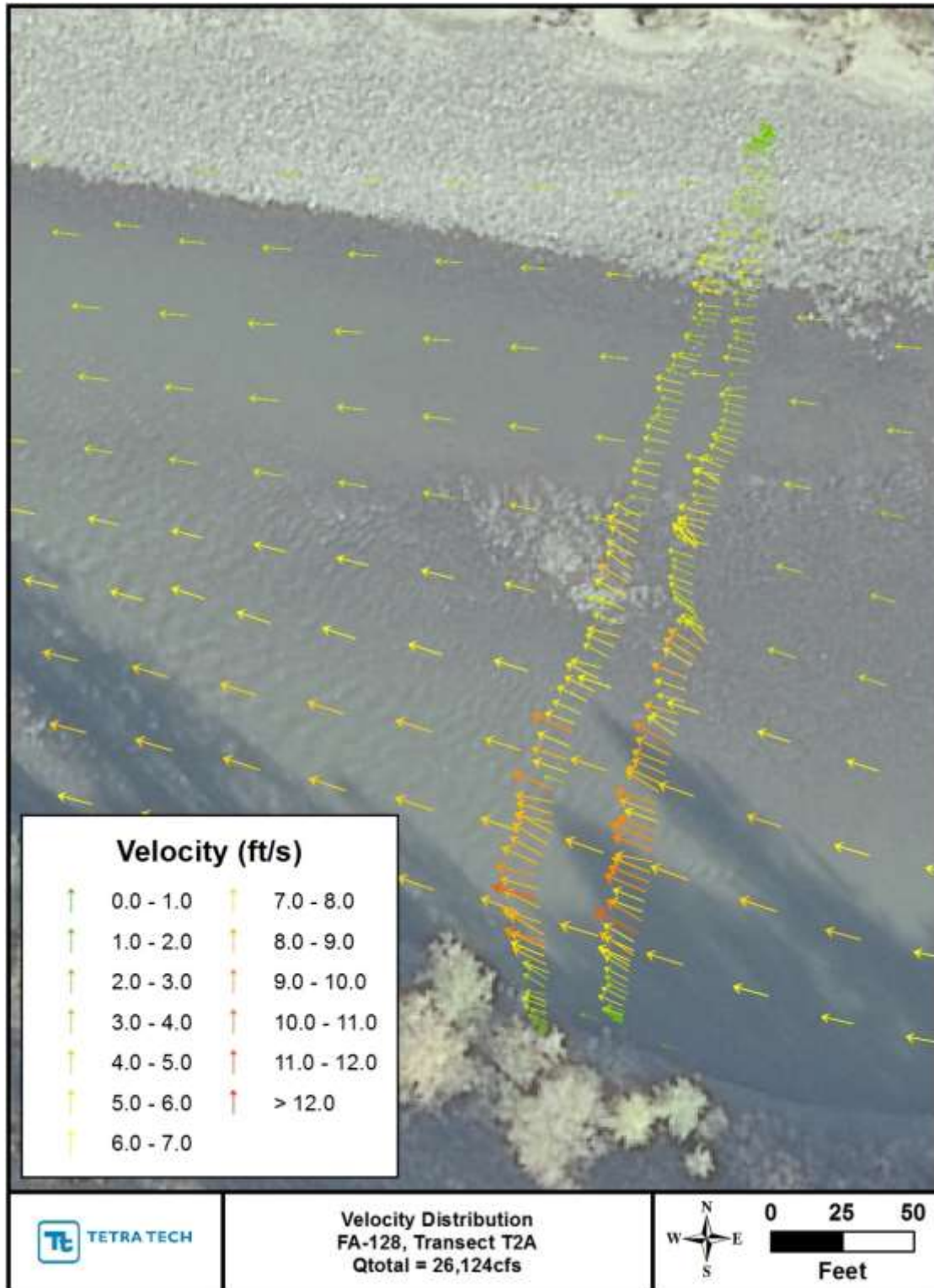


Figure 2.3-24. Comparison of measured and predicted velocity magnitude and direction at Transect 2A at 26,184 cfs (Sep 10, 2013).

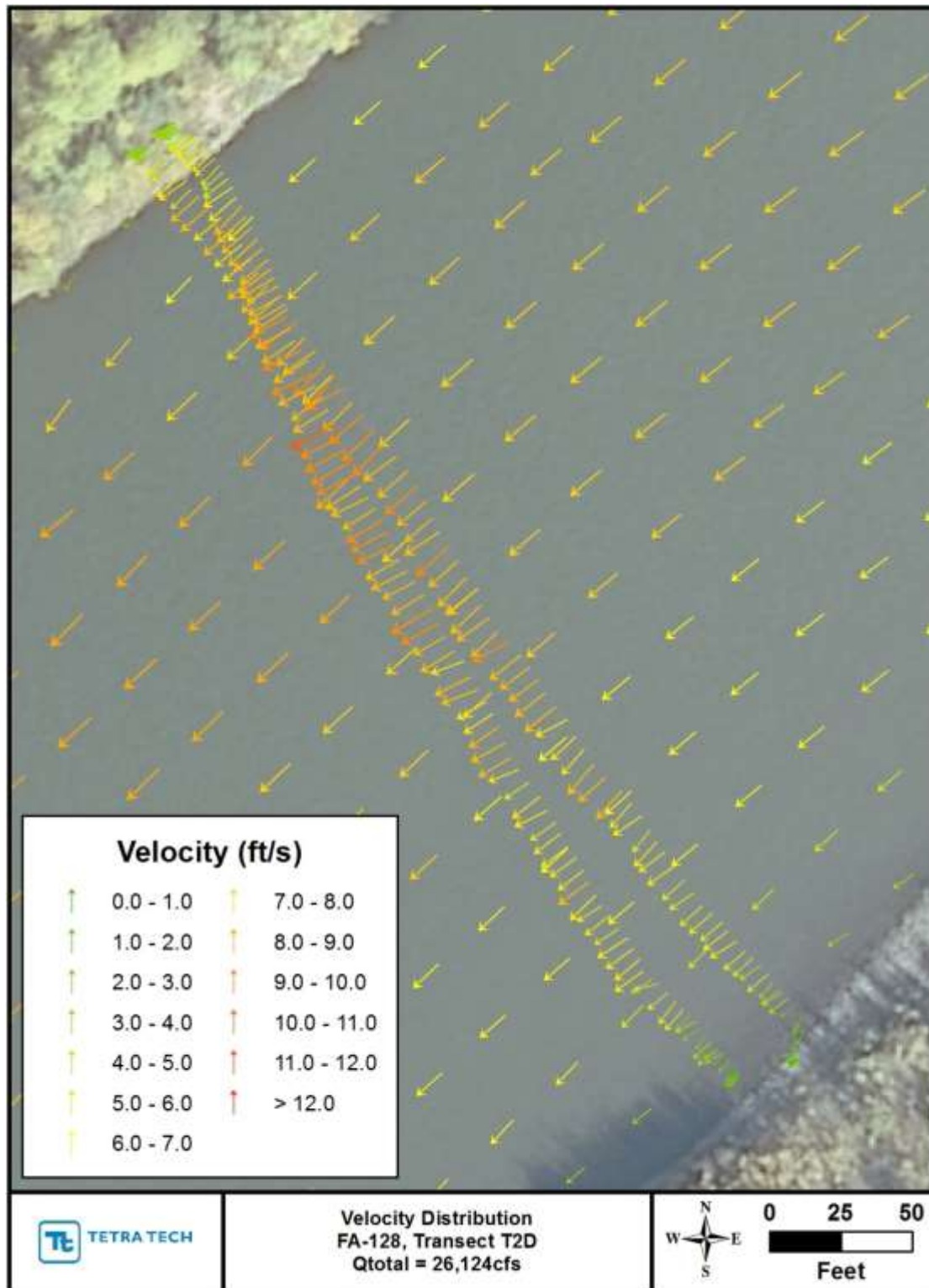


Figure 2.3-25. Comparison of measured and predicted velocity magnitude and direction at Transect 2D at 26,184 cfs (Sep 10, 2013).

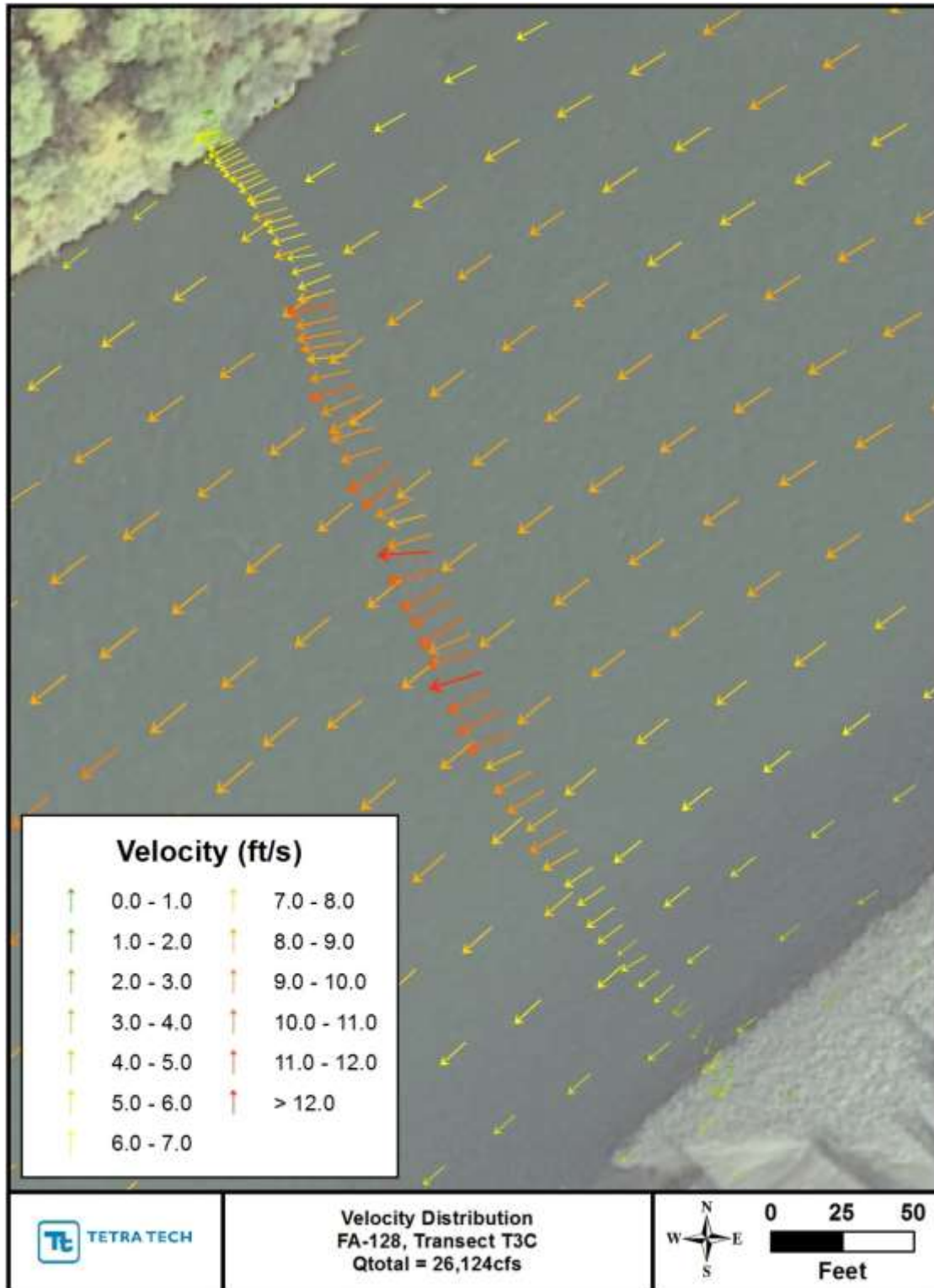


Figure 2.3-26. Comparison of measured and predicted velocity magnitude and direction at Transect 3C at 26,184 cfs (Sep 10, 2013).

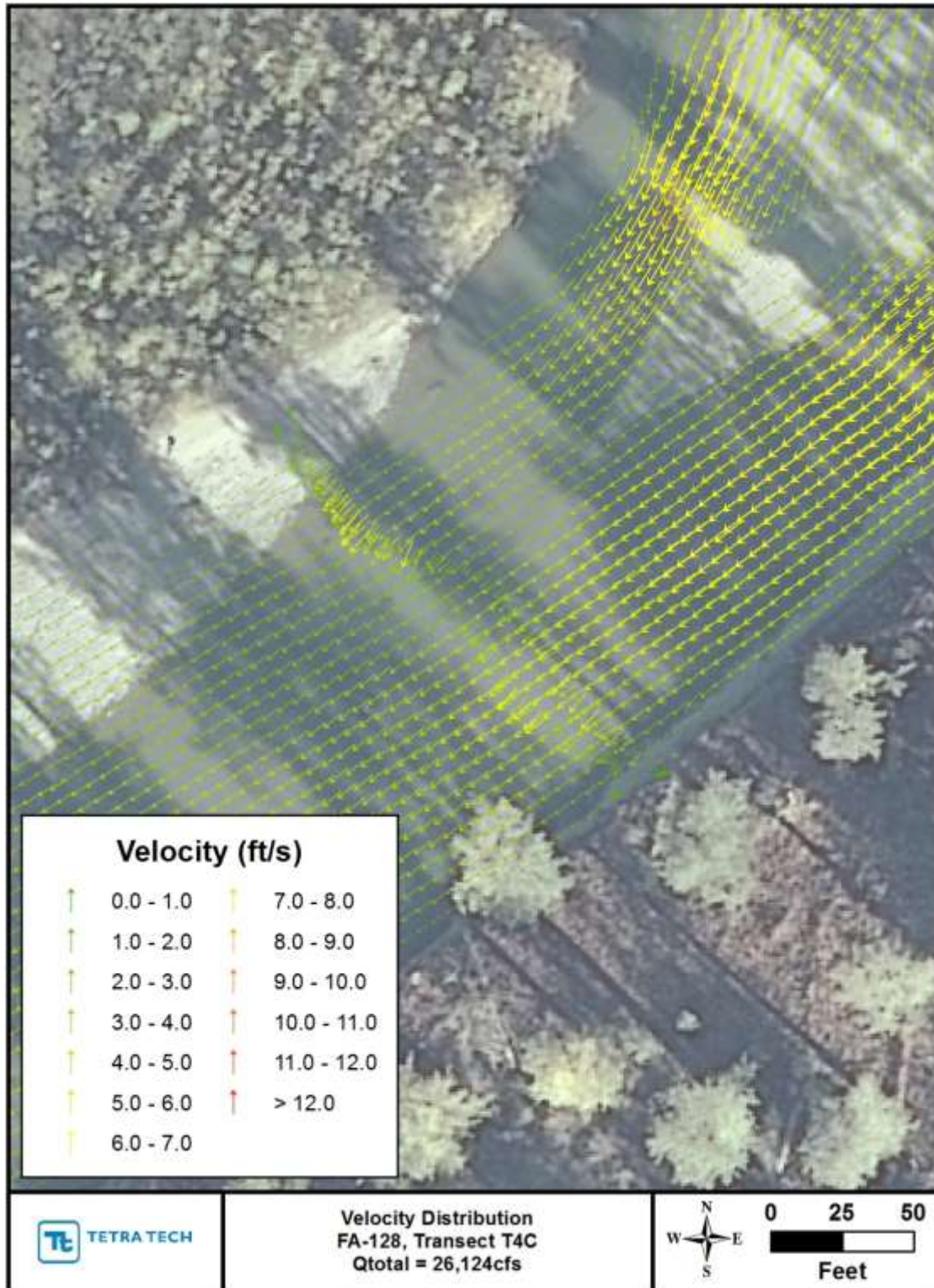


Figure 2.3-27. Comparison of measured and predicted velocity magnitude and direction at Transect 4C at 26,184 cfs (Sep 10, 2013).

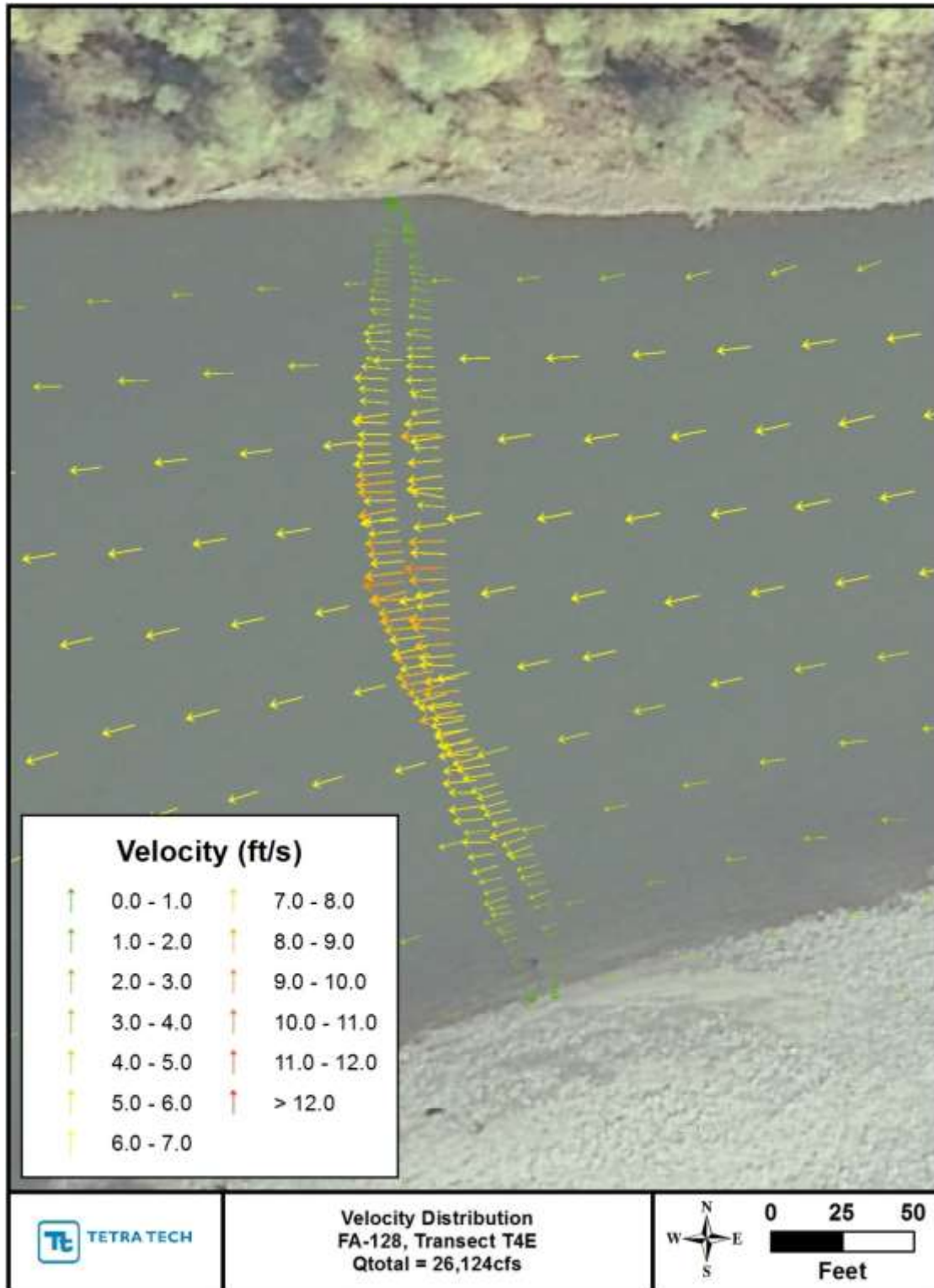


Figure 2.3-28 Comparison of measured and predicted velocity magnitude and direction at Transect 4E at 26,184 cfs (Sep 10, 2013).

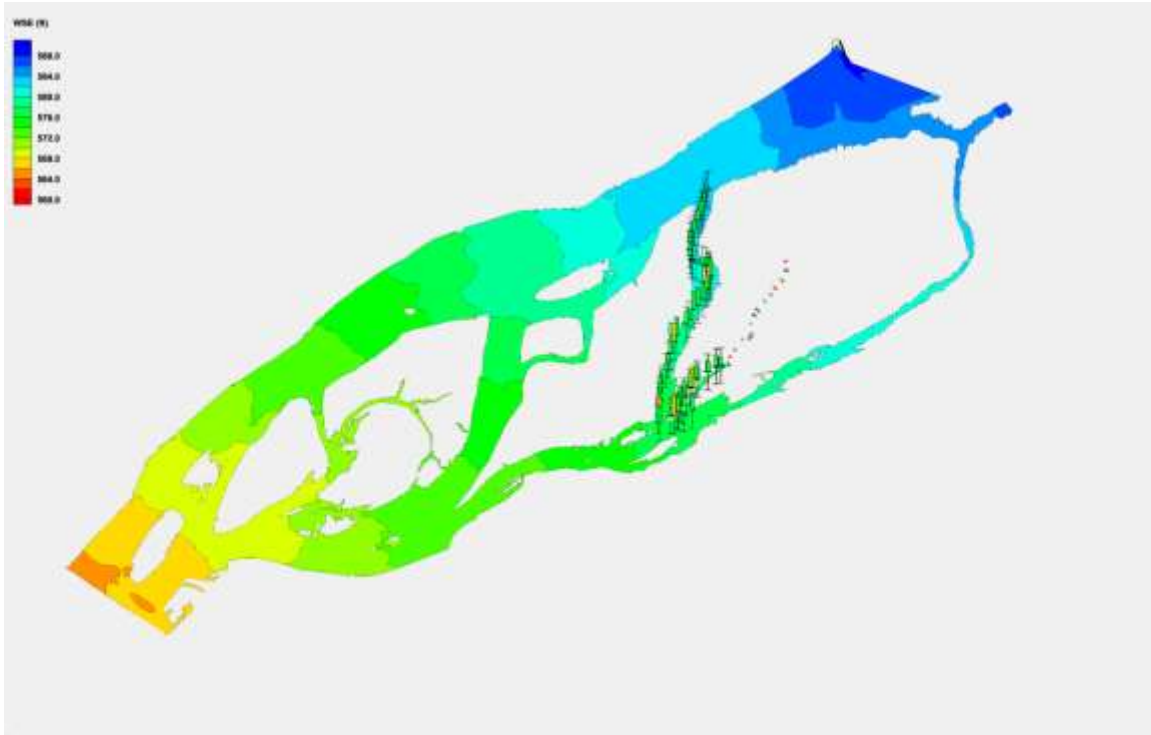


Figure 2.3-29. Screen capture from SMS showing differences between the measured and predicted water-surface elevations at 54,200 cfs (June 4, 2013) FA-128 (Slough 8A).

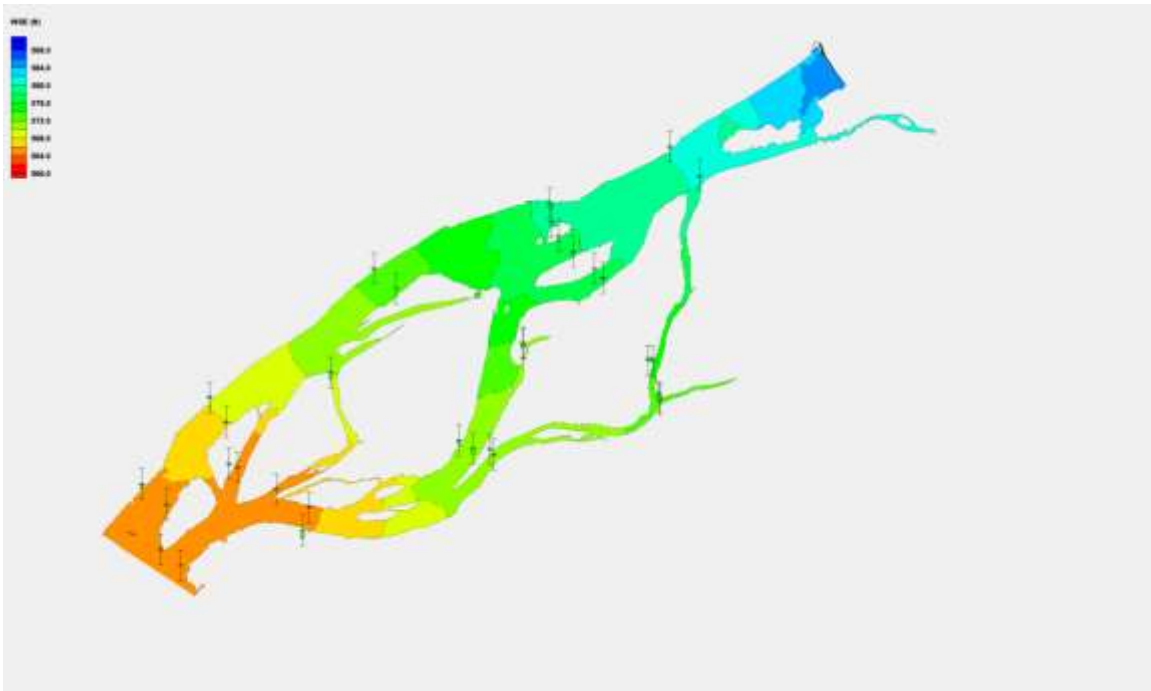


Figure 2.3-30. Screen capture from SMS showing differences between the measured and predicted water-surface elevations at 24,705 cfs (July 2, 2013) FA-128 (Slough 8A).

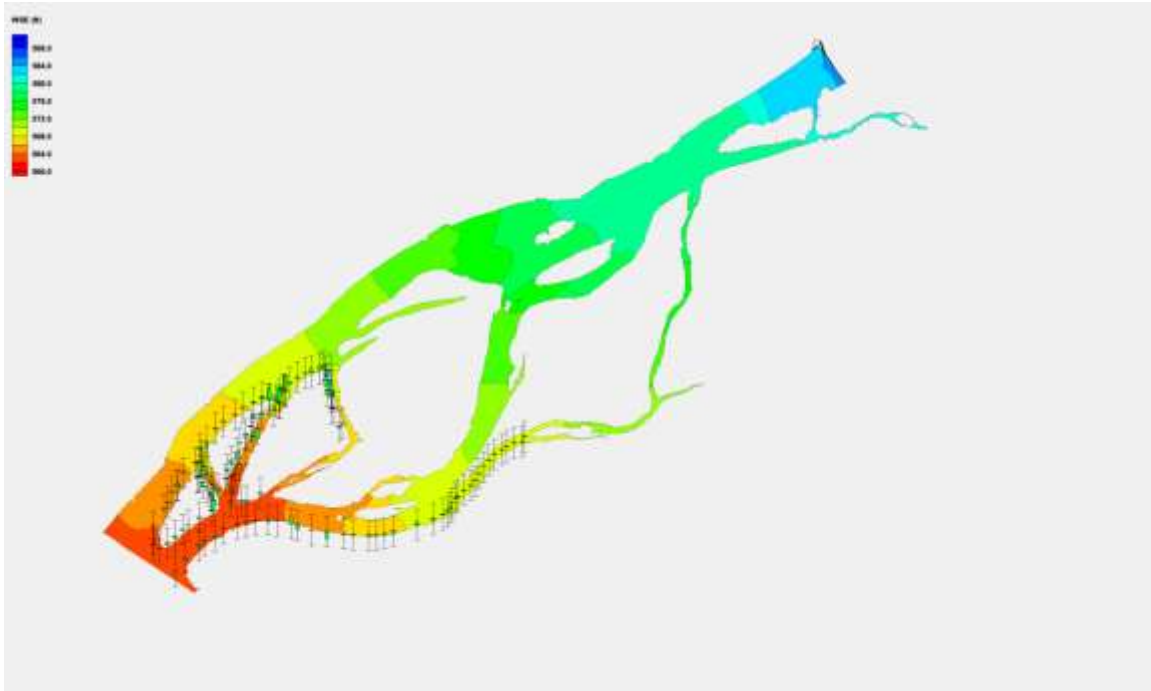


Figure 2.3-31. Screen from SMS capture showing differences between the measured and predicted water-surface elevations at 20,132 cfs (July 24, 2013) FA-128 (Slough 8A).

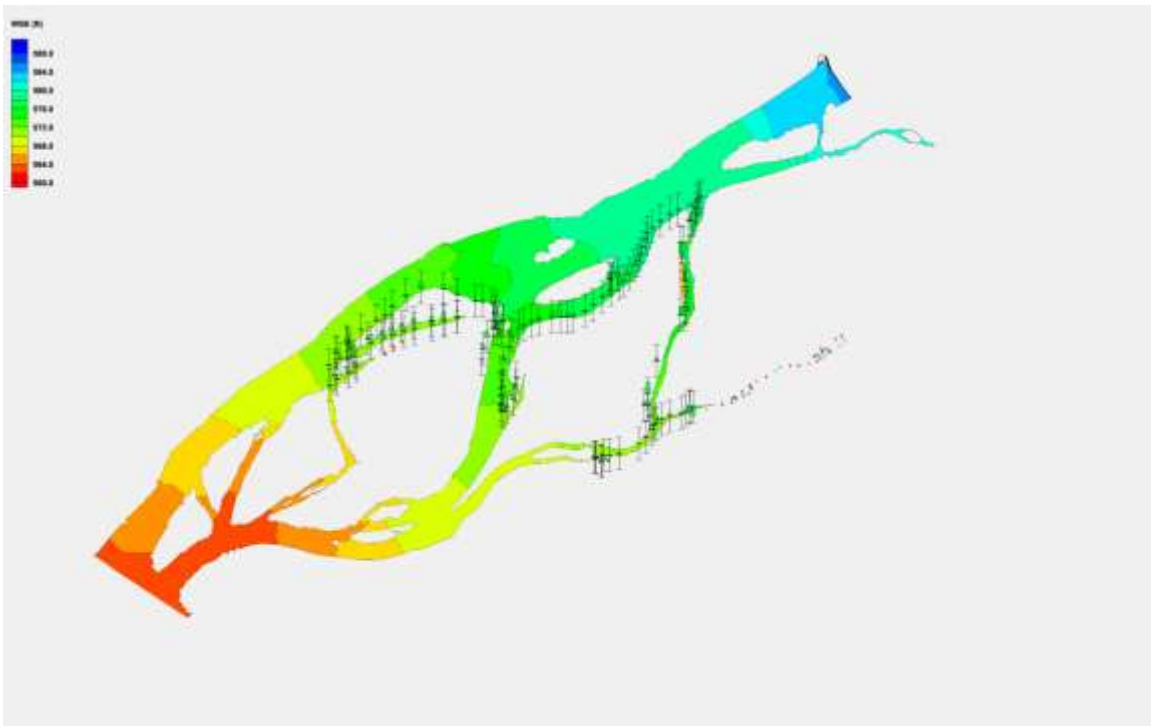


Figure 2.3-32. Screen capture from SMS showing differences between the measured and predicted water-surface elevations at 20,688 cfs (July 25, 2013) FA-128 (Slough 8A).

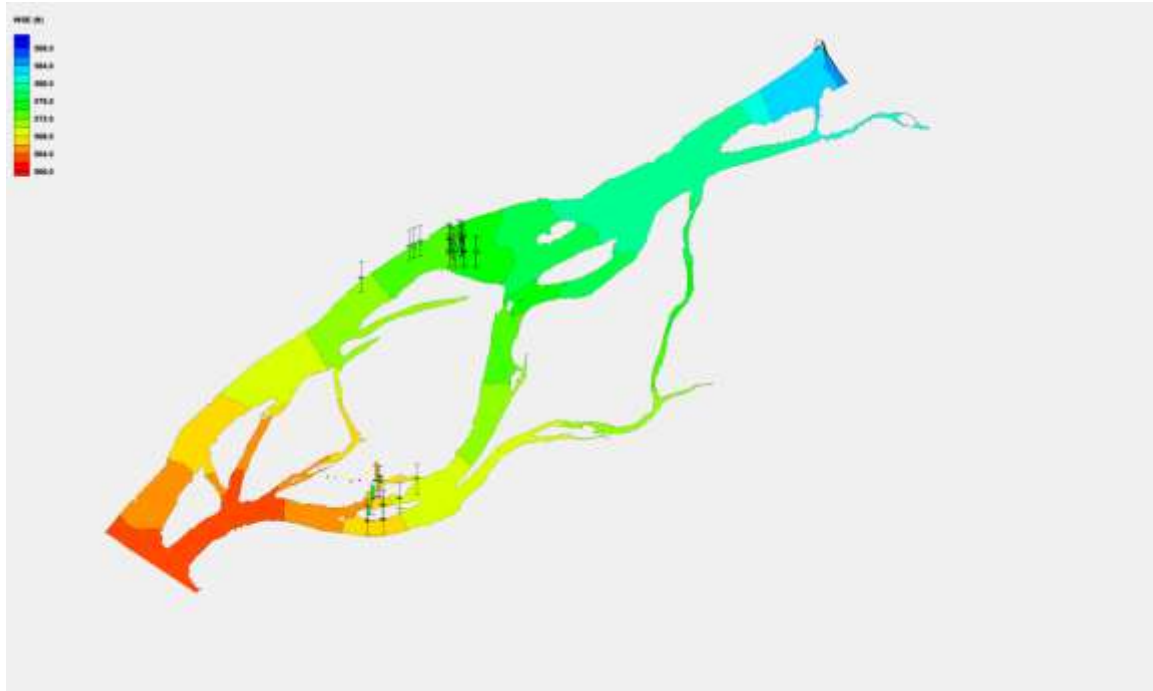


Figure 2.3-33. Screen capture from SMS showing differences between the measured and predicted water-surface elevations at 20,050 cfs (August 4, 2013) FA-128 (Slough 8A).

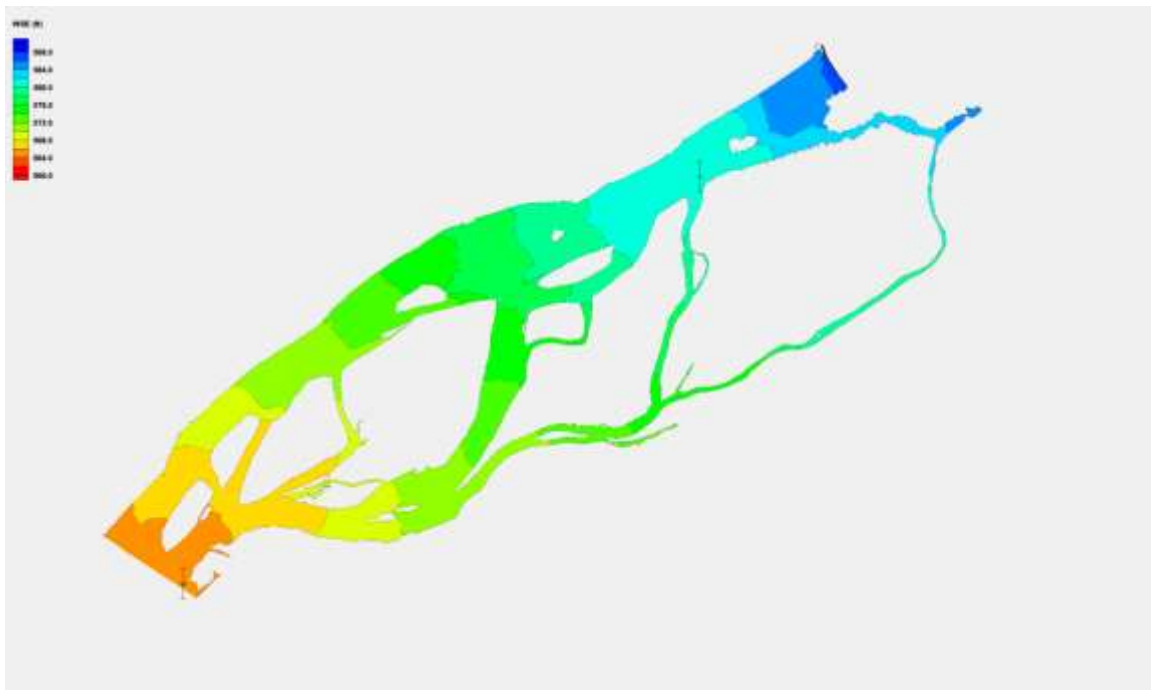


Figure 2.3-34. Screen capture from SMS showing differences between the measured and predicted water-surface elevations at 36,636 cfs (August 21, 2013) FA-128 (Slough 8A).

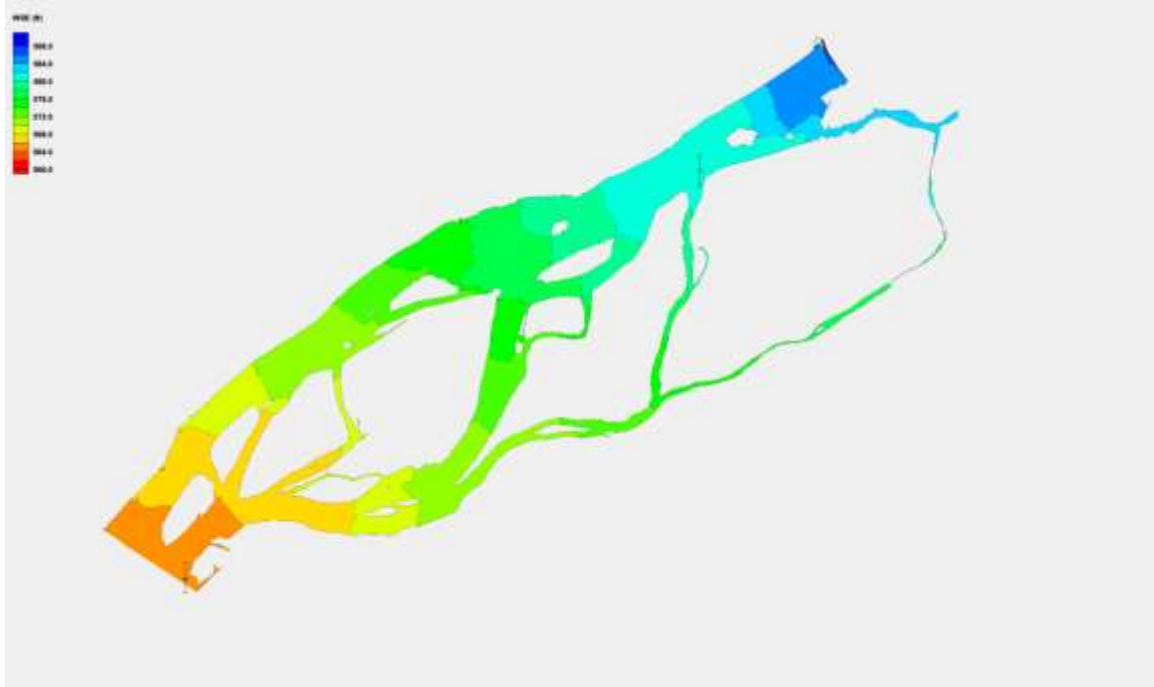


Figure 2.3-35. Screen capture from SMS showing differences between the measured and predicted water-surface elevations at 32,200 cfs (September 8, 2013) FA-128 (Slough 8A).

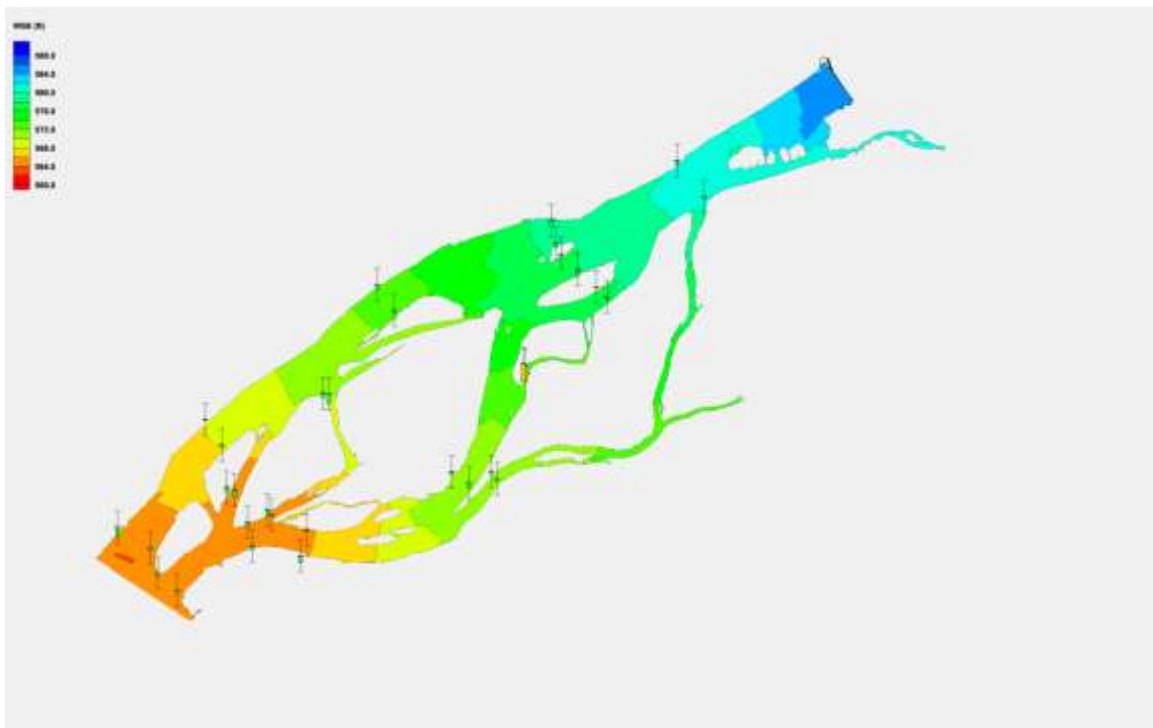


Figure 2.3-36. Screen capture from SMS showing differences between the measured and predicted water-surface elevations at 26,124 cfs (September 10, 2013) FA-128 (Slough 8A).

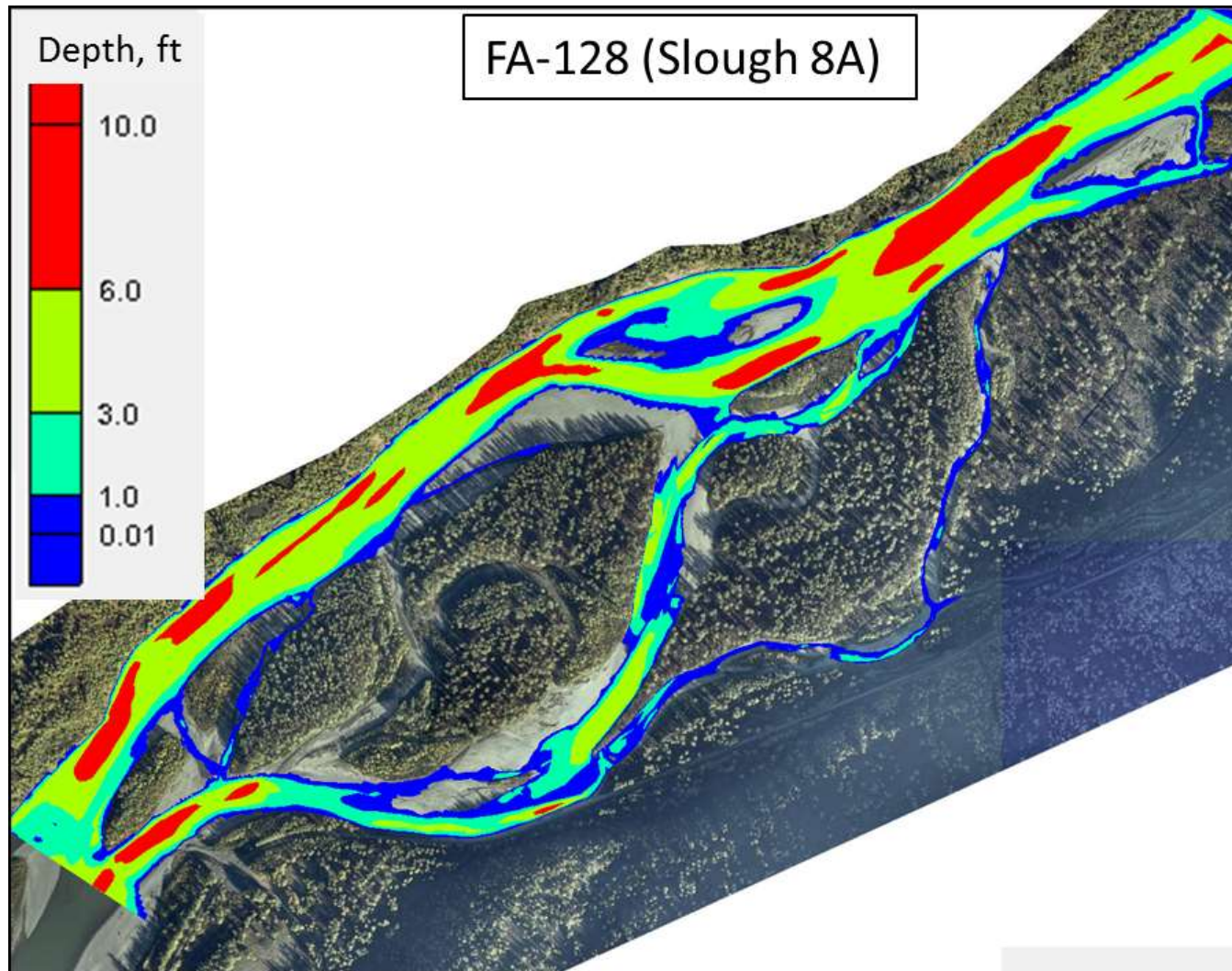


Figure 2.3-37. Flow depths at FA-128 (Slough 8A) for 12,000 cfs – initial run.

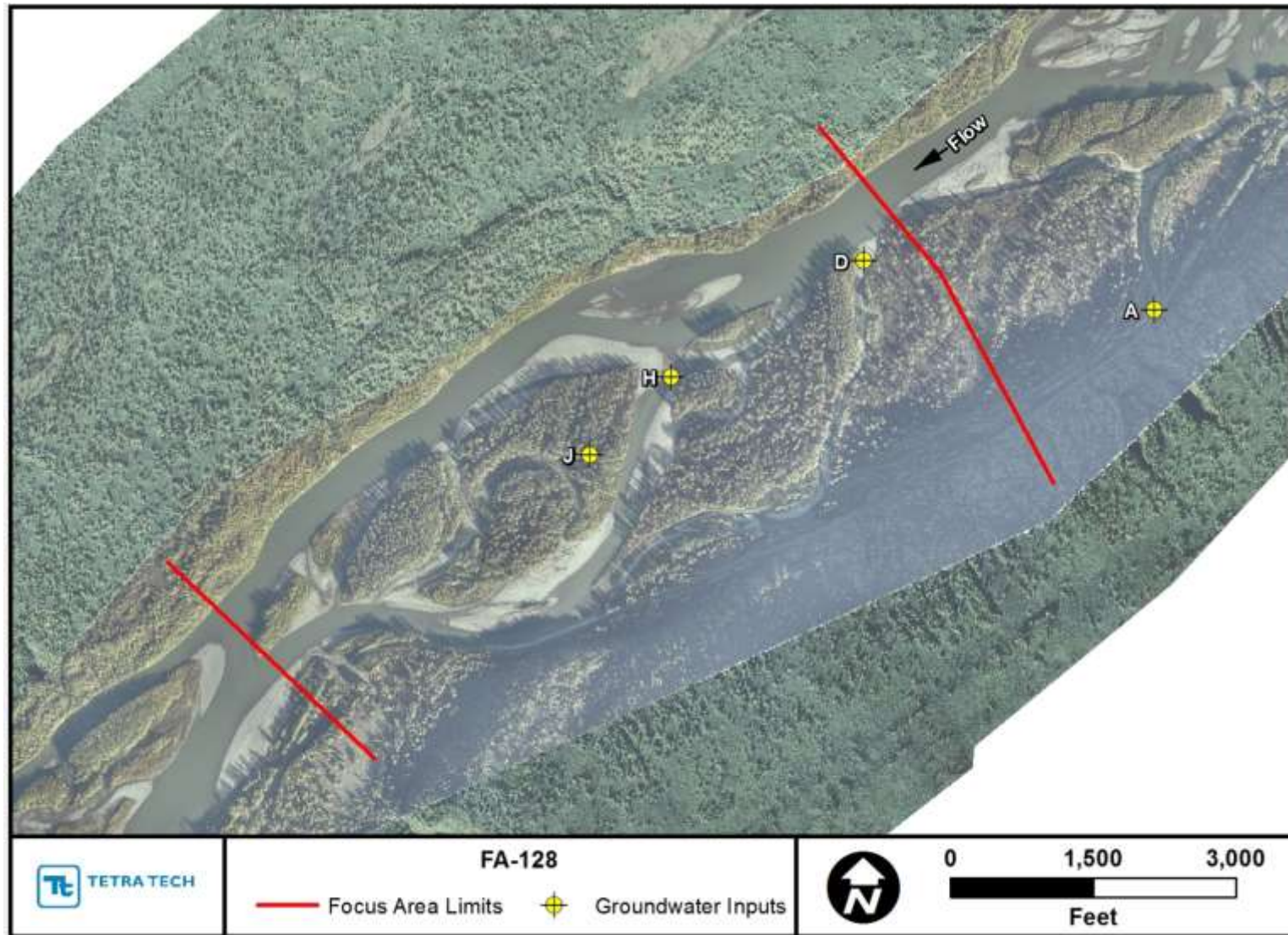


Figure 2.3-38. Location of the additional flows applied to the model to represent the groundwater flows in FA-128 (Slough 8A).

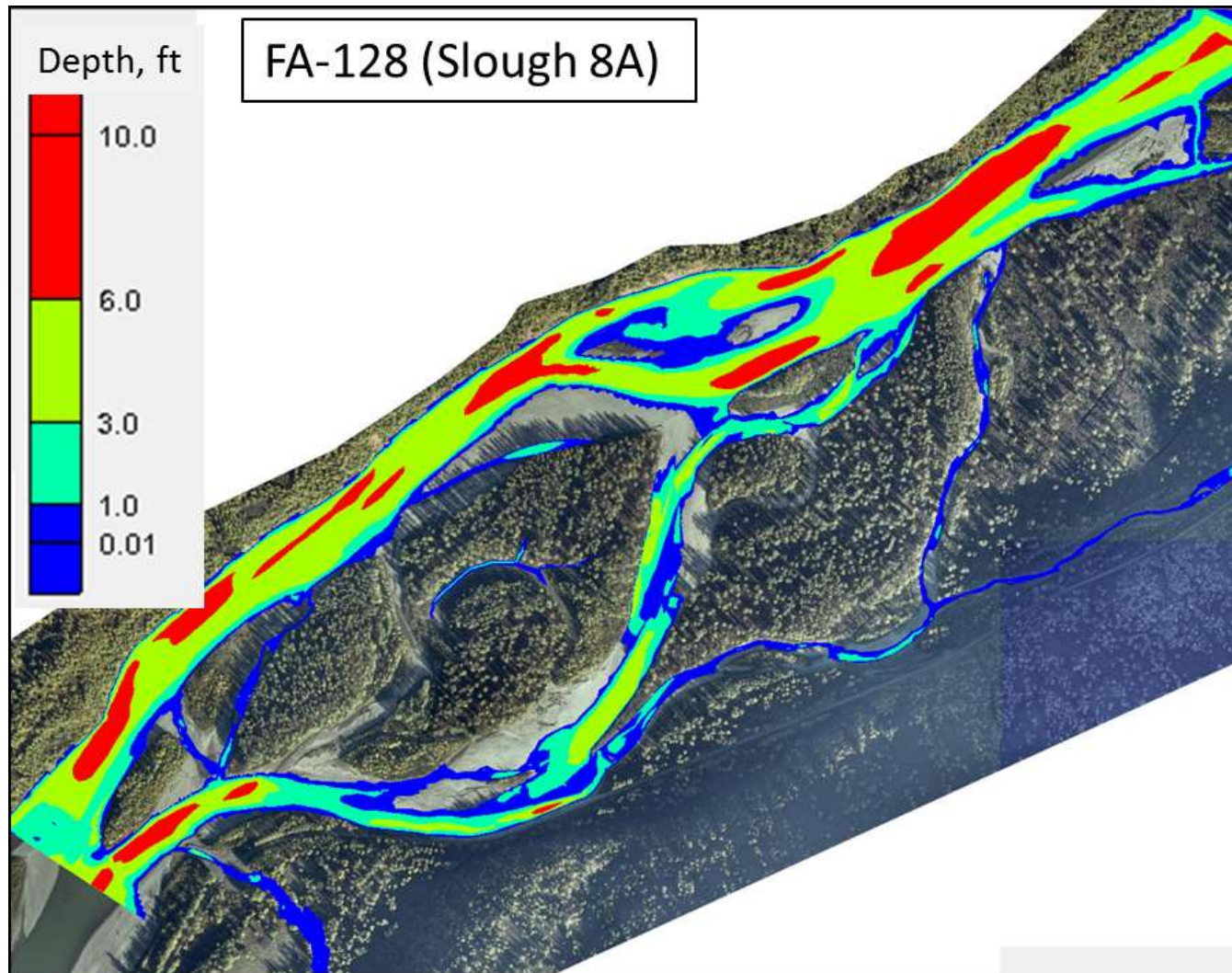


Figure 2.3-39. Flow depths at FA-128 (Slough 8A) for 12,000 cfs – run with point sources.

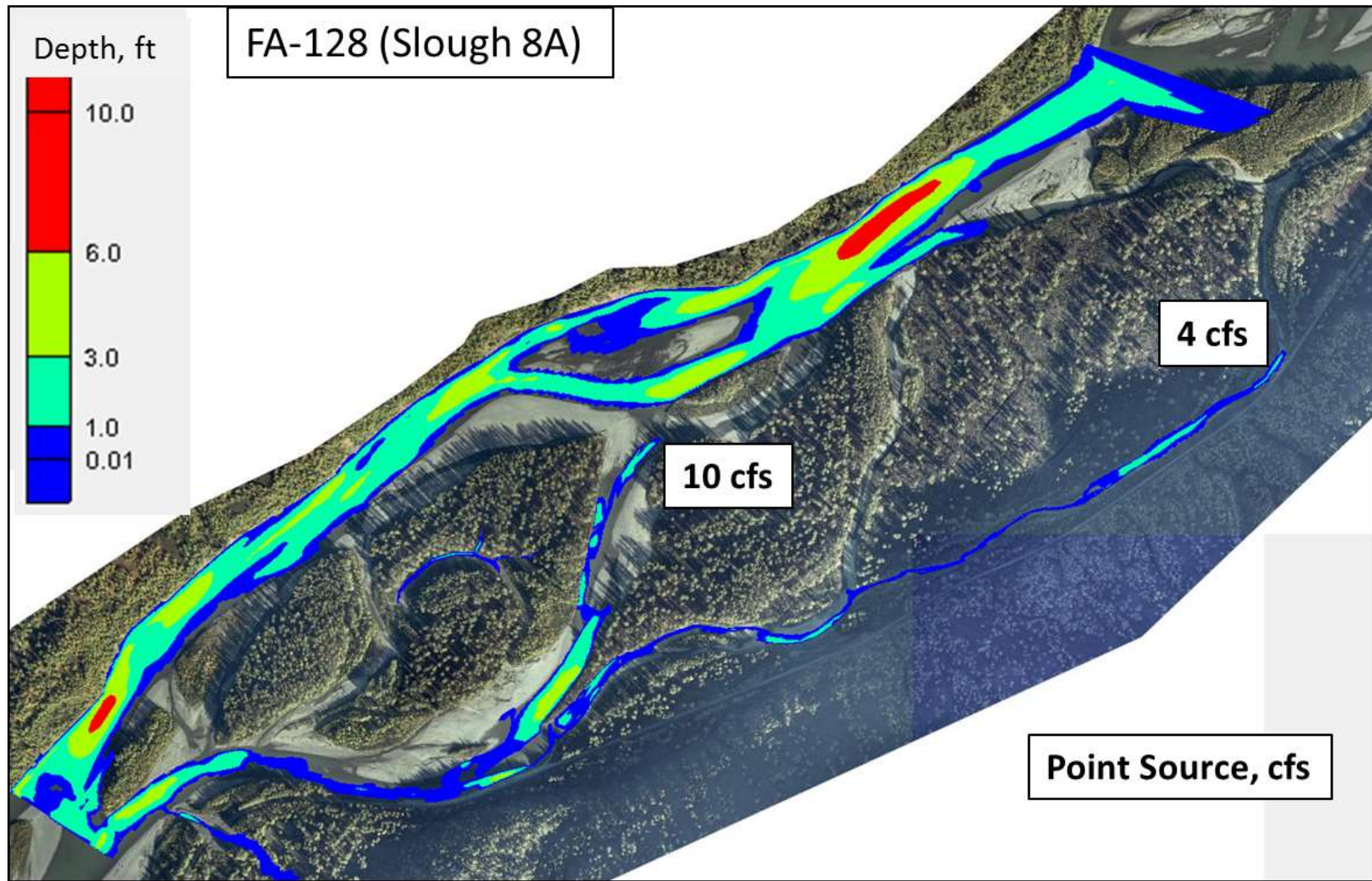


Figure 2.4-1. Predicted depth distribution at 2,000 cfs at FA-128 (Slough 8A).

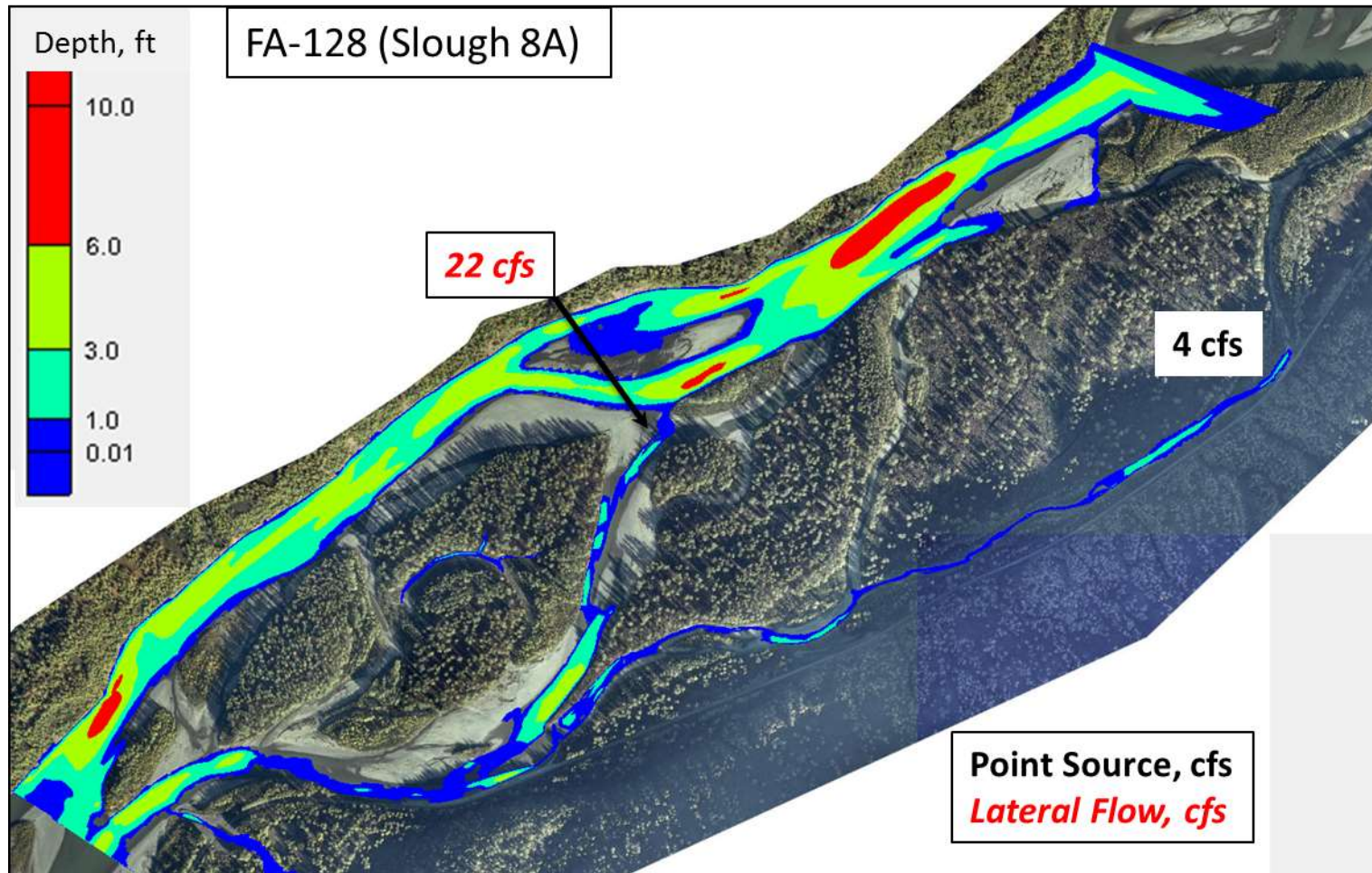


Figure 2.4-2. Predicted depth distribution at 4,000 cfs at FA-128 (Slough 8A).

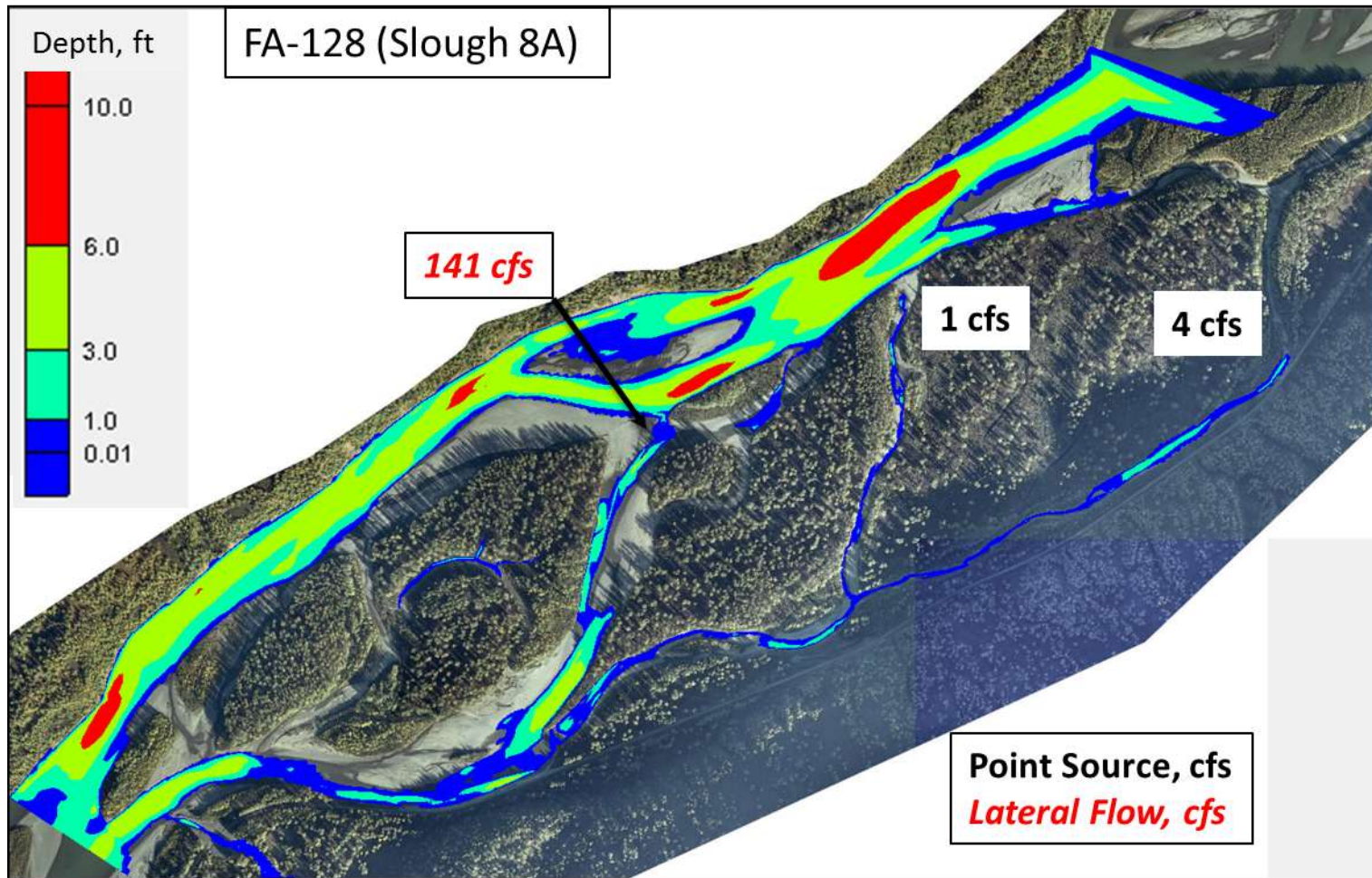


Figure 2.4-3. Predicted depth distribution at 6,000 cfs at FA-128 (Slough 8A).

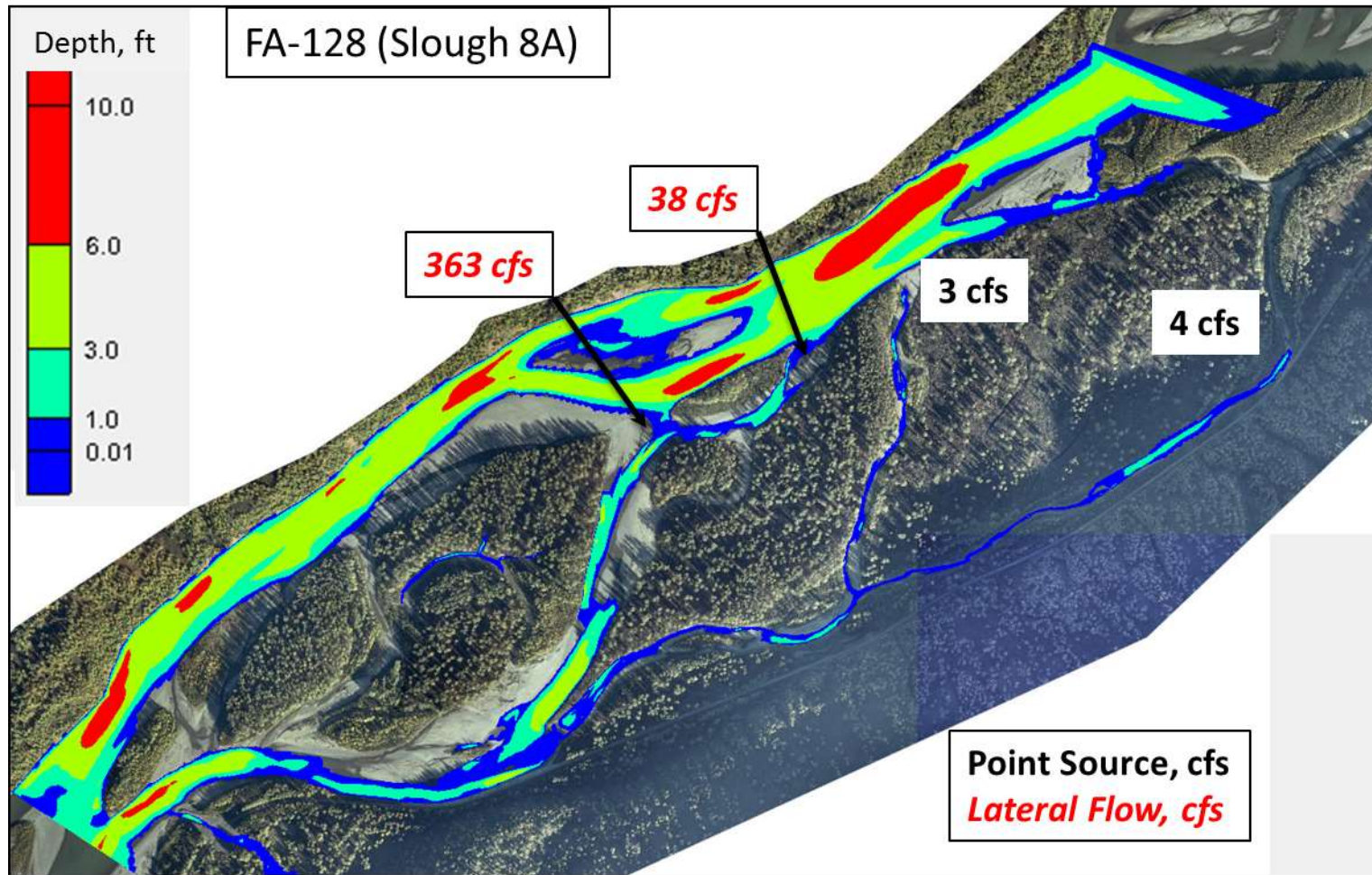


Figure 2.4-4. Predicted depth distribution at 8,000 cfs at FA-128 (Slough 8A).

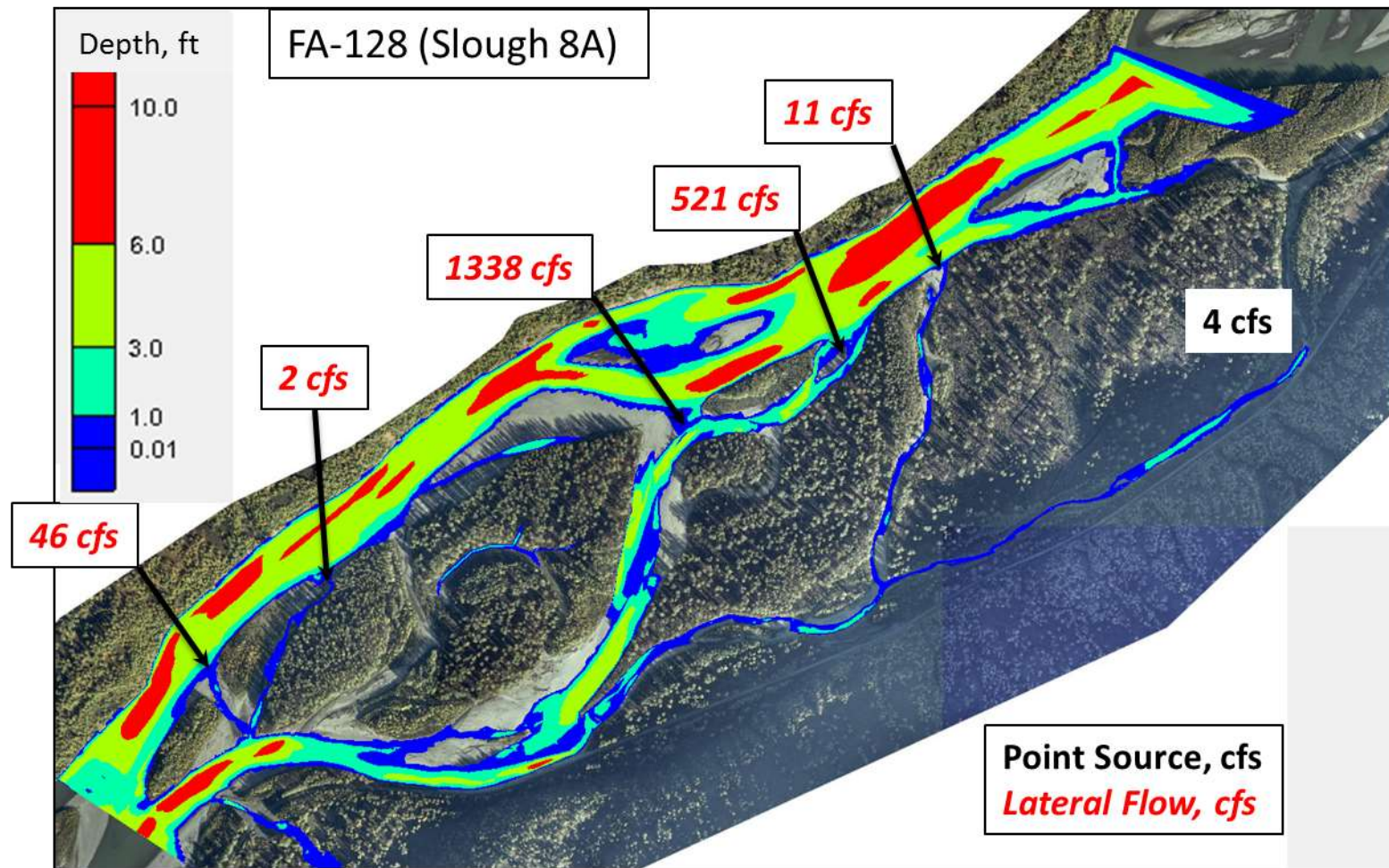


Figure 2.4-5. Predicted depth distribution at 12,000 cfs at FA-128 (Slough 8A).

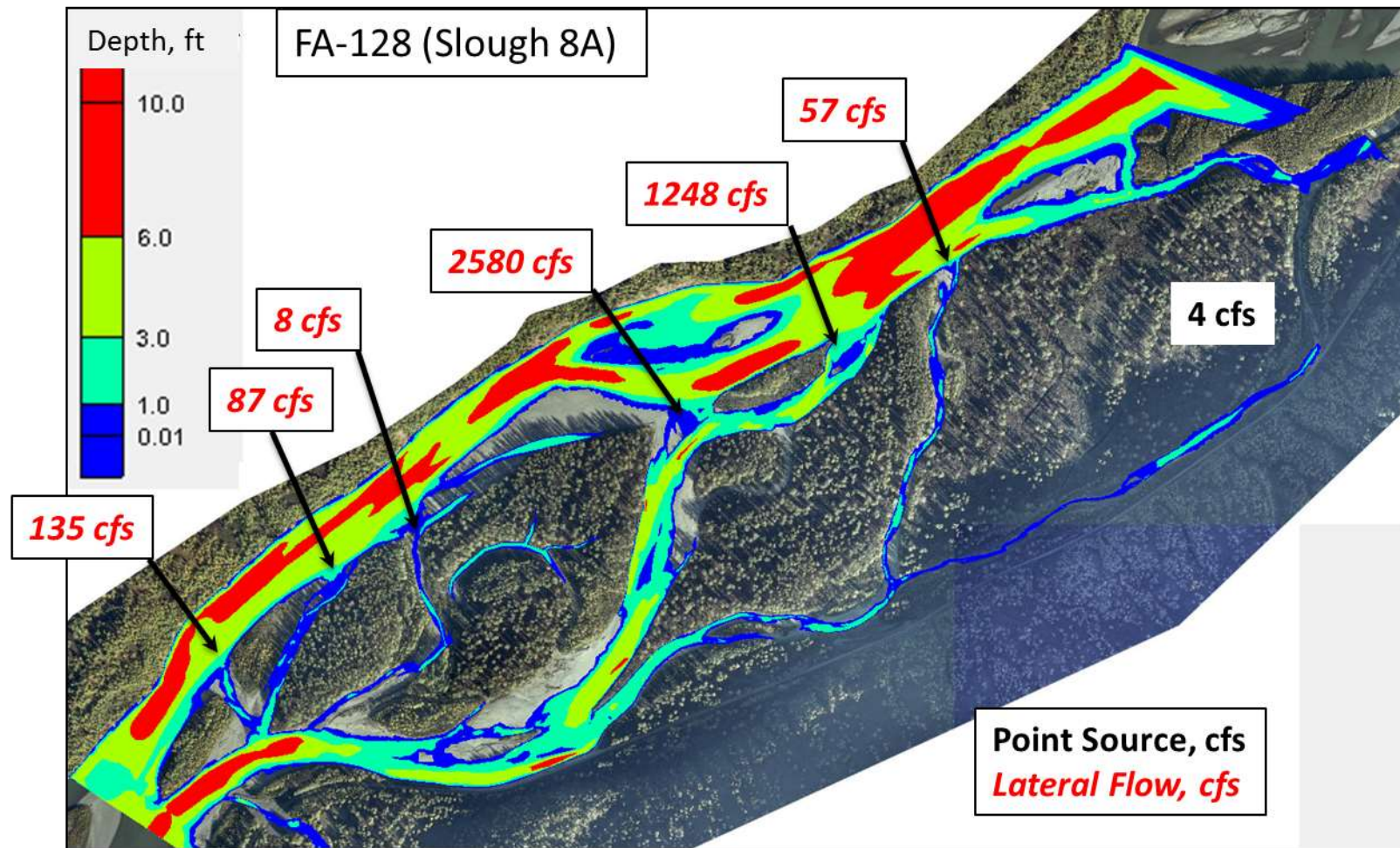


Figure 2.4-6. Predicted depth distribution at 16,000 cfs at FA-128 (Slough 8A).

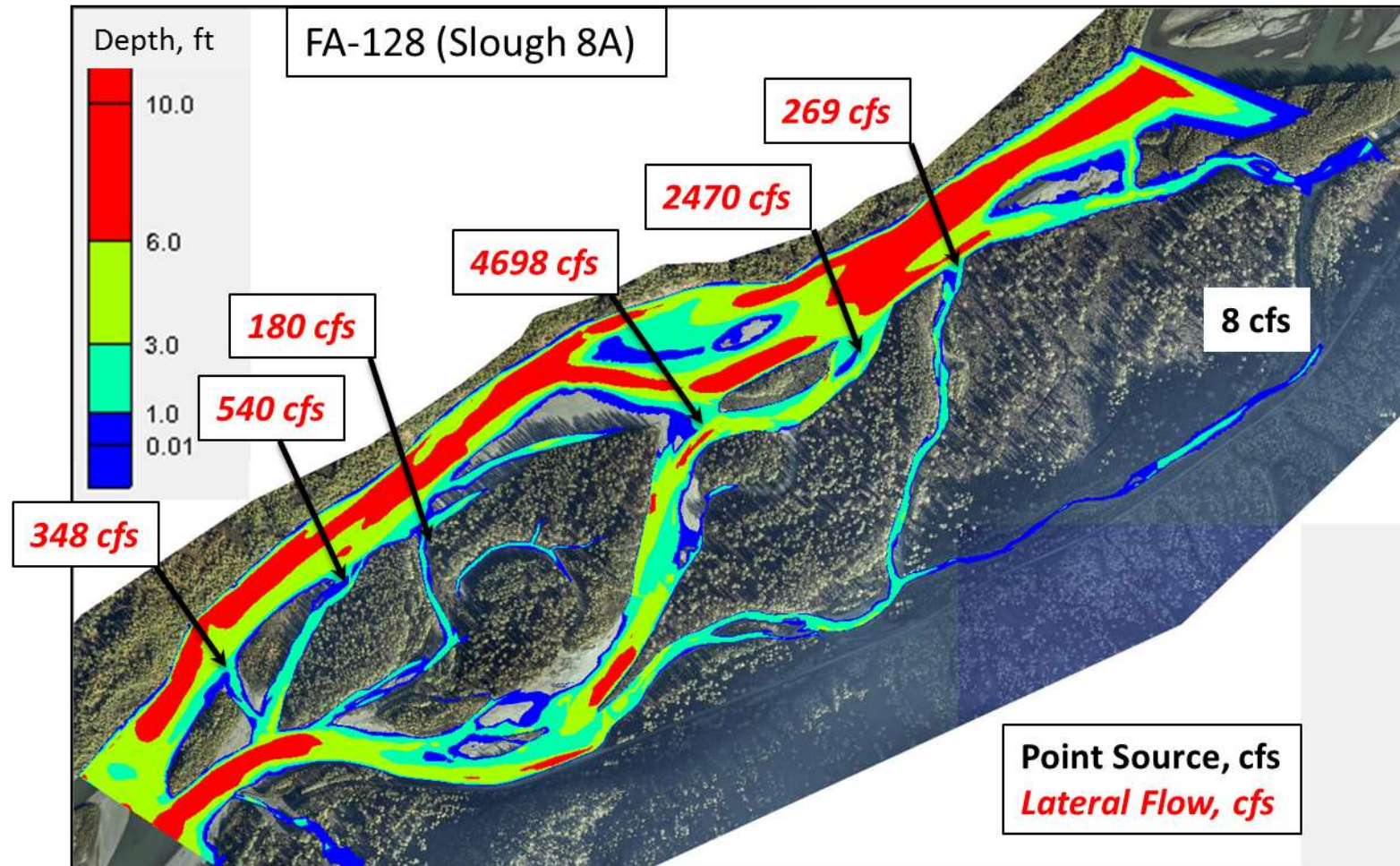


Figure 2.4-7. Predicted depth distribution at 22,000 cfs at FA-128 (Slough 8A).

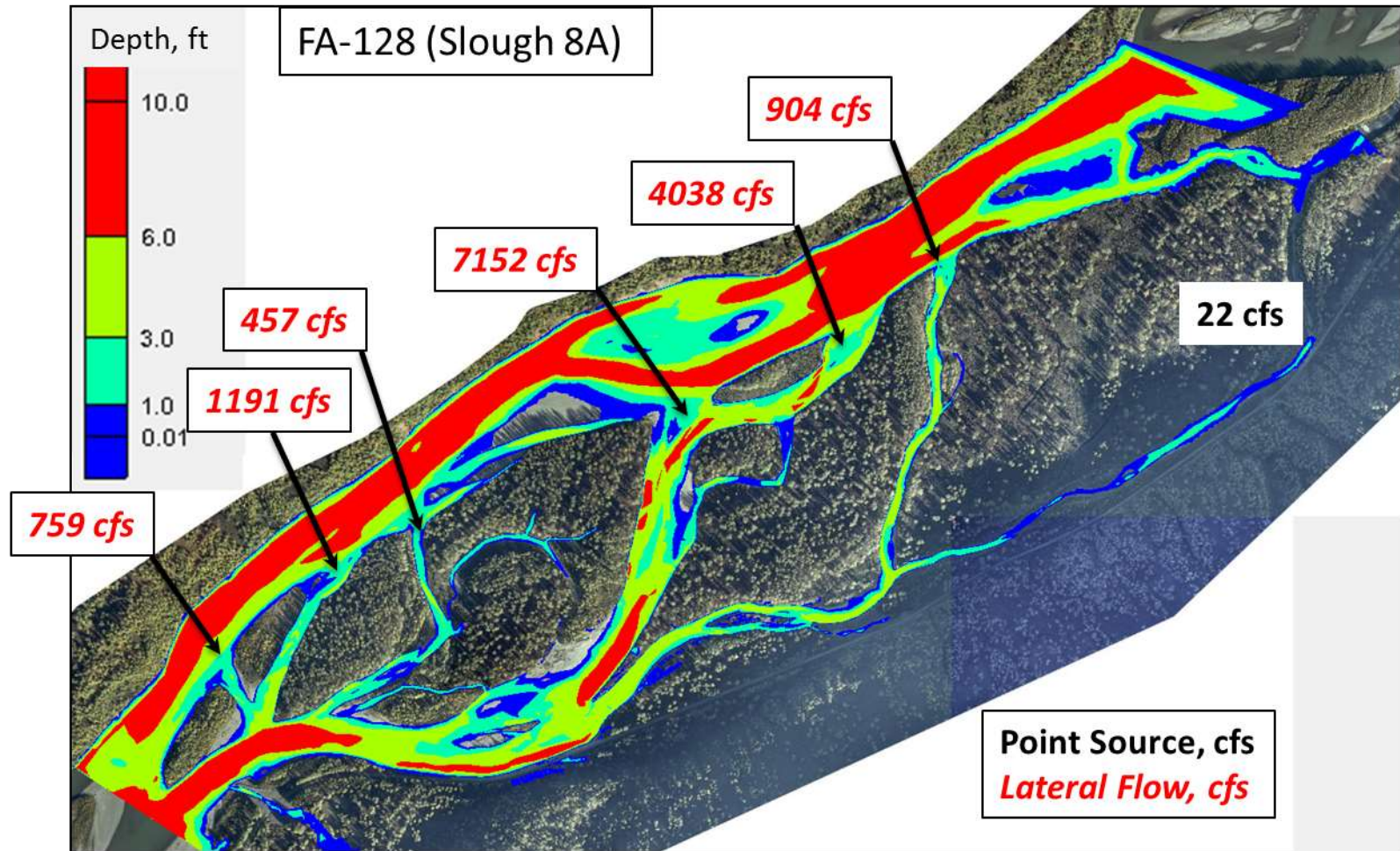


Figure 2.4-8. Predicted depth distribution at 30,000 cfs at FA-128 (Slough 8A).

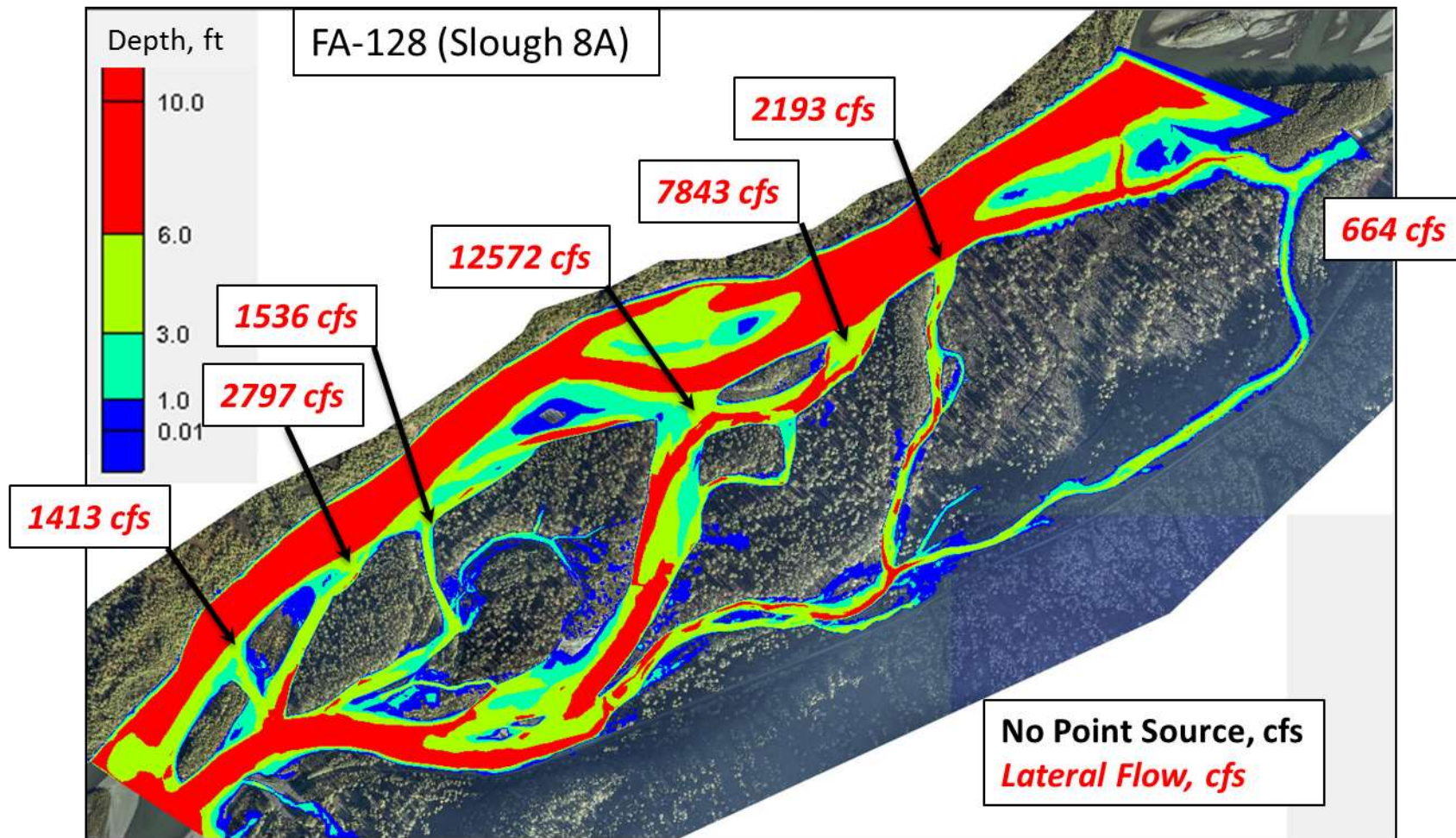


Figure 2.4-9. Predicted depth distribution at 50,000 cfs at FA-128 (Slough 8A).